To the Graduate Council:

I am submitting herewith a dissertation written by Masoud Naghedolfeizi entitled "A Life Assessment Methodology for Heat Exchanger and Steam Generator Tubing." I have examined the final copy of this dissertation for form and content and recommend that it be accepted in partial fulfillment of the requirements for the degree of Doctor of Philosophy, with a major in Nuclear Engineering.

Belle R Upadhyaya

Belle R. Upadhyaya, Major Professor

We have read this dissertation
and recommend its acceptance:

NE

John D. Landes

Robert E Uhrig

Arthur E Ruggles

Accepted for the Council:

Associate Vice Chancellor
and Dean of The Graduate School

A Life Assessment Methodology for Heat Exchanger and Steam Generator Tubing

A Dissertation
Presented for the
Doctor of Philosophy
Degree
The University of Tennessee, Knoxville

Masoud Naghedolfeizi
December 1994

ACKNOWLEDGMENTS

The author would like to express his sincere appreciation to his major professor, Dr. Belle R. Upadhyaya for his guidance, advice, support, and direction during the course of this research endeavor.

The author also expresses his gratitude to Dr. R. E. Uhrig, Dr. R. B. Perez, Dr. J. D. Landes, and Dr. A. E. Ruggles for serving on his doctoral committee and for their interest, advice and comments. Special thanks go to Dr. J. D. Landes for his technical discussions and useful suggestions.

The author is also grateful to the department head Dr. T. W. Kerlin for providing financial support, academic advice, help, and useful comments throughout his graduate studies.

Financial assistance from the Measurement and Control Engineering Center of The University of Tennessee is gratefully acknowledged.

The author also expresses his deepest gratitude to his parents, Akbar and Esmat Naghedolfeizi who have always encouraged and motivated him to pursue his educational goals, and to all of his family members for their love, encouragement, patience, and unconditional support. This dissertation is dedicated to them.

ABSTRACT

The development of an accurate technique for the service life prediction of steam generator tubes is influenced by two major problems in practice. These are: (1) availability of limited information regarding the in-service conditions of the tubes and (2) effects of material aging and degradation resulting from service exposure.

In an attempt to solve the above problems, this dissertation research focused on the development of a model-based methodology for the life assessment of steam generator tubes subjected to a certain degradation process. The methodology combines engineering analysis of the degradation process under study with the analysis of process field data and information to establish semi-empirical models to forecast the future trend in the degradation. The projection of this trend to a pre-defined allowable degradation level was used to determine the life expectancy of the component. The salient feature of this methodology is in its capacity to recognize the process nonlinearities and to identify the correct process trends which cannot be detected by simple applications of traditional forecasting techniques. This capacity greatly reduces the amount of required field data for a good forecast.

The semi-empirical prediction models were developed using both parametric and non-parametric techniques. The functional forms of the parametric models were determined based on both the approximated physics of the degradation process and the availability of field data for a reliable estimation of the model parameters. To improve the model prediction, the unknown process dynamics were enhanced by the

incorporation of an empirical dynamic formulation of field data.

The non-parametric models were established based on artificial neural network techniques. The neural network prediction (NNP) models were trained with a wide range of possible degradation paths generated by the process model. The trained NNP models perform an intelligent data mapping to match the trends in the input data to one of the learned process paths and thereby forecasting the future trends of the process within a specified time-frame.

The proposed life assessment approach was used to predict the wear process of a Once-Through Steam Generator (OTSG) tube within its 15th tube support as a complex application of trend forecasting. To implement the methodology, a tube wear process model was developed to simulate the process trend over time with regard to aging and degradation mechanisms resulting from service exposure. The simulated wear data were used to establish various semi-empirical prediction models to determine suitable models for process trend prediction with different block sizes of data.

The results show the degradation of friction coefficient and material aging could markedly increase the rate of tube wear with subsequent tube life reduction. They also indicated that the power-exponential model [$at^b exp(ct)$], developed based on this methodology, provided a more accurate prediction of the tube life than the power-law model (at^b) suggested in the literature. A significant improvement in the prediction of the power-law model was obtained by including a dynamic formulation of the historical data.

The results also demonstrated that NNP models perform extremely well for both

trend recognition and prediction, even with a limited amount of data. An attractive feature of NNP models is that they are far less noise-sensitive than parametric models. The estimation of residual life of tubing was demonstrated using both parametric and NNP models.

The methodology developed in this research is generic in nature and can be applied to the life assessment of both stationary components and rotating machinery.

TABLE OF CONTENTS

CHAPTER		PAGE
1.	**INTRODUCTION**	**1**
	1.1 General Background	1
	1.2 Degradation Mechanisms of Nuclear Steam Generator Tubing	6
	1.2.1 Common Tube Failure Modes	6
	1.2.2 Fretting-Wear Damage Mechanism	7
	1.2.3 Industrial Impacts	8
	1.3 Statement of the Problem and Objectives	10
	1.4 Significance of the Study and the Contributions of the Dissertation	15
	1.5 Organization of the Dissertation	18
2.	**LITERATURE REVIEW**	**19**
	2.1 Introduction	19
	2.2 Life Assessment Techniques	19
	2.2.1 Dynamic Methods	25
	2.3 Fretting-Wear of Heat Exchanger Tubes	27
3.	**METHODOLOGY FOR LIFE ASSESSMENT OF PLANT COMPONENTS.**	**32**
	3.1 Development of Life Assessment Models	32
	3.2 Parametric Prediction Models	34
	3.2.1 Applications	40
	3.2.2 Steam Generator Performance Degradation	40
	3.2.3 Life Prediction of Steam Generator Tubes	49
	3.3 Non-Parametric Models Using Artificial Neural Networks	52
	3.3.1 Introduction	52
	3.3.2 Artificial Neural Networks	54

3.3.3 Neural Network Methodology for Predicting Steam Generator Tube Degradation 57
3.3.4 Rationale 61

4. STEAM GENERATOR TUBE WEAR MODEL 65

4.1 Introduction 65

4.2 Tube Wear Model Development 67

4.2.1 Contact Deformation Model 68

4.3 Parameter Identification of the Tube Wear Model 79

4.3.1 Coefficient of Friction 79
4.3.2 Shear Stress Yield Point 83
4.3.3 Normal Contact Forces 86

4.4 Comments on the Wear Model 87

4.5 Mechanics and Patterns of Tube Wear in OTSG Systems 88

4.6 Summary 89

5. DEVELOPMENT OF A MATHEMATICAL MODEL FOR TUBE/SUPPORT INTERACTION IN MULTI-SPAN STEAM GENERATOR TUBES 92

5.1 Once-Through Steam Generators 92

5.2 Flow-Induced Vibration in an OTSG 94

5.2.1 Vortex Shedding 96
5.2.2 Random Turbulent Buffeting 97

5.3 Simulation of Impact Forces 98

5.3.1 Solution Procedure 104
5.3.2 Simulation of Tube-to-Support Contact forces for an OTSG Tube 105

5.4 Parametric Study of Contact Forces and Contact Duration Time . . . 113

5.5 Summary 116

6. IMPLEMENTATION OF THE LIFE ESTIMATION METHODOLOGY TO THE WEAR OF STEAM GENERATOR TUBING 119

6.1 Tube Wear Data Acquisition Methods 120

6.2 Experimental Studies of Tube Wear Mechanisms in Heat Exchangers 122

6.3 Simulation Procedure for Tube Wear Degradation 123

6.4 Development of Parametric Prediction Models 132

6.4.1 Case Study #1: Normal Tube Wear Degradation 133
6.4.2 Case Study #2: Rapid Tube Wear Degradation 141
6.4.3 Dynamic Parametric Models 148

6.5 Non-Parametric Prediction Models Using Artificial Neural Networks 152

6.6 Residual Life Estimation 163

6.7 Parametric Sensitivity Analysis 169

6.8 Simulation of Uncertainties 175

6.9 Summary and Suggestions for Implementation 178

6.9.1 Summary 178
6.9.2 Suggestions for Implementation 180

7. SUMMARY, CONCLUSIONS AND RECOMMENDATIONS FOR FUTURE RESEARCH 182

7.1 Summary 182

7.2 Conclusions 185

7.3 Recommendations for Future Research 189

REFERENCES 191

APPENDICES 200

A. STEAM GENERATOR TUBE FAILURE MODES 201

A.1 Tube Wall Degradation Mechanisms 201
A.2 Tube Plugging Trends and Forced Power Outages 206

B. MASS AND STIFFNESS MATRICES 210

C. LISTING OF COMPUTER PROGRAMS 211

VITA 231

LIST OF TABLES

TABLE **PAGE**

1.1 Cost survey of steam generators used in the U.S. nuclear power plants ($ represents 1 million dollars) [1]. 5

3.1 Values of constant parameters of steam pressure model and the overall heat transfer coefficient equation. 44

3.2 Time dependent models of the UTSG steam pressure. 47

5.1 Design data for a typical Once-Through Steam Generator (OTSG) used in Oconee power plant [17,74]. 95

5.2 Computational efficiency of the finite element model of OTSG tube vibrations. 109

6.1 Values of constant parameters of the tube wear process model. 129

6.2 Estimated values of the parameters of the prediction models for the case of smooth wear data. 135

6.3 Estimated values of the parameters of the prediction models for the case of noisy wear data. 139

6.4 Structural and Training Information of the NNP Models. 157

LIST OF FIGURES

FIGURE		PAGE
1.1	History of world-wide number of steam generator tubes plugged [1].	3
1.2	Effect of chemical corrosion degradation on the tubes of PWR steam generators [76].	9
1.3	Effect of mechanical degradation on the tubes of PWR steam generators [76].	9
3.1	Variations of a UTSG steam pressure versus percentage reduction in the overall heat transfer coefficient.	42
3.2	Trend prediction of the steam pressure variations using both a quadratic and a dynamic regression models.	48
3.3	Trend prediction of the steam pressure deviations using both a simple and a linear dynamic regression models..	50
3.4	Flow chart showing a life assessment procedure of steam generator tubes due to the wear mechanism.	53
3.5	Typical structure of a multi-layer artificial neural network.	56
3.6	Schematic diagram of a hypothetical steam generator tube degradation region.	59
3.7	Schematic diagram of a typical non-parametric prediction model using artificial neural networks.	62
4.1	Shakedown process during the deformation of a rolling element.	69
4.2	Schematic diagram of the interaction mechanism between a tube and tube support.	71
4.3	Penetration of asperities of one surface onto the opposing surface [71].	76
4.4	Frictional behavior of ion-coating test [66].	82
4.5	Patterns of wear scars on a pulled out tube from an OTSG of Duke Power's Oconee unit [76].	90
5.1	Schematic diagram of a typical Babcock & Wilcox Once-Through Steam	

Generator unit [74]. 93

5.2 Cross-flow velocity profile between the 15th support tube and the upper tube sheet in an OTSG uint [17]. 102

5.3 Schematic diagram of the four-span model of an OTSG tube. 107

5.4 Simulation of tube displacement at the 15th tube support of an OTSG system due to the excitation forces of Equation (5.9). 111

5.5 Simulation of contact force history at the 15th tube support of an OTSG system due to the excitation forces of Equation (5.9). 111

5.6 Frequency response of the tube displacement at the 15th tube support due to the excitation forces of Equation (5.9). 112

5.7 Frequency response of the contact forces at the 15th tube support due to the excitation forces of Equation (5.9). 112

5.8 Variations of the contact forces at the 15th tube support with clearance. 115

5.9 Variations of the contact duration time at 15th tube support with clearance. 115

5.10 Variations of the contact forces with tube-to-support misalignment at the 15th tube support. 117

5.11 Variations of the contact duration time with tube-to-support misalignment at the 15th tube support. 117

6.1 Variation of the wear mechanism with time for tubes with Incoloy 800 and Monel 400 materials (carbon steel is the tube support material) [15]. 124

6.2 A computer algorithm for the estimation of tube wear amount. 127

6.3 Simulation of tube wear process using a time varying friction coefficient. 130

6.4 Trend prediction of a normal tube wear degradation using semi-empirical parametric models with three different block sizes of data. 136

6.5 Trend prediction of a rapid tube wear degradation using semi-empirical

parametric models with two different block sizes of data. 142

6.6 Effect of noise on the estimation of parameters of the Power-Exponential model for two block sizes of data each having 5 and 10 data points, respectively. 144

6.7 Effect of noise on the prediction of Power-Exponential model. 145

6.8 Trend prediction of a rapid tube wear degradation using a high order parametric model. 147

6.9 Trend prediction of a rapid tube wear degradation using a nonlinear dynamic regression model. 150

6.10 Trend prediction of a rapid tube wear degradation using a simple linear dynamic regression model. 151

6.11 Effect of noise on the prediction of the linear dynamic model. 153

6.12 Data structure of the training patterns of the NNP models. 155

6.13 Trend prediction of various tube wear degradation trajectories using NNP models with 3 different block sizes of data. 158

6.14 Effects of 4% and 6% noise levels on the prediction of a 3-point NNP model. 160

6.15 Effects of 4% and 6% noise levels on the prediction of a 5-point NNP model. 162

6.16 Schematic diagram of residual life estimation using parametric prediction models. 165

6.17 Schematic diagram of residual life estimation using NNP models. 165

6.18 Residual life estimation of a typical OTSG tube when a parametric model is used for the trend prediction of a normal tube wear degradation. 166

6.19 Residual life estimation of a typical OTSG tube when a NNP model is used for the trend prediction of a normal tube wear degradation. 168

6.20 Variation of tube wear with the exponent parameter of the coefficient of friction. 171

6.21 Variation of tube wear with the aging factor of the shear yield stress point. 171

6.22 Variation of tube wear with the rate parameter of the contact forces. . . . 173

6.23 Variation of tube wear with the rate parameter of the contact duration time. 173

6.24 Effect of random variations of the contact forces on tube wear. 177

6.25 Effect of force biasing on tube wear. 177

A.1 Tube plugging trends of Babcock & Wilcox steam generators [76]. 207

A.2 Tube plugging trends of Combustion Engineering steam generators [76]. 207

A.3 Tube plugging trends of Westinghouse steam generators [76]. 208

A.4 Percent of forced power outages due to corrosion degradation mechanisms [76]. 208

A.5 Percent of forced power outages due to mechanical degradation mechanisms [76]. 209

LIST OF ACRONYMS

ANN	Artificial Neural Networks
ASME	American Society of Mechanical Engineers
EPRI	Electric Power Research Institute
NNP	Neural Network Prediction
OTSG	Once-Through Steam Generator
PWR	Pressurized Water Reactor
UTSG	U-Tube Steam Generator

CHAPTER 1

INTRODUCTION

1.1 General Background

Heat exchangers and steam generators are widely used in fossil and nuclear power plants, and in chemical industry processes. Their safe and reliable operations are crucial for plant performance, increased production and economy. To ensure reliable operation of these components, it is essential to gain a good and realistic understanding of degradation mechanisms which can lead to the failure of such equipment. This knowledge is useful for both estimating equipment life and for establishing a sound and effective schedule for plant monitoring and maintenance programs. This in turn will help to reduce unexpected and costly shut-downs of the plants due to degradation problems in these equipment.

The degradation of tubes in heat exchangers and steam generators causes the most failure rates in these devices. Tube degradation process could occur due to four major causes:

1. Thermal and mechanical stresses,
2. Fatigue and creep,
3. Wear and fretting, and
4. Corrosion.

Depending on the operational and environmental conditions, one or more of the above causes can damage the tubes. Damaged tubes could be identified by available inspection procedures such as eddy current and ultrasonic testing [60]. Since the replacement of a damaged tube can be extremely tedious, time consuming and costly, the current practice is to plug damaged tube so that they no longer function.

A recent survey of world-wide nuclear steam generator tube plugging [1] indicates that the number of tubes plugged per year from 1976 to 1991 has approximately increased by 6000 (see Figure 1.1). This generates a major concern about the performance of steam generator systems in power plants. The removal of tubes from service increases steam generator pressure drop which causes power losses [1,2]. Some power plants have reported a large pressure drop (up to 70 psi) in their steam generators due to steam generator performance degradation and tube plugging [2]. Although certain limits for pressure drop are considered in the design of steam generators, the current trends in pressure drops in some nuclear steam generators are not encouraging [1,2] mainly from the viewpoint of satisfactory operation in the future.

Many operating steam generators or heat exchangers in process industries have been working for a long period of time, and because of this, aging related problems are emerging. The failure and degradation of steam generator or heat exchanger tubes could be accelerated because of aging. The tube damage mechanisms could also be aggravated as the tube material properties and environmental conditions are changed. Reference [1] gives steam generator historical world-wide tube plugging data for a number of nuclear power plants during the time span of 1976 through 1991. The data

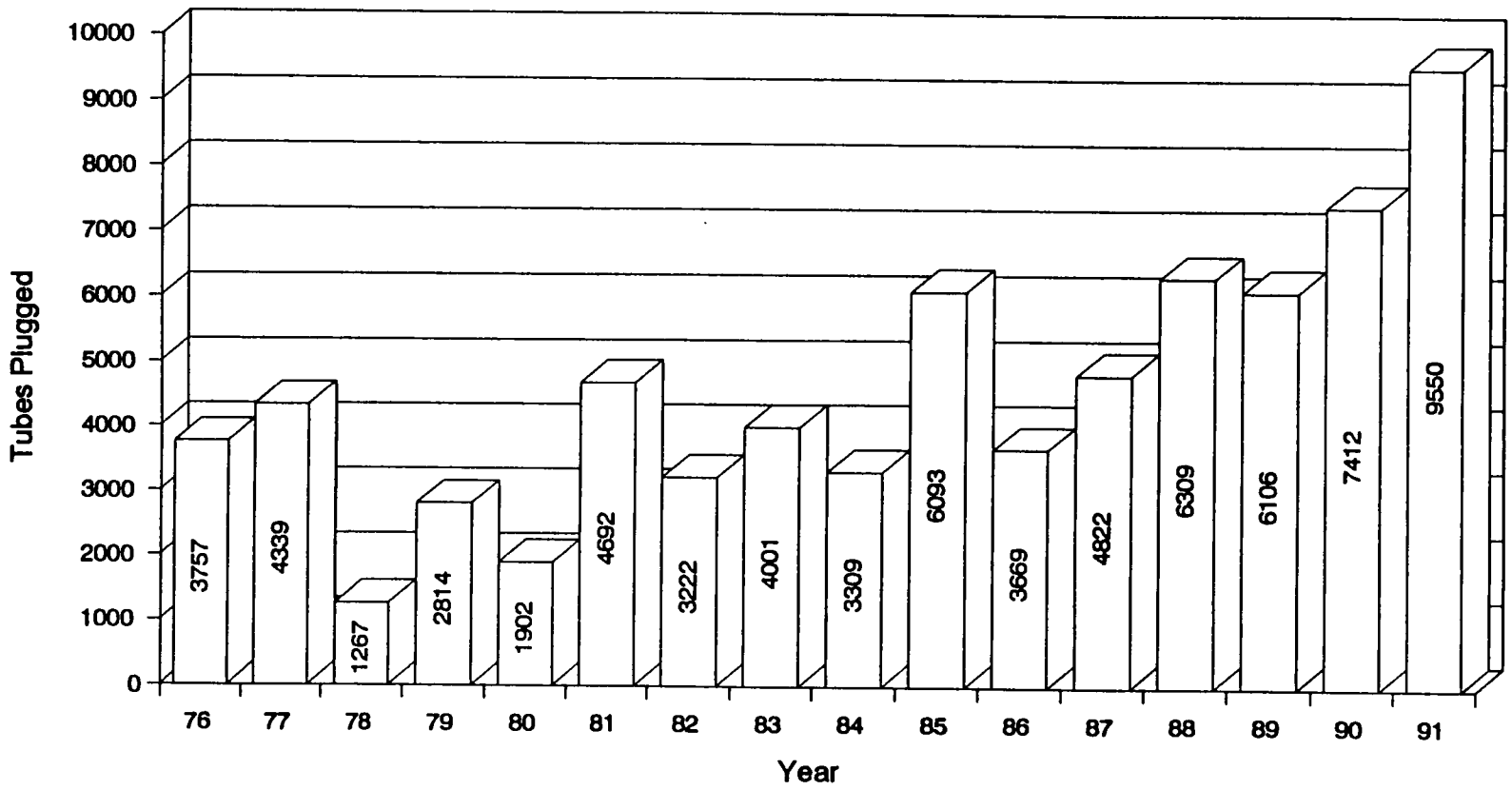


Figure 1.1: History of world-wide number of steam generator tubes plugged [1].

have shown a rapid increase in tube plugging rate since 1988. This indicates that problems related to aging and degradation in steam generators are increasingly affecting the performance of nuclear plants. To resolve these problems, a better planning is required, both for managing steam generator degradation and aging issues and for planning tube monitoring schedule. Indeed, in recent years (from 1986 to 1991) many U.S. nuclear power plants have reported a better cost reduction in the expenses of steam generator related problems than that during 1980 through 1984 [1] (see Table 1.1). This is primarily attributed to a more systematic and effective program for handling steam generator degradation problems. The cost reduction related to aging and degradation problems (of any plant component) can be substantially reduced by implementing predictive methods for the estimation of residual life or service life of components during their operation. The knowledge of service life or remaining life of operational components would improve system monitoring and maintenance procedures. This could benefit a plant in two ways:

1. Increase overall plant reliability.
2. Reduce the number of unscheduled outages.

It can also give a plant manager the opportunity to make qualified decisions (for taking maintenance actions at a suitable time) in the interest of plant production.

Although, in recent years much research and progress have been made in improving reliability of steam generators and heat exchangers, considerable work still remains to be carried out. Power outages due to steam generator problems do still occur in nuclear power plants [1]. Power industry could also suffer severe losses (case of accident) due

Table 1.1: Cost survey of steam generators used in the U.S. nuclear power plants ($ represents 1 million dollars) [1].

	U. S. YEARLY AVERAGES						SAVINGS	
	ACTUAL 1980-1984		TARGET 1986-1991		ACTUAL 1991		TARGET 1986-1991	ACTUAL 1991
LOST CAPACITY	NO.	COST($)	NO.	COST ($)	NO.	COST ($)	($)	($)
S/G REPLACEMENT	1.5%	$51	.5%	$17	.5%	$17	$34	$34
FORCED & EXTENDED OUTAGES	4.2%	$145	2.5%	$86	1.9%	$66	$59	$79
REPAIR & MAINTENANCE								
TUBE PLUGGING	2242	$5	2000	$4	5469	$11	$1	($6)
TUBE SLEEVING	3181*	$32	3000	$30	3351	$34	$2	($2)
RAD. EXPOSURE	4670 mr	$5	4000 mr	$4	6000** mr	$6	$1	($1)
STEAM GENERATOR REPLACEMENT	1.2	$120	.6	$60	.5	$50	$60	$70

* Revised (Second Millstone 2 sleeving campaign occurred in 1985 rather than 1984 as previously reported)
** Estimated

to unexpected failure of heat exchangers and steam generators. Therefore, it is necessary to develop methods and techniques to adequately estimate service or remaining life of a component much in advance of its failure time. In addition, the development of such methods could also show how long a component can satisfactorily operate if it survives beyond its design life limit. This is important for economic reasons, since retaining the existing component in operation will be more cost-effective than a premature component replacement.

This dissertation develops a methodology for the life assessment analysis of steam generator tubes subjected to a certain degradation mechanism. As a complex application of life prediction, the methodology is used to forecast the service life of a Once-Through Steam Generator (OTSG) tube degrading from fretting-wear damage mechanism.

1.2 Degradation Mechanisms of Nuclear Steam Generator Tubing

1.2.1 Common Tube Failure Modes

The degradation processes of nuclear steam generator tubing are usually divided into two broad categories: (1) chemical corrosion and (2) mechanical degradation [76]. In the former, the four modes of the tube degradation are thinning, pitting, primary-water stress-corrosion cracking (PWSCC), and intergranular attack/stress corrosion cracking (IGA/SCC). In mechanical degradation, the common modes of tube damage mechanisms are wear, fatigue, and impingement. Denting is considered as a potential

tube damage precursor rather than as a separate tube degradation process [42,76]. It usually assists the initiation of stress-corrosion cracking.

Corrosion related damage mechanisms are generally more common in recirculating steam generator units, whereas mechanical degradation processes are more dominant in once-through steam generators.

Fretting-wear damage mechanism, which is related to the subject of this study, is described in the following subsection. The description of other damage mechanisms are presented in Appendix A.

1.2.2 Fretting-Wear Damage Mechanism

Flow-induced vibrations in tubular heat exchangers and steam generators can cause dynamic interaction forces between a tube and its support. These interaction forces will lead to the wear of tubes with consequent reduced tube life.

Fretting-wear, which is one of the wear mechanisms, is common when a normal force acts on contacting surfaces between two bodies and thereby causes the two bodies undergo relative oscillatory sliding motion with very small amplitudes. It is a combination of mechanical, chemical, and other wear mechanisms such as adhesion, corrosion, and fatigue. This type of wear is very common in tubular heat transfer equipment where the oscillatory behavior of tubes causes periodical contacts between tubes and tube supports. Fretting-wear is considered as a very first tube damage mechanism which occurs in steam generators and heat exchangers. This is because of the existence of flow-induced vibration forces [3-12,17] from the time a steam generator

or heat exchanger becomes operational. Wear of steam generator tubes is usually associated with tube thinning which accelerates the initiation of cracks because of fatigue or other damage mechanisms. Therefore, it is important to predict the amount of tube wear before catastrophic or unanticipated tube failures occur during the operation time of a steam generator.

1.2.3 Industrial Impacts

The industrial impacts of the tube degradation mechanisms on the plants of three vendors of steam generators are shown in Figures 1.2 and 1.3. For the chemical degradation processes, stress corrosion cracking affects the largest percentage units of plant populations; with 41.2% for Westinghouse plants, 50% for Babcock & Wilcox plants, and 60% for Combustion Engineering plants (see Figure 1.2). Figure 1.3 indicates that wear and fatigue are the most dominant mechanical damage mechanisms in the plants of all three steam generator vendors. The affected plant population by wear for Westinghouse is 70.2%, for Babcock & Wilcox 87.5% and for Combustion Engineering 73.3%. Wear by itself does not contribute significantly in forced outages and tube plugging; however, it markedly accelerates the tube failures caused by fatigue and stress corrosion cracking.

A survey of industrial effects of tube damage mechanisms on the U.S. power plants are given in appendix A.

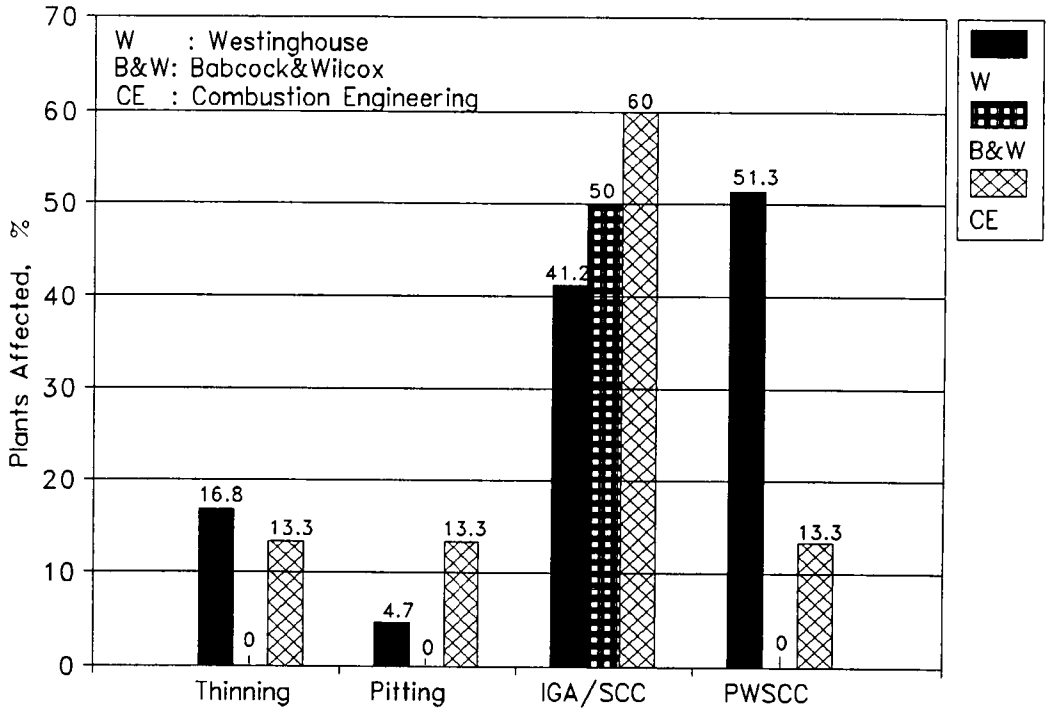


Figure 1.2: Effect of chemical corrosion degradation on the tubes of PWR steam generators [76].

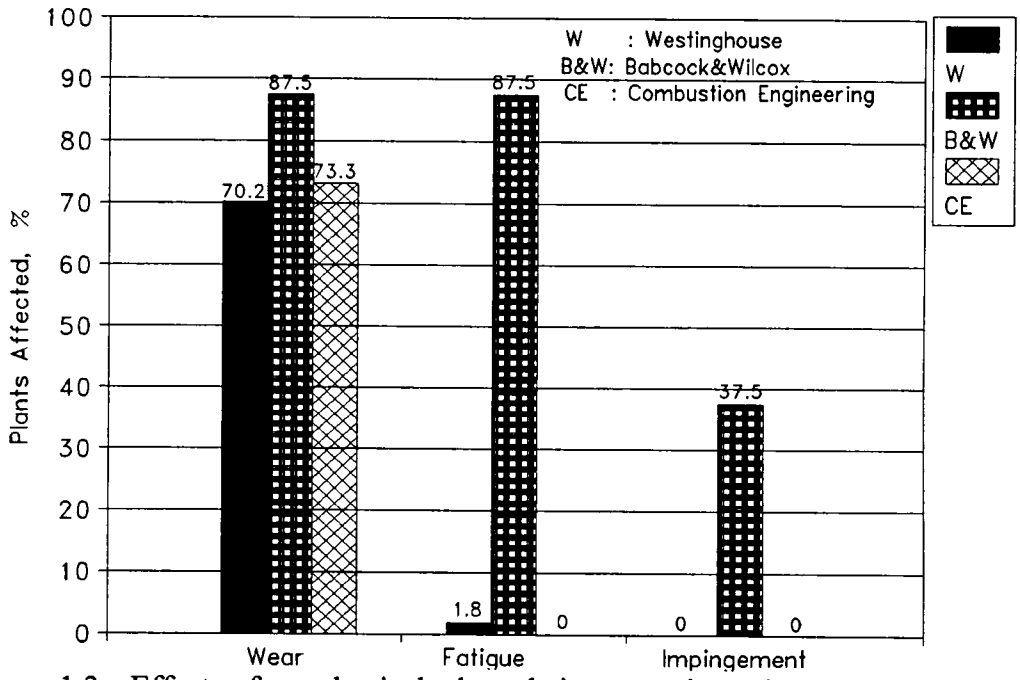


Figure 1.3: Effect of mechanical degradation on the tubes of PWR steam generators [76].

1.3 Statement of the Problem and Objectives

In recent years, there has been a growing need in the power plant industry to forecast the service life of aging plants and structural components which have been in operation for extensive periods of time. As mentioned in section 1.1, the potential benefits of a reliable life prediction technology are prevention of costly forced outages, increase of plant availability, establishment of inspection criteria and maintenance schedule, safe and reliable operation, and extension of plant operation life beyond the original design life.

In practice, however, there are two critical problems associated with the development of an accurate life prediction methodology. These are

- Availability of only limited amount of information regarding in-service condition of the component under study.
- Effect of material aging and degradation resulting from service exposure.

These problems are most acute in systems where service inspections are performed with a large time interval.

The literature review presented in Chapter 2 shows that the above problems have not been adequately addressed in the life assessment analysis performed by many investigators. Still, most available life prediction techniques depend strongly on statistical and/or a time series analysis of failure or lifetime data. To establish a more reliable life prediction technology, some investigators have emphasized the physics of failure and the degradation process and thus develop techniques for the life assessment of the component under study. However, many of these techniques are mostly suitable

for design life calculations since they assume standard material properties and the existence of design operating conditions.

The foregoing problems are implicated in the life assessment analysis of many power plant components including heat exchanger and steam generator tubing. For instance, a wealth of data and information on the service condition assessment of steam generator tubes requires either continuous monitoring or frequent post service inspections. However, this is not feasible for most industrial steam generators or heat exchangers. Continuous monitoring is practically impossible with today's measurement instruments. Frequent off-line examination and service inspection are not common practices in industrial plants either. This is because of obvious restrictions on the number of plant shut-downs and start-ups, reduced production and revenues, and the cost of service inspection process. For example, in a nuclear power plant the service inspection of steam generators is performed during the refueling cycle of the plant and has a cycle time of 12-18 months. Therefore, a large time interval between each service inspection does not permit the acquisition of sufficient data and information to merely apply time series or statistical techniques for forecasting purposes. Also, the lack of detailed information pertaining to material properties and actual service loadings over the life of the component does not permit to make a reliable estimation of service or remaining life from design calculation. These problems are quite evident especially for the wear of steam generator or heat exchanger tubes when the nonlinearities associated with tube aging and degradation complicate the correct identification of wear trends.

It is the purpose of this study to develop a methodology to estimate the service or

the remaining life of a typical Once-Through Steam Generator (OTSG) tube degrading from fretting-wear damage mechanism. In this approach, first a damage model based on the physics of the degradation process under study (wear of tubes) was developed to characterize the process trends as the tube ages and degrades over time. Then, the model was used in conjunction with available field data to construct semi-empirical models to predict future process trends and thus to determine the service life of the component with respect to a pre-defined allowable degradation (or alarm) level. The salient feature of the model is in its capacity to recognize the process nonlinearities and to identify the correct process trends which cannot be detected by mere applications of traditional forecasting techniques. This capacity greatly reduces the amount of required data for a good forecast. Therefore, the field data are mainly used to estimate or tune the model parameters and to improve the prediction.

Thus, the methodology combines a deterministic model of the tube wear process with the available process field data and information to assess the service or remaining life of tubing.

The tube wear process model was developed based on an elastic/plastic contact deformation model of tube-to-support interactions (see Chapter 4). It correlates the wear process with the tube-to-support contact forces resulting from periodical impacts between the tube and its support plate. It also incorporates factors or parameters which reflect the effects of aging and environmental degradation mechanisms on the process trends. The key role of the model is to identify the correct trends of the tube wear process so that the information pertaining to the process data is optimized for

establishing semi-empirical prediction models. The application of this model to the wear process of an OTSG tube within the upper tube support (15th) plate[1] was investigated in this study.

Semi-empirical prediction models were developed in both parametric and non-parametric forms. The parametric models establish mathematical relationships between the tube degradation and the tube operating time with a certain number of constant parameters. The general mathematical forms of the models were identified based on the characteristics of the process model[2] and the model parameters were estimated using regression analysis on the process field data. The extent and complexity of parametric models depend on the availability of statistically sufficient field data for the estimation of model parameters. This is an important issue in practical situations where a meaningful estimation of model parameters requires more data points than the number of model parameters. This is due to the fact that almost always field data are contaminated with measurement noise which can sometimes markedly affect the estimation process. This implies that complex prediction models, incorporating several parameters, should be used when more data become available. Improvements in the

---

[1] At this location, high cross-flow steam velocity causes tube wear more than at any other location.

[2] It is important to distinguish the difference between a process model and a parametric prediction model. A process model may not be explicitly expressible as a function of time. Examples of such a model are steam generator tube wear damage mechanism (see Chapter 6) and tube crack propagation [63-65] which are in closed mathematical form with respect to time. However, if a damage process model can be described as a direct function of time, it may also be used as a parametric prediction model.

prediction of the parametric models were also demonstrated by combining an empirical dynamic formulation of the field data with the models.

The artificial neural network methodology was applied as a non-parametric approach to estimate future values of the tube wear degradation process within a specified time-frame in an innovative manner. In this technique, backpropagation neural networks [80-84] were used to establish computational models for short term, intermediate, and long term predictions. The key issue in using such a technique is to prepare proper data sets for the training of neural network prediction models. The data sets should be large enough to cover a desired range of all possible paths of the tube wear degradation mechanism. In this study, the process model of the tube wear mechanism was employed to produce such data sets.

It should be emphasized that the methodology employed here to develop semi-empirical prediction models is in general a model-based technique by which a degradation process can be correlated with the component service or remaining life through extracting maximum information from the process data. The complete details of semi-empirical prediction models, both parametric and non-parametric (artificial neural network), will be presented in Chapter 3.

The other objective of this study is to perform a sensitivity analysis of the tube wear model in order to identify those parameters which have a greater influence on the tube wear behavior during aging and degradation of tubes over time.

The objectives of the proposed research were accomplished through the completion of the following tasks.

1. Development of a time-dependent tube wear model.
2. Identification of the wear model variables. This includes the characterization of material aging and environmental degradation processes, resulting from service exposure, on the dynamics of these variables.
3. Simulation of tube-to-support contact forces. This requires the development of a finite element vibration model of a multi-span tube. Parametric study of the contact forces were also performed to characterize the variations of the contact forces with the tube/support clearance.
4. Implementation of the methodology to the life prediction of OTSG tubes. This requires the integration of tasks 1, 2, and 3 in order to establish a process model for the characterization of tube wear trends over time. It also includes the development of semi-empirical prediction models to estimate the service life of tubes with respect to maximum allowable wear amount.
5. Simulation of uncertainties in the tube wear model. This study identified the impact of model uncertainties on tube wear trends.

1.4 Significance of the Study and the Contributions of the Dissertation

Although there has been a good amount of work on the wear process of heat exchanger tubes in recent years, there are several important issues which need to be

studied in greater details. In the literature, the wear process of heat exchanger tubes has been mainly studied from the viewpoint of design considerations (see Chapter 2). These studies provide useful design guidelines and give some insight into the parameters affecting the wear process. However, wear is a time dependent process and its characteristics can change over time due to aging and degradation of materials [63,71]. Wear literature on heat exchanger tubes does not present a method of estimating the tube wear rate from the viewpoint of aging and degradation of the tube material which is very important for a realistic tube life assessment. This study offers a model-based prediction approach by which the wear trends of steam generator tubes can be forecast from information optimization of the available tube wear data. The importance of this approach is that it does not require significant field data to obtain a good prediction of the process trends. This is due to the fact that the approach is developed based upon the physics of the wear degradation process (as described in Section 1.4); thus, the prediction process tends to be more deterministic in nature. The other significance of this work is that the proposed life assessment approach will be generic and applicable for any degradation or failure process which is as complex as the wear process or simpler. In fact, the application of the methodology to forecasting the performance degradation of steam generators, which is a simpler case than that of the tube wear process, has resulted in a very good and robust prediction as demonstrated in Chapter 3.

The original contributions of the dissertation research are the following:

1. Development of a model-based life prediction methodology. The

methodology includes the development of a tube wear model which can identify the dynamics of tube wear process (on an average) because of aging and environmental degradation of tube material over time. The wear model was combined with the analysis of field data (tube wear data obtained from eddy current testing) to formulate suitable prediction models for the tube life assessment analysis.

2. Development of non-parametric prediction models using artificial neural networks. The neural network models are trained with the data generated from the wear process model in an innovative fashion, and are then classified as short-term, intermediate-term and long-term prediction models.

3. Improvements in life prediction by introducing an empirical dynamic characterization of the field data in conjunction with the parametric prediction models. This will help to capture those dynamics of the process data which can not be modeled deterministically or a priori. It also helps reduce, to some extent, the impact of model uncertainties on the prediction.

4. The methodology developed in this research is generic in nature and may be applied to life assessment of both rotating machinery and stationary components.

The design data used in this study were acquired from reports and publications listed in the REFERENCES at the end of this dissertation. The material in chapters 3-6

are the original contribution of this dissertation. For a summary of the method used in this study, see section 3.2.

1.5 Organization of the Dissertation

This dissertation is organized in seven chapters and three appendices. Following an introductory chapter, a review of pertinent literature is presented in Chapter 2. Chapter 3 focuses on the development of a life assessment methodology for steam generator tubing. It also describes the procedures of developing semi-empirical prediction models using both regression analysis and artificial neural networks. Chapter 4 deals with the development of a tube wear model suitable for the life assessment analysis. Identification of the tube wear model parameters is also presented in this chapter. Chapter 5 describes mathematical simulation of contact forces due to vibratory response and tube/support dynamic interaction of a multi-span OTSG tube. A parametric evaluation of the contact forces is also performed in this chapter. Chapter 6 presents the implementation of the life assessment methodology for the tubes of an OTSG system. Residual life estimation and parametric sensitivity analysis are also presented in this chapter. Concluding remarks and avenues for future research are stated in Chapter 7.

CHAPTER 2

LITERATURE REVIEW

2.1 Introduction

The broad scope of the subject of this study required a literature survey in two major areas. In order to examine and evaluate the existing techniques for life assessment of engineering components it was necessary to review related literature on engineering reliability, life prediction, and failure analysis of such components. In the review, the focus of attention was to identify techniques for trend prediction of degradation processes, especially with a limited amount of process field data and information.

In order to investigate the current advances in the fretting-wear damage mechanism of tubular heat transfer equipment, it was necessary to study the pertinent literature on dynamic interactions between tube and tube supports in these equipment. The investigation also included the proposed models of tube life prediction due to wear degradation mechanisms.

2.2 Life Assessment Techniques

Life assessment analysis is the process of determining service life of a component with regard to its operation in a given environment. The analysis methods traditionally

fall into two broad categories: (1) probablistic approach and (2) dynamic approach. In the former, the analysis is established based on the underlying concept of system reliability [47-49]. The reliability of a system is defined as the probability that in a specified operational and environmental conditions a component or a system will perform its duty without failure for a given period of time [49]. This definition is fundamental for deriving other measures of life assessment and prediction such as failure rate, mean-time-to-failure, and hazard functions [48,62]. These probablistic quantities are employed to develop reliability and lifetime models for a data set of lifetimes obtained from a population of identical components operating under similar environmental and operational conditions. The validity of such models depends strongly on two conditions. First, to maintain the quality of lifetime data, the similarity of operational and environmental conditions must be preserved. Second, the data base must be statistically large enough to make meaningful inferences about the characteristics of the entire population. This is normally a more critical condition since its violation may introduce extensive model uncertainties.

The probablistic life assessment methodology has been applied in various engineering disciplines. Perhaps electronic industry has benefited and enjoyed this method more than any other industry. The reason is that electronic equipment and components (such as transistors, VLSI circuits, etc.) are sufficiently inexpensive and small so that large random samples can be tested to failure, relatively cheaply, under controlled environmental and operational conditions [48,49]. The other reason is that the nature of failure in such components tends to be more random and instantaneous.

This satisfies the condition of independent and identically distributed random variables for statistical analysis. Thus, it is possible to obtain excellent reliability data and thereby to establish relatively accurate life or failure models for such components, and these models have been published widely [47,48,62]. Experience has shown that these models provide reliable predictions of potential failures in practical applications. This is largely due to the fact that the real-world environmental and functional conditions are very similar to those of test conditions.

The use of probabilistic approach has also been successful for many electrical components such as electric insulations and cables [51].

The probablistic life assessment techniques have been applied to mechanical components and structures with some success. In these techniques, the reliability or useful life of a component is basically estimated via damage models of the component's failure modes. Notable example of mechanical failure modes are fatigue, creep, and wear. For instance in the case of fatigue, the traditional approach to life assessment analysis of a component has been the prediction of fatigue crack initiation lives [63,65]. A review of literature [51,63,64] indicates that in such methods, damage models or probability of failure functions are developed based on statistical inferences either on laboratory data or historical failure data. Experience shows that these models have relatively limited applications in real-world situations [63-65]. This is due to the very obvious fact that they require extensive amount of quality data to produce reliable life predictions. The problems associated with producing a large data base for mechanical components are as follows. The laboratory testing of mechanical components are time

consuming and expensive to operate and therefore it is not feasible to have a large sample of components to be tested to failure. Unlike electronic components, if not impossible, it is extremely difficult to simulate operating and environmental regimes similar to those of the real-world situations. Mechanical equipment is often subjected to wide ranges of operating stress and/or environmental variations (which may be quite unknown or random in some situations). For example, steam generators or heat exchangers may experience more thermal and mechanical stresses during transient conditions (temperature may vary rapidly) than during normal operating conditions. They may also operate at different environmental conditions. For instance, the intensity of chemical corrosion process in such components may vary over time because of operating environment. Therefore, failure models developed under controlled laboratory conditions may not always be applicable in practice. In fact, the literature review reveals that fatigue damage models developed for metallic materials in non-corrosive or benign environment are not generally valid for the same materials in corrosive or aggressive environment [63-65].

The other important issue is that many mechanical or chemical failures are not random or instantaneous in nature. Prime examples are fatigue, corrosion, creep, and wear mechanisms. These are of the gradual degradation type, and thus manifest their own physics of failure. Therefore, statistical and probablistic analysis may not always yield a correct physical damage model for a given degradation process especially with a limited amount of data. In fact, the current trends in developing models for fatigue crack initiation or propagation indicate that the use of physics of failure methods such

as fracture mechanics techniques is preferable to that of probablistic methods [63-65].

From the foregoing discussion and the literature review, it is clear that the lack of statistically sufficient failure data and information imposes serious constraints on the utilization of probablistic life assessment methods to real-world applications. Nevertheless, the ease of implementation (and sometimes as the only alternative tool) have encouraged many investigators to employ such techniques for various mechanical failure analysis, particularly for situations where the failure modes are either physically too complex to analyze or they are basically random in nature. Some probablistic or statistical failure, damage, and life models of mechanical degradation processes are described in References [17], [50], and [63-65].

Dominion Engineering company [50] performed statistical analysis on the steam generator tube degradation data (mainly for PWSCC and corrosion) to construct failure models as a direct function of time. They concluded that a cumulative Weibull distribution is most suitable for steam generator tube degradation analyses. However, many of these models resulted in overly conservative estimations of tube failures.

In an attempt to predict tube cracking in the upper regions of OTSG units, Davis et al [17] developed a high order damage model based on a combined engineering and probablistic analysis. The model results showed that both steady and flow-induced vibration stresses were major contributors to the tube cracking problems. However, a relatively large variance between the model prediction and the field data indicated that additional data were needed for a reliable estimation of the model parameters. The model also required an extensive amount of information about the steam generator

operating history for its analysis.

Liaw [55,56] developed a life prediction methodology for steam pipes which operate at elevated temperatures but in the sub-creep temperature range. He used the concepts of elastic-plastic fracture mechanics to formulate procedures for the remaining life prediction and inspection criteria of steam pipes. The methodology was employed to forecast the fatigue crack growth life of circumferential cracks in a steam pipe. However, its application was somewhat limited since it required a data bank to include the effects of variability of constants in the fatigue crack growth model. The effects of material degradation and aging resulting from service exposure were not considered in his analysis. His work, in general, demonstrated an excellent engineering analysis of steam tube failures at elevated temperatures which are mainly suitable for design calculations.

Simonen and Jaske [43] developed a computer simulation model to predict the damage to the tube material used in petrochemical heaters. The model was applied to forecast the service lives of tubes which operate at elevated temperatures and under sustained and cyclic loading conditions. It provided a more accurate estimation of the tube life prediction in comparison with that of traditional simple stress tube rupture models. However, its main drawbacks were the need for detailed descriptions of operating conditions throughout the tube life and the neglect of aging and material degradation effects. It also required extensive material data and information for the constants of the model.

Cohn [44] performed a comparison of tube stress and remaining life using a

multiaxial stress approach versus the traditional design approach of uniaxial stress. He investigated the combined effect of creep damage mechanism resulting from high temperature operation and multiaxial stresses because of loading conditions on the tube rupture life estimation. Based on this investigation, he concluded that rupture life based on the traditional design approach may be significantly optimistic at stress levels below 8 ksi. He also emphasized that frequent non-destructive examinations of the tubes were needed to obtain important information on fabrication defects, service-induced defects, and material conditions.

2.2.1 Dynamic Methods

In the dynamic method, the life assessment analysis is carried out by using the analysis of historical failure or lifetime data. The method dynamically trends the degradation process(es) responsible for the failure of a component with respect to a defined degradation level and thereby predicts the life of a component. The trending techniques are usually developed based on a time series of historical failure or degradation data because a time series represents a description of the past. This suggests that if a degradation process correlates well with its past history, then the past data are indicative of what we may expect in the future. Therefore, it is possible to postulate an underlying mathematical dynamic model that is representative of the process.

The life, degradation, or failure prediction models established in this manner are also able to capture the dynamic nature of change over time in a degradation process,

including trends in historical data. Depending upon the type of application, the models may be mathematically expressed as univariate or multivariate regression models [52,53].

Over the past three decades, dynamic and stochastic models have found a wide range of applications from signal processing to stock market forecasting. However, their applications to life assessment analyses have been somewhat limited. Perhaps the first practical application of dynamic models to life estimation is described in a paper recently published by Upadhyaya and his colleagues [53]. In the paper, the authors correlated the residual life of a component with its degradation modes via a multivariate dynamic regression model. This is defined as

$$Y(t) = \sum_{i=0}^{n} a_{1i}x_1(t-i) + \sum_{i=0}^{n} a_{2i}x_2(t-i) + \ldots + \sum_{i=0}^{n} a_{mi}x_m(t-i) + \theta$$

where x_i, i=1,2,..., m are the signatures derived from the data of the degradation modes, a_{ki}, k=1,2,..., m; i=1,2,..., n, are the model parameters, and θ is a bias term. They examined and evaluated the performance of the approach by fitting several dynamic models to the data obtained from experimental testing of small induction motors. The predictions of the models for the residual life estimations agreed very well with those of actual values. They also concluded that the inclusion of nonlinear terms in the dynamic models improved the prediction for their case study. This study particularly demonstrated that unlike probablistic methods, the dynamic approach does not necessarily require the knowledge of a component's population to perform life assessment analysis. This implies that the life assessment process is a system or

component specific.

While the above case study shows encouraging results, there are certain constraints that restrict the pure application of such models to life assessment analysis. These are:

1. Sufficient data for training of the models so that they can capture the process dynamics effectively.
2. Equally spaced time intervals in data.
3. No special rule to determine the optimal order of models (only by trial and error).
4. Usually suitable for a short-term prediction since the error introduced by the bias term may propagate into the prediction system.

Perhaps the first constraint is more critical in practice since the collection of a large amount of degradation or failure data in some equipment or components like steam generators is not always feasible as explained in Chapter 1. Therefore, the dynamic approach appears to be more applicable when sufficient data are available.

2.3 Fretting-Wear of Heat Exchanger Tubes

The study of fretting-wear damage mechanism in tubular heat exchangers has grown rapidly in recent years. Since this mechanism is caused by contact interaction forces between tubes and tube supports, many investigators [13,14,16,19-33] have conducted theoretical and/or experimental works to study these forces. The works of these researchers show that significant progress has been made in characterizing and in estimating these forces and their associated contact parameters such as area and time duration. Their works provide a good knowledge of tube contact parameters which are

quite essential for a reliable assessment of tube fretting-wear rate. A few researchers [5,14,15,29,30] have also tried to relate the tube-to-support dynamic interaction parameters to fretting-wear mechanism and thereby to estimate the service life of tubes. The following review summarizes their studies performed in this area.

Perhaps Ko and Roger [16] were the first researchers who conducted both experimental and analytical investigations of tube-to-support dynamic interactions for a prototype multi-span heat exchanger tube. The goal of their investigations was to primarily characterize factors influencing the interactions and subsequently to correlate them to the tube wear process. Although their work did not present a relationship to describe the tube wear rate as a function of tube-to-support dynamic interaction parameters (such as contact forces), they suggested that the trend of the tube wear process over time, obtained based on long duration tests, may be expressed as follows:

$$W = a\,t^{b} \tag{2.1}$$

where 't' is time and 'a'and 'b' are constants to be determined based on factors associated with tube-to-support interaction characteristics (such as contact forces), materials, and temperature.

Later, Ko and Basista [18] performed extensive experimental investigations to analyze the dependency of tube wear rate on tube-to-support interaction characteristics. Their investigations showed that the tube wear rate can be correlated with a force function 'F' that represents the integrated area of the force histogram of the shear force component of the contact forces. The authors observed that the application of this force function into the following relation produced good results that agreed well with the

experimental results.

$$\dot{W} = a F^{b} \tag{2.2}$$

where W is the wear rate and 'a' and 'b' are constants determined experimentally.

Pettigrew [5] also conducted a set of both experimental and theoretical investigations on the wear of heat exchanger tubes. Based on these investigations, he stated that the tube wear rate depends on normal and oblique forces and a sliding distance characterized by the dynamic interaction of tube-to-support. Thus, he suggested the following relationship which correlated well with his experimental results.

$$\dot{W} = A \left[\frac{1}{t} \int F_n ds \right]^{b} \tag{2.3}$$

where W is the wear rate, t is time, F_n is the normal component of the contact forces, s is the sliding distance, and 'A' and 'b' are constants to be determined experimentally. The author also supported the application of Equation (2.2) to the wear estimation of heat exchanger tubes.

A similar study was conducted by Fisher and his colleagues [30] for a multi-span steam generator tube. The study took into account the effects of contact parameters, namely: tube-to-tube support eccentricity, clearance, and preload on the amount of tube wear rate. They utilized the model of Equation (2.2) along with statistical analyses of these effects to calculate the wear amount. The results indicated that eccentricity and preload have the strongest effect on the wear rate. They also concluded that if tube-to-support clearance is increased by 100% the wear rate could increase by 10 percent.

Many other researchers such as Connor et al [37], Goyder and Teh [25], and Frick

et al [34] developed various tube wear models based on the Archard wear relationship [70,71]. It correlates a wear volume, V, with the normal force between the wearing surfaces, F, the sliding distance, S, and the empirical wear coefficient, K, as follows:

$$V = KFS \tag{2.4}$$

Connor [37] combined the above equation with the characteristics of tube-to-support contact forces to predict the life of tubes. Frick and his colleagues [34] modified the wear equation by replacing the normal force and sliding distance with a work rate term, W, to obtain a tube wear model as follows:

$$V = KWT \tag{2.5}$$

where T is total time. Goyder and Teh [25] characterized the tube wear in terms of tube-to-support impact rates, the tangential tube velocity, and a wear coefficient in a form similar to Equation (2.2).

It should be noted that the majority of the wear models proposed by these investigators are empirical in nature and the validity and applicability of them are yet to examine in practice. Nevertheless, the suggested models can be used to assess the service life of heat exchanger tubes if a value for an allowable wear amount is given. However, the life assessment obtained in this manner is mostly suitable for design purposes where it is assumed that standard tube material properties and design operating conditions exist. The assessment cannot be reliable if the interest is in the in-service life estimation of individuals which are subjected to aging process and different operating or environmental conditions. This is due to the fact that the existing tube

wear models do not consider the role of factors such as aging or environmental variations on fretting-wear damage mechanism. In fact, such factors can alter tube physical properties or tube-to-support dynamic behavior. For instance, the surface hardness or the surface roughness changes over time due to aging and degradation mechanisms resulting from corrosion and fatigue processes [63,70-72]. Tube-to-support dynamics can also change because of variations in tube/support clearances and due to the increase in tube-to-support eccentricity over time. The consequence of these changes leads to variation in the tube wear rate and thereby the life assessment of tubes. Therefore, it is necessary to develop a methodology which can adequately describe the effects of such aging and degradation processes on the tube wear damage mechanism.

In addition, the methodology should effectively make use of the process field data in order to update the models and to improve their predictions for a more realistic life assessment analysis. This is an important issue since in practice a damage process like wear may be involved with a number of unknown mechanisms that can not be characterized by a mere application of experimental and/or analytical investigations. This issue has not been addressed in the open literature and needs to be studied.

CHAPTER 3

METHODOLOGY FOR LIFE ASSESSMENT OF PLANT COMPONENTS

3.1 Development of Life Assessment Models

The assessment of the remaining or service life of a component requires a variety of data and information. The broad areas of data and information may be classified as damage mechanisms, loading conditions, strength of the component materials (against the damage mechanism) and environmental conditions. These data are used in a model of life assessment or damage accumulation (with respect to time) in order to estimate the remaining or service life of a component. The methods for developing models of life assessment or damage accumulation usually fall into three broad categories:

1. Those involving theoretical modeling, the acquisition of loading condition history, and the use of standard material data.
2. Those associated with post service inspection and testing that need direct access to the component for measurement and sampling.
3. Those based on probabilistic and statistical inferences using failure rate models which are usually developed for a population of similar individuals.

Approach (1) usually requires the knowledge of operational history, physics of the situation, and loading and environmental conditions. Since this approach is based on

the physics of the situation, it allows the life assessment process to be more deterministic in nature which is very useful for design purposes. However, it may not give a good prediction during the actual operation of a component since it depends on standard material data which can be different from actual data obtained from post service examinations. Approach (2) applies stochastic techniques and analysis to past data and experience in order to extrapolate or forecast future trends of the component life process. Since this approach ignores physical details of the system, a good prediction needs a large enough base of relevant data. This requires more frequent post service inspections and examinations. However, there are obvious restrictions on this matter from the point view of economy, production, and the number of shut-downs and start-ups. Approach (3) utilizes standard statistical lifetime distribution models for a class of individuals. The type of the model and its parameters are determined based on statistical and probabilistic inferences on a group of similar individuals. This method could give a general idea about the life assessment of a component. However, it may not give a reliable life assessment of a specific component. This is due to the fact that there may be several variables and conditions associated with one individual which is not true for another individual from the same class. Therefore, if there is a serious interest in the life assessment of each individual this method is not recommended.

The integration of methods (1) and (2) could result in a better approach for resolving the issue of life assessment analysis. The new approach has both the luxury of deterministic models (based on method 1) and the utilization of field data (used in

method 2). In this approach, the deterministic models developed for damage mechanisms or life assessment of a component must include certain parameters that reflect the effects of aging and environmental degradation processes that may occur during the life of that component. These parameters may have their own aging models which can be combined with the damage mechanism models. The complexities of the combined model (process model), specification of what parameters are to be regraded as known and unknown, and solution details of the unknown parameters depend on the amount of available data and information. In this approach, the primary task of the process model is to identify general trends of a process as accurately as possible. Then the engineering analysis of the characteristics of the process trends, in conjunction with the available (field) process data will be used as a formal basis for establishing semi-empirical prediction models. The semi-empirical models are developed using both parametric and non-parametric techniques.

3.2 Parametric Prediction Models

Parametric models are perhaps the most used and well-known paradigms in the analysis of lifetime data and in problems related to the modeling of aging, degradation, or failure processes. The key issue in applying parametric models to the prediction is to obtain a correct model type for the process under study. The identification of the model type may be acquired by purely empirical methods. Usually, several types of failure or lifetime models (for example; Exponential, Weibull, and Log-normal) are examined with the existing process data. Then, statistical analyses (such as residual

analysis, coefficient of determination, and hypothesis testing) on the models are used to select the best type of model that satisfactorily describes the distribution of the data. Also, graphical observations of data characteristics are used to decide about the choice of model. Such techniques usually need a large amount of data to ensure a proper type of model for a given application. It is obvious that for the situations where a limited amount of data is available, the type of model identified by these methods does not imply any correctness of the model. For such cases, the knowledge and information about the physics of the process can be utilized to obtain a correct type of model.

In this investigation, the engineering analysis of the physics of the process under study (here steam generator tube wear degradation) was employed to develop proper univariate parametric models where time is the only variable. The models were then used to predict the future trends of the process and thereby to forecast the remaining time left during which the related process component(s) may satisfactorily operate with regard to a prescribed degradation level.

The estimation of model parameters were obtained by using regression techniques on the existing process data. Therefore, the mathematics of the parametric prediction models is the same as that of the regression analysis, but the type of regression model depends on the engineering analysis of the process trends.

The major concern arising from this method is the impact of model uncertainties on the process trend prediction. The model uncertainties can result in a faulty prediction since they arise from incomplete knowledge as well as inaccurate characterization of the process trends. One way to minimize and offset their impacts is to combine the

model with a time series of historic field data. In a broad sense, this is a valid and scientific solution since most degradation mechanisms (including the tube wear process) are normally correlated with their past histories which can be described by a time series. This idea is also supported by the fact that the nature of these mechanisms is generally systematic and continuous with respect to time.

The inclusion of the past data into the prediction model may also offer another advantage. It can capture those dynamics of the process data which cannot be characterized or modeled by engineering analysis. This in turn will help to reduce the variance of the prediction error and thus help obtain a better estimation. It is obvious that the estimation will be improved as more field data become available.

Based on this approach, the following procedure is proposed for the life assessment of a plant component.

1. Develop a model of degradation process. The model can be mathematically represented in a general form as

$$U = F(\theta, X, t) \tag{3.1}$$

where U is a measure of progress in a degradation process, $\theta = (\theta_1,\theta_2,\theta_3,...,\theta_n)$ is a vector of model parameters, $X = (x_1,x_2,...,x_n)$ are model variables and t is time. For example, in the wear of steam generator tubes, U is the amount of tube wear or metal removed from the tube surface, θ is a wear rate coefficient, and $\{x_i\}$ are contact forces, contact time duration, tube materials properties, and a coefficient of friction.

2. Establish models for those model variables that change with aging and

degradation processes. This is given by

$$X = F_1(\alpha, U, t) \tag{3.2}$$

where $\alpha = (\alpha_1,\alpha_2,\alpha_3,...,\alpha_n)$ is a vector of parameters. It is always possible that variations in some model parameters depend on the behavior of the component degradation process. Examples of such a situation are tube-to-support contact forces and contact time which vary with the progress in the wear of tube at the tube support plate. In a tube wear process, the yield strength of tubes or contact forces can also vary because of material aging, fatigue, or environmental degradation mechanisms [63,66].

3. Combine steps 1 and 2 to obtain a general relationship for the degradation process under study. Thus

$$U = G(\beta, t, U) \tag{3.3}$$

where $\beta = (\beta_1,\beta_2,\beta_3,...,\beta_n)$ is the vector of final model parameters. This relationship implies that the combined relationship for the degradation process may have a closed form. Notable examples are tube wear process in heat exchangers and steam generators and fatigue crack propagation of materials [63-65].

4. Establish parametric prediction models based on the process model of Equation (3.3) so that the degradation process is described as a direct function of time. The prediction models are indeed univariate models where time is the only model variable. That is

$$Y = H(\gamma, t) \tag{3.4}$$

where $\gamma = (\gamma_1,\gamma_2,\gamma_3,...,\gamma_k)$ are constant parameters of the model. As stated earlier the type of model is determined based on the characteristics of the process model. However, it is sometimes necessary to compromise between the type of model and the amount of available data in order to estimate the model parameters. For example, complex models with a number of parameters may be applied when more data become available.

5. Apply regression techniques to fit the model to the existing process data. As described earlier, the estimation of Y can also include a time series of past data. This is expressed as follows

$$Y(t) = H(\gamma, t) + \sum_{i=1}^{m} a_i Y(t-i) + \theta \tag{3.5}$$

where Y is field data of the degradation process over time t, θ is the bias of estimation, and a_i, i = 1,2,...,m are the time series parameters. A least-squares minimization was used to estimate both the model and the time series parameters.

$$\min_{(\gamma, a_1, a_2, \ldots, a_m)} \sum_{k=1}^{N} [Y(k) - H(\gamma, t) - \sum_{i=1}^{m} a_i Y_i(k-i)]^2 \tag{3.6}$$

6. Finally, determine the anticipated useful life of the component under study by extrapolating its degradation process trends, obtained from Equation (3.5), to a defined allowable degradation level (or alarm level).

It follows from the above that a reliable life assessment methodology requires two

key components: (1) a correct trending technique (of degradation processes) and (2) an accurate definition of a permissible degradation level.

It is necessary to point out that the dynamic model described by Equation (3.5) usually produces very good results for a near future prediction. Such a model may not be used for a long term forecasting since the bias term 'θ' will propagate (sometimes with a large order of magnitude) into the model. Strictly speaking, such models are one-step ahead predictors since the bias term cannot propagate into the prediction system. However, if the root-mean-squared value of the bias is much smaller than the values of the process data, the model may be used as a few step ahead predictor as well. The choice value for the number of past data points 'm' depends usually on the application type and the amount of available data. As a rule of thumb, the value of m may be chosen from one to three. Care should be exercised in using a large value of m since as m increases more parameters have to be estimated[3] and also over-fitting of the data might occur.

Finally, it should be noted that the significance of the proposed approach is its ability to characterize systematic trends of a process without using an extensive amount of engineering modeling or detailed field data. This method is quite suitable for life or damage assessment of heat exchanger and steam generator tubes where usually limited field data are available.

---

[3] This is a potential problem when a limited amount of data is available.

3.2.1 Applications

To demonstrate the capabilities of the proposed methodology, two applications of the methodology are presented. The first is the forecasting of the performance degradation of steam generators. This case study simply and clearly demonstrates how the model-based methodology can be used to develop parametric models to predict the performance degradation of steam generators due to fouling effects. The author has also performed a more detailed analyses of this case study in Reference [54], including the effects of tube plugging events.

The second is the life prediction of steam generator tubes degrading from fretting-wear damage mechanism. The service and residual life of a typical Once-Through Steam Generator (OTSG) tube is predicted due to a fretting-wear mechanism that occurs at the 15th tube support plate. Since fretting-wear is considered to be one of the most complex tube damage mechanisms [15,16,63], the performance of residual life estimation methodology can be fully examined and evaluated.

3.2.2 Steam Generator Performance Degradation

The performance degradation of steam generators is usually defined as the drift of steam pressure over time because of fouling and/or tube plugging problems. Fouling in steam generators reduces the effective overall heat transfer coefficient between the primary and the secondary fluids. It results in steam pressure drops and consequently degrades the performance of such components. It is desired to forecast the future trends of steam pressure drop for a U-Tube Steam Generator (UTSG) unit which is faced with

the fouling problem.

To predict such a trend, the first step according to the proposed methodology, is to obtain a degradation model of the steam pressure. Engineering analysis of thermal-hydraulic processes in a steam generator can be employed to develop a relationship for the variation of steam pressure as a function of the overall heat transfer coefficient. This can be achieved either by analytical approaches (which could be quite difficult and tedious for a complex system such as a steam generator), or by a parametric study of thermal-hydraulic model of the steam generator[4]. In this study, such a relationship was developed based on a parametric evaluation of the UTSG steam pressure variations versus changes in the overall heat transfer coefficient. The result of the parametric evaluation is shown in Figure 3.1. It is realized that a quadratic function provides the best statistical fit to the trends of the steam pressure variations. Thus,

$$P = a_0 + b_0 U_n + c_0 U_n^2 \tag{3.7}$$

where P is the steam pressure deviation from the set point, U_n is reduction in the heat transfer coefficient (%), and a_0, b_0, and c_0 are constant parameters of the equation as shown in Table 3.1.

The heat transfer coefficient degrades over time as a result of tube fouling effects. The Fouling causes an additional thermal resistance to heat flow between the primary and the secondary fluids in a steam generator unit. Fouling models are mainly characterized based on the growth of deposit thickness and/or thermal resistance

---

[4] The UTSG model of Reference [91] was used in this study.

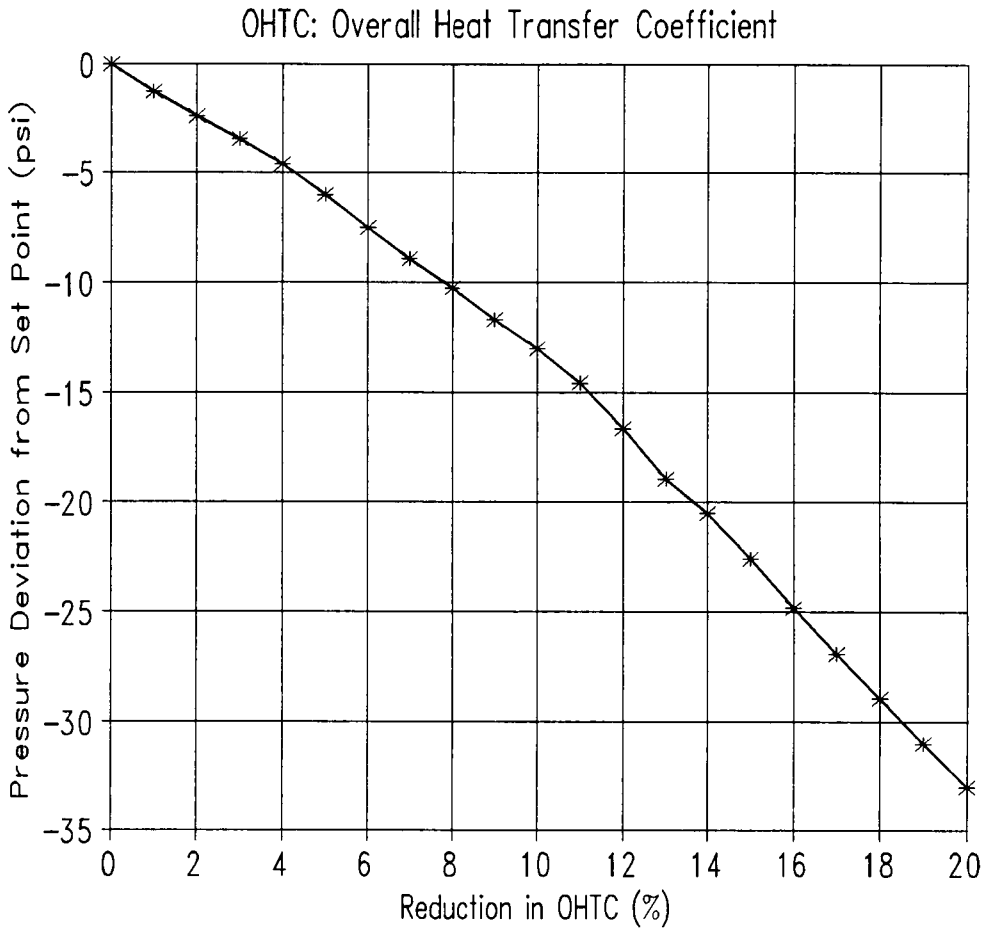


Figure 3.1: Variations of a UTSG steam pressure versus percentage reduction in the overall heat transfer coefficient.

[88-90]. The growth model of thermal fouling resistance with respect to time is often described as an exponential function [88-90]. The model is defined as:

$$R_f(t) = R_{f\infty}(1-e^{-t/\tau}) \tag{3.8}$$

where

R_f = Thermal fouling resistance (hr-ft^2-°F/BTU)

$R_{f\infty}$ = Final thermal fouling resistance

t = Time

τ = Time constant calculated from the experimental data.

The integration of the above equation with the heat transfer coefficient relation results in the following relationship (see Reference [54] for details):

$$\frac{U_f(t)}{U_0} = \frac{1}{1+U_0 R_{f\infty}(1-e^{-t/\tau})} \tag{3.9}$$

where

U_f = Fouled overall heat transfer coefficient

U_0 = Clean overall heat transfer coefficient.

Table 3.1 presents typical values of the constant parameters of the above equation.

The value of U_0 (approximately, 2000 btu/hr-ft^2-°F) is usually a known quantity and it does not change significantly with time. The quantity R_∞ does not exceed 1.5×10^{-4} (hr-ft^2-°F/btu) for nuclear steam generators. Therefore, it is expected that the value of

Table 3.1: Values of constant parameters of steam pressure model and the overall heat transfer cofficient equation.

Equation Number	**Parameters of the Equation**	**Root Mean Squared Error**
(3.7)	a_0 = -0.198 b_0 = -1.0473 c_0 = -0.0311	0.225
(3.8)	$R_{f\infty}$ = 1.5e-04, τ = 32	----------
(3.9)	$R_{f\infty}$ = 1.5e-04, τ = 32, U_0 = 1960	----------

$U_0 R_\infty \leq 0.3$. If Equation (3.9) is expanded in a converging series[5], the following relation can be approximated by neglecting terms of order greater than one (this is fairly a good approximation since $(U_0 R_\infty)^2 \leq 0.09$).

$$\frac{U_f(t)}{U_0} \cong 1 - U_0 R_{f\infty}(1 - e^{-t/\tau}) \tag{3.10}$$

The above equation is combined with the steam pressure model to derive a time dependent degradation model of the steam pressure as follows (step 3 of the methodology).

$$\begin{aligned} P(t) &= a_0 + b_0 x(t) + c_0 x(t)^2, \quad \text{where} \\ x(t) &= 1 - U_0 R_{f\infty}(1 - e^{-t/\tau}) \end{aligned} \tag{3.11}$$

The historic data of the steam pressure variations can be used to estimate the constant parameters of the above model. However, the estimation process can be complex and cumbersome if the values of τ and $R_{f\infty}$ are not known[6]. Note that the values of τ and $R_{f\infty}$ are to be estimated by heat transfer evaluation of the fouling process in the steam generator. This usually requires visual inspection of a typical fouled tube in a steam generator, eddy current examination, and laboratory testing of the deposit materials. Thus, it is possible that the values of τ and $R_{f\infty}$ are not always available. In this case, some simplifications should be performed in Equation (3.11) in

---

[5]For $x<1$

$$\frac{1}{1+x} = 1 - x + x^2 - x^3 + \ldots + x^n$$

[6]In this case the estimation of parameters requires a non-linear least squares technique with a possibility of having a non unique solution.

order to facilitate the estimation of parameters. A second order expansion of $\exp(-t/\tau)$[7] reduces Equation (3.11) to

$$P(t) = \alpha_0 + \alpha_1 t + \alpha_2 t^2 \tag{3.12}$$

where parameters α_0, α_1, and α_2 are easily estimated by a linear-least squares technique. In this equation the values of τ and $R_{f\infty}$ along with other parameters (a_0, b_0 and c_0) are integrated into parameters α_0, α_1 and α_2. Thus, the steam pressure degradation model described by Equation (3.12) does not directly require the knowledge of τ, and $R_{f\infty}$.

A time series of the historic field data of the steam pressure can be combined with the above model to improve the prediction and to capture those dynamics of the steam pressure process which cannot be characterized by engineering analysis. This is described as

$$P(t) = \alpha_0 + \alpha_1 t + \alpha_2 t^2 + \sum_{i=1}^{m} a_i P(t-i) + e \tag{3.13}$$

where e is error of prediction and $\{a_i\}$ are constant parameters.

The prediction of future trends is obtained in two ways. In the first scheme, just the steam pressure model described by Equation (3.12) was used to fit the process data. The variance of the fit and a future prediction of the steam pressure variation are shown in Table 3.2. In the second scheme, Equation (3.13) with n=2 (P(t-1) and P(t-2)) was applied to forecasting. As shown in Table 3.2 and Figure 3.2, the model provides a more accurate estimation of the future prediction and a better approximation of process

---

[7]This is a good approximation if $(t/\tau) \leq 0.6$, which is usually the case for steam generators.

Table 3.2: Time dependent models of the UTSG steam pressure.

Model	Mathematical Representation	σ^2	One Point Prediction	Actual Value
1	$P(T) = 0.174 - 3.23T - 0.033T^2$	1.85	-27.90	-28.50
2	$P(T) = 0.645 - 5.0T$ $0.55T^2 - 0.6847P(T-1)$ $1.3382P(T-2)$	0.17	-28.1	-28.50
3	$P(T) = 0.403 - 3.467T$	2.23	-27.1	-28.50
4	$P(T) = 1.416 - 4.451T - 0.279P(T-1)$	2.05	-27.9	-28.50
σ^2 = Variance of error for the 9 data points used in the model				

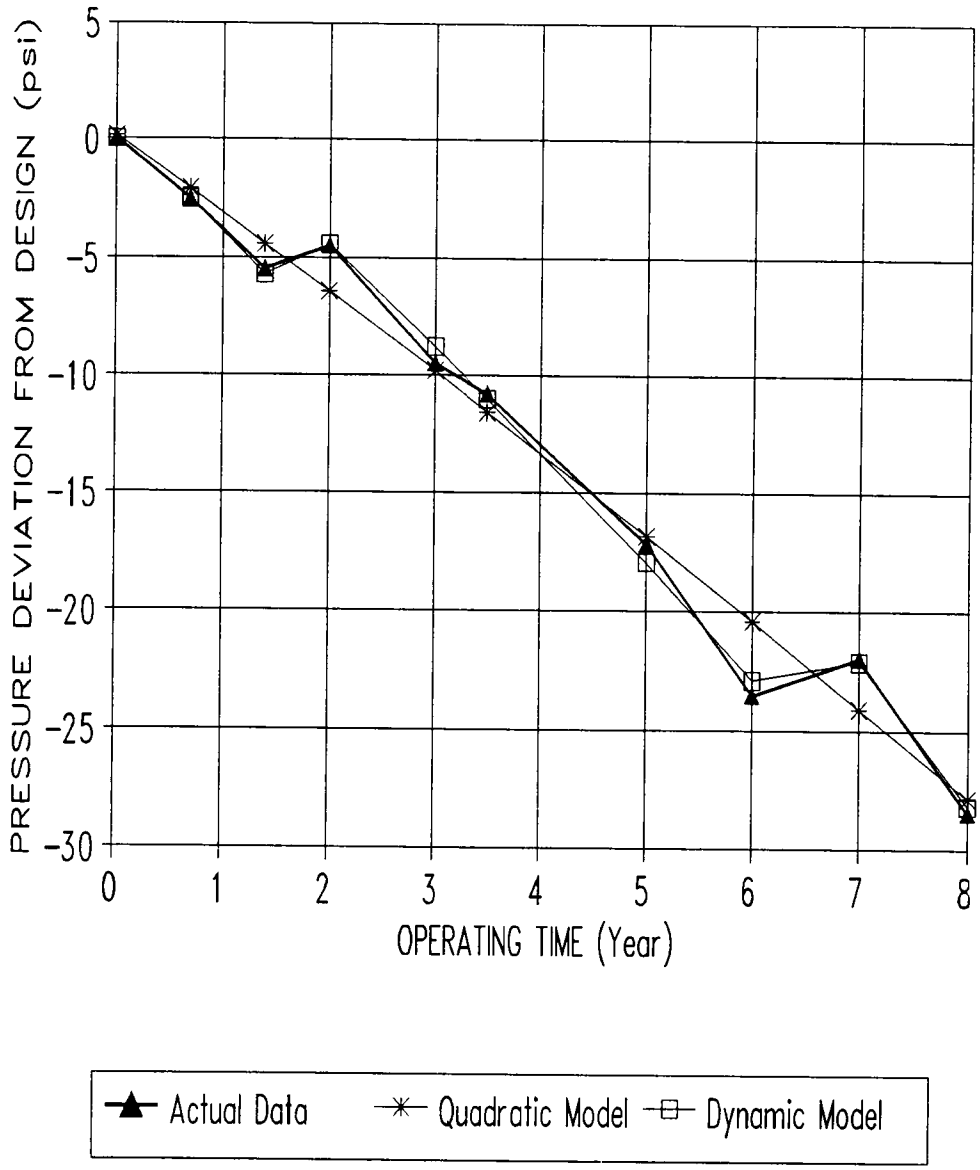


Figure 3.2: Trend prediction of the steam pressure variations using both a quadratic and a dynamic regression models.

trends in comparison with the results of the first scheme. This shows the dynamic model is able to adequately explain the nonlinearities of the process trends and thereby produce more reliable and accurate results.

Given the maximum allowable steam pressure drop, either of these schemes can be used to determine the remaining time that the steam generator is able to function satisfactorily.

A simulation of model uncertainty is also performed. The uncertainty is introduced as errors in the modeling of steam pressure degradation process. It is assumed that the steam pressure varies linearly with time rather than quadratically. Thus a linear model is fitted to the steam pressure process data to estimate the trends of the process. Table 3.2 presents the model parameters, the variance of fit, and the prediction of a future value. The model predictions are also plotted in Figure 3.3. A comparison between the results of the linear and the quadratic models indicates that the linear model is less accurate in estimating the steam pressure variations. However, by adding a dynamic term to the model (model 4 of Table 3.2) a more accurate prediction of the trend is obtained as shown in Table 3.2 and Figure 3.3. This shows that the inclusion of a time series of the process data with a prediction model can reduce the effect of model uncertainties to some extent.

3.2.3 Life Prediction of Steam Generator Tubes

The fretting-wear mechanism is one of the major damage mechanisms of heat exchanger and steam generator tubing (especially at the beginning of their service life)

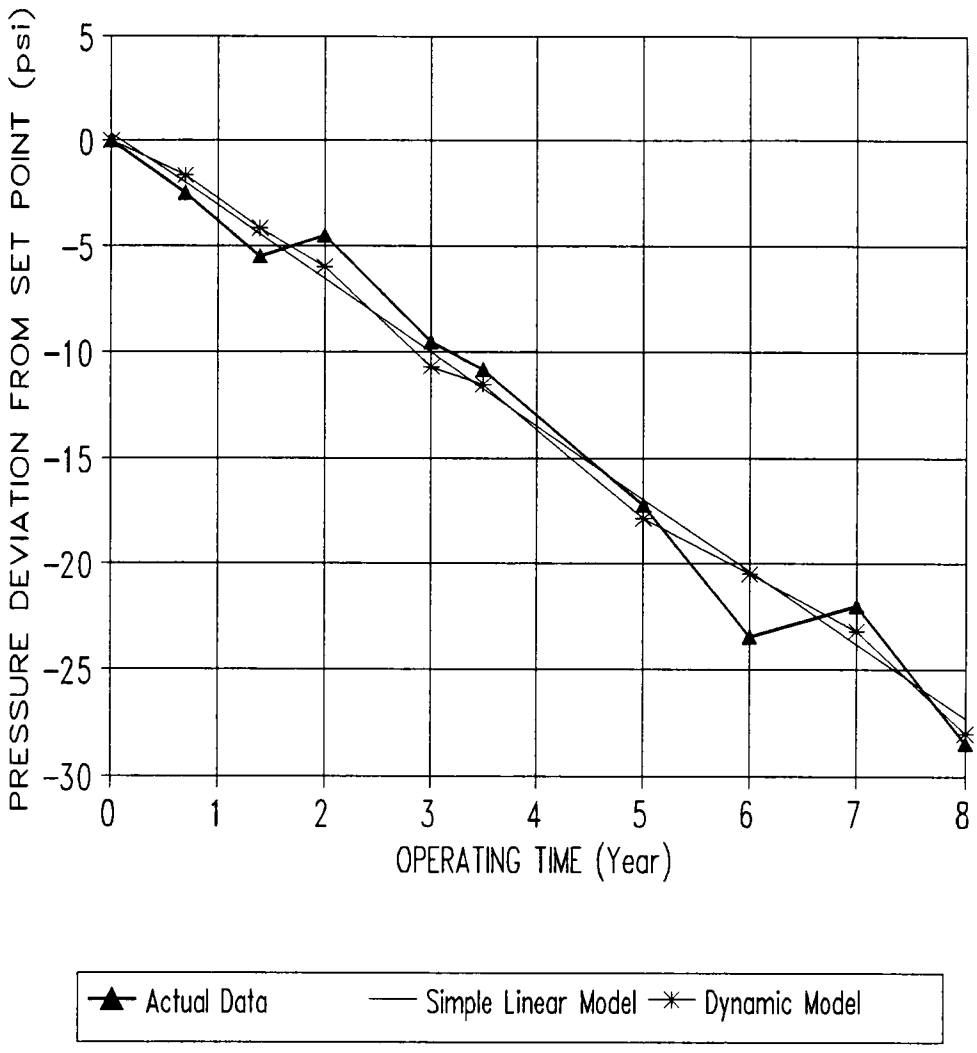


Figure 3.3: Trend prediction of the steam pressure deviations using both a simple and a linear dynamic regression models.

[1,5,9,15]. Prior knowledge and experiments on fretting-wear mechanism confirm the dependency of this mechanism on loading conditions, tube-to-support contact area, contact time, and contact surface conditions (such as roughness and hardness) [63,16]. To characterize the role of these variables on the tube wear process, a wear model of heat exchanger tube must be first developed as required by the proposed methodology. This will be performed in Chapter 4. Then, the behavior of model variables due to aging and degradation process must be investigated according to the second step of life assessment procedures. This may require additional model development and analysis. However, considerable attention must be paid to the variables that significantly influence the tube wear process.

One of the most important variables in the tube wear process is the contact force between a tube and its tube support. In a steam generator these forces are developed by flow-induced tube vibrations causing dynamic interactions between tubes and tube supports. In fact to a large extent, the magnitude and the duration time of such forces are the primary factors which are responsible for the wear of tubes. The characterization of these factors depend upon several parameters such as tube modulus of elasticity, support stiffness, tube excitation frequency, tube/support clearance, and misalignment between tubes and tube supports. A parametric study could reveal the trends in the variation of contact forces versus the variation in such parameters. Some of these parameters could also change over time because of environmental and/or mechanical degradation. For instance, the mechanical wear of a tube within its tube support or tube thinning due to chemical corrosion increases tube-to-support clearance

which consequently varies the contact forces and the contact time. Experimental or theoretical models are usually available to describe the changes of such parameters over time (for example, models of chemical corrosion tube thinning of steam generators). The integration of these models with the results of the parametric study will give a time dependent relationship which describes the changes in the contact forces as a result of aging and degradation processes.

The other variables of tube wear model such as the friction coefficient and the strength of tube materials may also change with aging and degradation. Previous research and investigations regarding the characteristics of these variables should be utilized to develop or establish aging models for such variables. The integration of these models with the fretting-wear model will result in a time varying wear process model, suitable for the life assessment analysis (see Chapter 6).

Given the allowable wear amounts and tube wear field data, the model can be utilized to construct parametric prediction models for the estimation of the remaining or service life of tubes during the operation of a steam generator. The flow chart of this procedure is shown in Figure 3.4. The overall procedure is somewhat similar to that described in section 3.2.2.

3.3 Non-Parametric Models Using Artificial Neural Networks

3.3.1 Introduction

Over the past decade, Artificial Neural Networks (ANNs) or computational neural networks have been applied with success to a variety of problems. The general

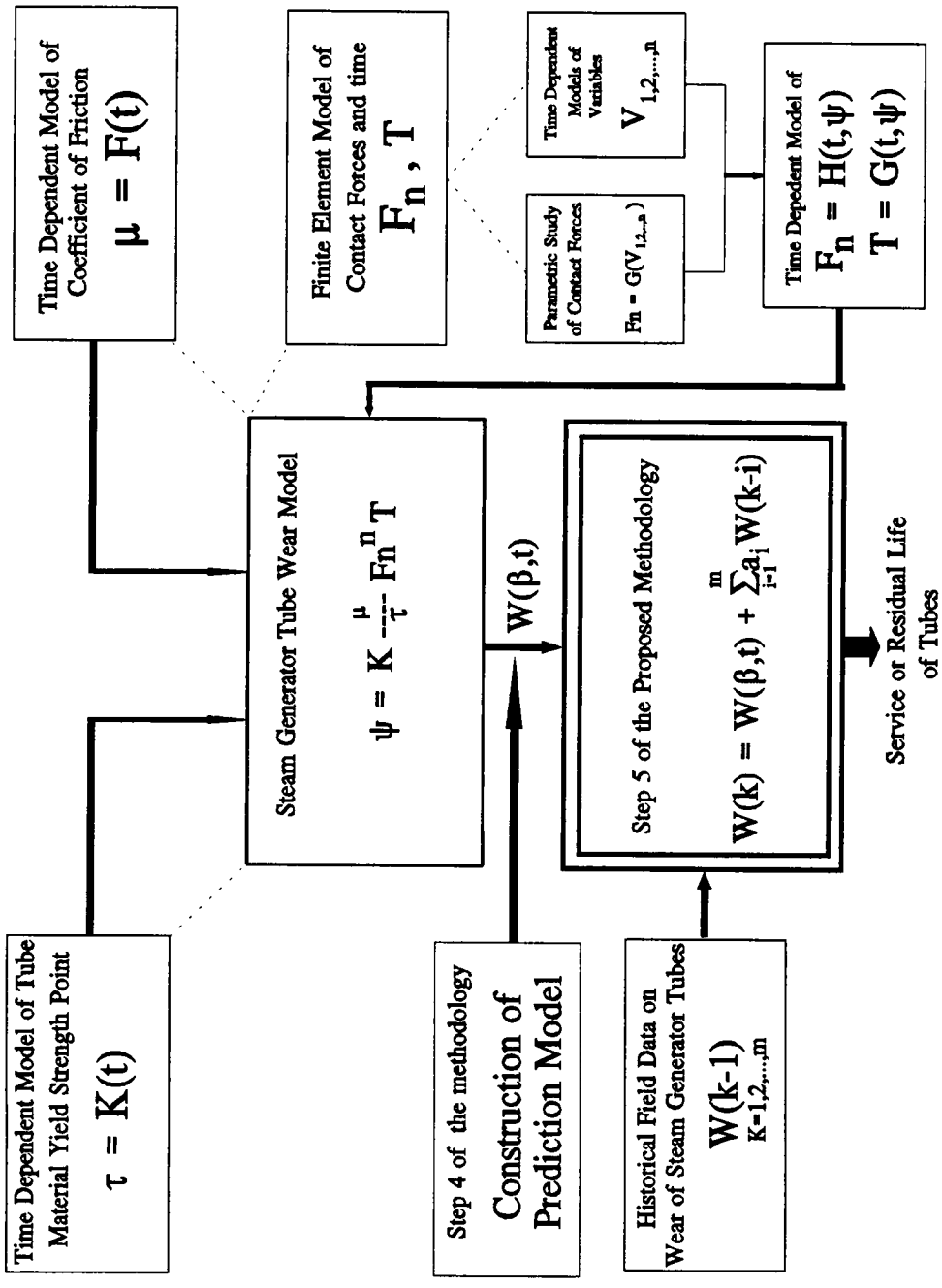


Figure 3.4: Flow chart showing a life assessment procedure of steam generator tubes due to the wear mechanism.

applications of ANNs span a wide range of domain including pattern recognition, data and signal processing, pattern mapping, data compression, and speech recognition. For some of these problems, ANNs provide a powerful alternative to classical computing methods which may not perform very complex well for nonlinear systems. Notable examples are speech recognition and pattern classification and recognition.

The prime advantage of neural networks is that they generate their own models between input and output variables through learning from known examples or patterns. This feature differs them from traditional computing techniques that require a priori information or a specific form of model of the relationship among input/output variables. Other advantages are: prediction from incomplete data, robustness, and fault tolerance.

In this study, a non-parametric methodology based on ANNs is used for the prediction of steam generator tube degradation process. Prior to the description of the approach, a brief explanation of ANN paradigm is presented. Further details of ANNs are available in many publications and literature [80-84].

3.3.2 Artificial Neural Networks

Artificial neural networks are non-parametric computational models developed from a desire to mimic or to emulate the very basic functions of biological nervous systems. A typical neural network model is composed of a large number of Processing Elements (PEs), analogous to the biological neurons, and operates in a massive parallel distributed processing architecture. A processing element performs a weighted sum of the input

elements and thresholds this sum using a nonlinear activation function. The PEs are arranged in layers or slabs which are fully or randomly interconnected to other PEs in adjacent layers by link with variable weights. A multi-layer neural network consists of a sequence of layers starting from an input layer and ending in an output layer. The input layer receives external input vector values and the output layer presents the responses of the network to such input values. Layers located between input and output layers are known as hidden layers. Hidden layers provide the capability to perform complex nonlinear mapping between the input and the output variables. A typical multi-layer neural network is shown in the Figure 3.5.

The operation of ANNs includes two phases: (1) learning and (2) recall. In the learning phase, the network is trained with a set of known patterns which contain both inputs and their corresponding (desired) outputs. During this phase, the connection weights associated with each PE are adjusted by a learning algorithm so that the generated network response reaches the desired output with a minimum error. The training time depends usually on the complexity of the application, the architecture of the network, and the training algorithm. Presently, there is not specific rule that defines the required training time.

In the recall phase, the performance of the network is examined and evaluated by presenting the inputs of unseen patterns (not used in training) to the network. If the network generates responses that match closely to the outputs of the patterns (with similar error rate found for the training patterns), then the network has learned the relationship(s) between the inputs and outputs of the entire patterns. Several trials on

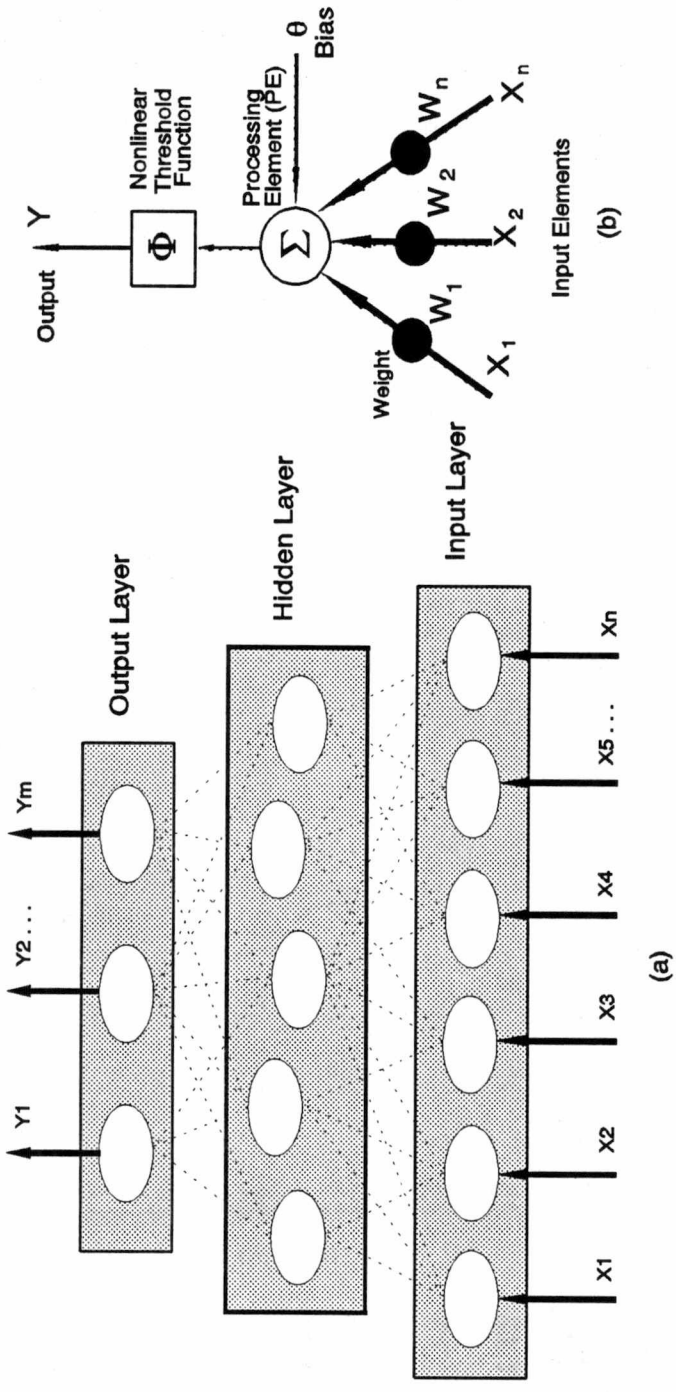


Figure 3.5: Typical structure of a multi-layer artificial neural network.

both the network structure and the amount of training time may be required to obtain a suitable network for a given application.

There are many types of neural network architectures: Hopfield, Kohonen self-organizing feature map, counterpropagation, and multi-layer perceptron with backpropagation training algorithm. However, in various applications (from finance to engineering), backpropagation networks (BPNs) have been favorably used over other networks. The inherent ability of back- propagation networks to form arbitrary complex nonlinear decision boundaries enables them to solve many complex problems [80-82]. In addition, they possess many other features such as supervised learning, nonlinear pattern mapping, ease of implementation, and good performance reported by many investigators. They are also available in many commercial software systems. Based on these features, backpropagation neural networks were utilized for the application in this study. A detailed description of BPNs and other neural networks are available in the literature [80-83].

3.3.3 Neural Network Methodology for Predicting Steam Generator Tube Degradation

The first step in applying neural networks to a given application is to assess the amount of required data for network training. The training data set should be large enough to cover a desired range of possibilities. For the case of predicting degradation processes of steam generator tubes, the networks have to be trained with a variety of tube degradation data, systematically collected over a long period of time, in order to create accurate and meaningful neural network prediction models. This type of data

should be normally supplied via power utilities or industries dealing with steam generator problems. However, real-world databases for such an application either currently do not exist or contain very limited amount of information [42]. In this situation, the required data may be generated based on the simulation models of the physics of tube degradation processes.

The models of tube degradation processes are usually developed by analytical and/or experimental techniques either in closed or in direct mathematical forms. The mathematics of the models describes the general trends of the process and the values of model parameters characterize the process trends of a specific component (for example a steam generator tube). For a typical steam generator tube a range of values of the model parameters are established rather than their exact values. Nuclear steam generator tube failure analyses indicate that this range could be relatively large from one tube to another [42,88]. Using this range of values in the tube degradation models, it is possible to generate a sufficiently large database to encompass all possible tube degradation trajectories (paths) that may occur during the life of a given tube. Figure 3.6 illustrates a hypothetical region that a given tube degradation process may belong to. This region includes many paths which characterize the progress of tube degradation with time.

The data generated in this manner can be processed in many ways for training different neural network prediction models; e.g, short-term, intermediate-term, and long-term. The training data set includes many patterns acquired from the tube degradation paths. Each pattern contains both input and output vector variables. The input

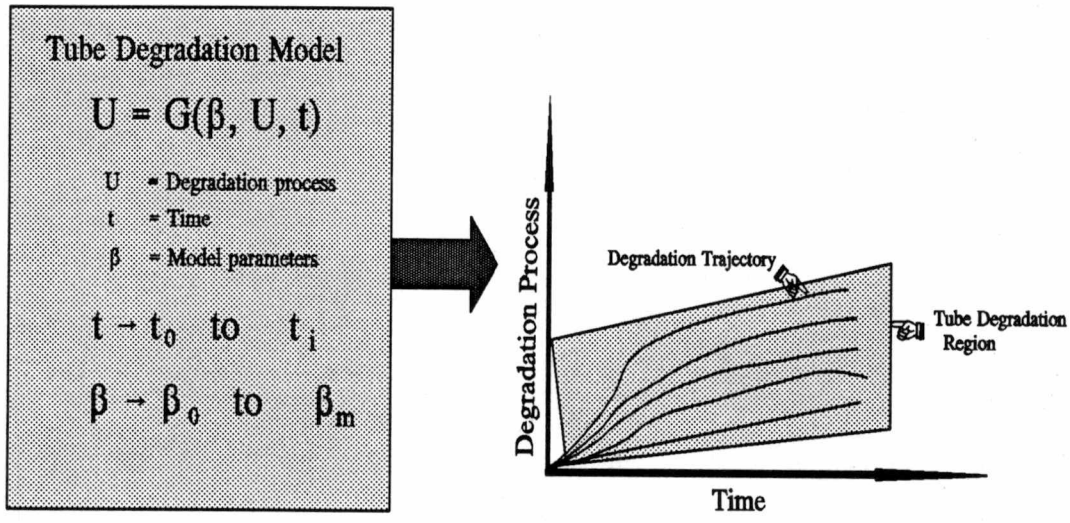


Figure 3.6: Schematic diagram of a hypothetical steam generator tube degradation region.

variables are composed of the historic values of the tube degradation within a specific time-frame and some of their mathematical properties. The time-frame of the input vector spans from the current time to a few points back in time with equally spaced time intervals. The size of this time-frame depends on the type of a desired prediction model or the amount of available data. The data properties considered in this study are the area under the input values and the degradation rate from one input to another which is determined as the difference between two inputs. These properties provide information about the data characteristics which represent to some extent certain dynamics of the data. Therefore, the inclusion of these properties in the input vector may offer two major advantages:

(1) improve the training phase of the neural network since more information is utilized for pattern recognition and classification.

(2) enhance the prediction since the characteristics of the data are regarded as additional input signatures which may compensate to some degree for the uncertainties associated with the process model.

The output vector contains the predicted values of the tube degradation which are arranged with equal time steps. The number of output elements depends on the type of the desired prediction model. For, example, if the output vector contains 3 elements, the prediction model may be classified as a short term. In this study, an *n*-point Neural Network Prediction (NNP) model is composed of *n* elements in the output vector and

$n+m$ elements in the input vector[8], where m corresponds to the number of data properties. Based on this convention, for instance, a three point prediction model takes 3 historic data points plus 2 values of data properties of a given tube degradation process (e.g, wear) and forecasts the next 3 future values of the process. Figure 3.7 shows the schematic diagram of the neural network approach for the construction of a typical non-parametric prediction model.

The neural network prediction (NNP) model constructed in this manner can be used to forecast the real degradation process of steam generator tubes. This is due to the fact that the model is trained based on the data generated from the physical models of a tube degradation mechanism and some features of the data. The data also encompass all possible trajectories of tube degradation trends. Therefore, if the physical models of the process adequately describes the general trends of the real-world data, it is expected that the NNP models provide a plausible forecast of the process trends.

3.3.4 Rationale

There are several reasons that encourage the application of NNP models to the life assessment analysis. They are:

(1) NNP models may produce a more reliable prediction than parametric models when a limited amount of real-world data is available. This is due to the fact that NNP models have learned to emulate the physics of the process via training. Thus, when a

[8] Via experimental procedure, it was found that this type of structure provides a sufficient length of prediction with a good accuracy for the applications of this study. Note that in general this can be different.

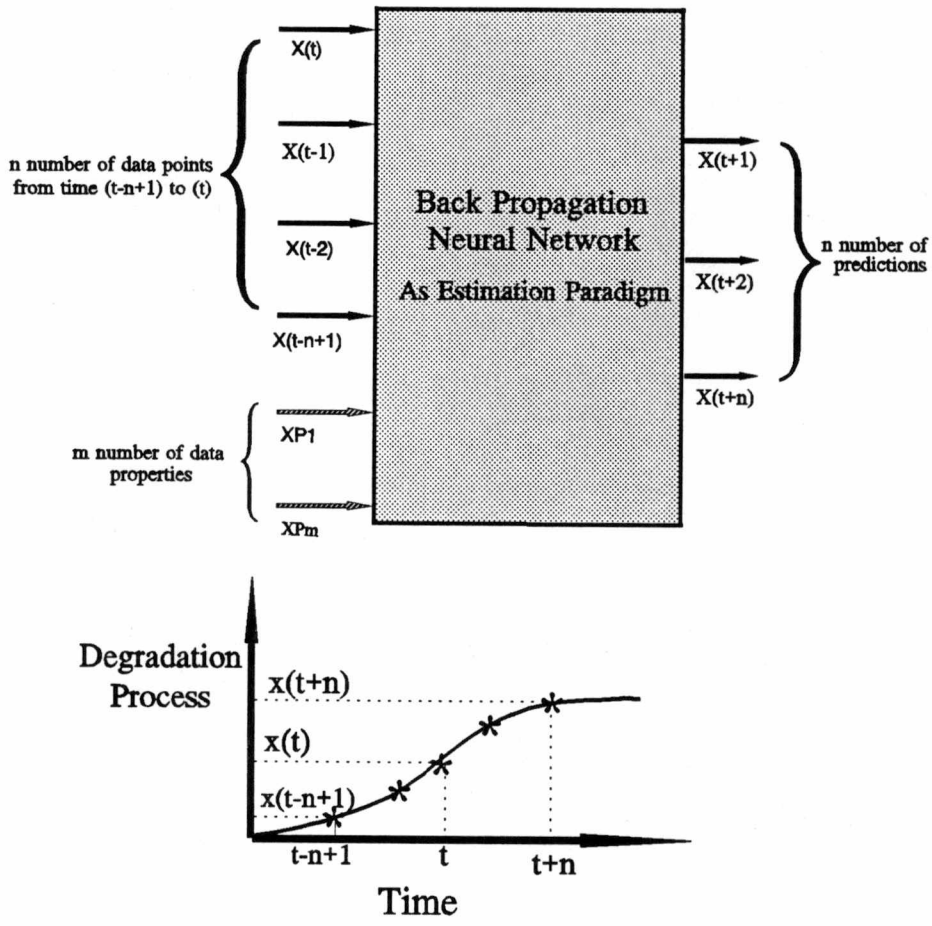


Figure 3.7: Schematic diagram of a typical non-parametric prediction model using artificial neural networks.

portion of the data is presented to them, they are able to perform an intelligent data mapping to match the trends of the data to one of the learned process trajectories and thereby to forecast the future values of the process trends. However, this may not be the case for regression or classical models. In the regression models even if the functional forms of the models are known, the estimation of model parameters would require statistically sufficient data.

(2) NNP models are fault tolerant and thus measurement noise should not affect their performance as much as those of classical models.

(3) NNP models can be trained once and used for a class of tubes subject to the same degradation mechanism. However, classical prediction models may require the estimation of model parameters for each individual tube.

(4) NNP models are especially suitable for cases when the degradation (process) models are mathematically in closed form (e.g., tube wear and fatigue crack propagation). In such cases, the process model can be directly used to generate data for training of the NNP models. However, for the case of parametric prediction models the functional forms of such models with respect to time must be estimated based on the characteristics of the process model. This may introduce some error in identifying future trends of the process.

The main drawbacks of NNP models are (1) the need for equally spaced time intervals in the data sets and (2) possible collapse in the prediction if the functional form of the tube degradation process is inaccurate. The former is not a main concern since usually (if not always) tube degradation measurements are performed during every

year or every refueling outage in nuclear power plants. However, a poor choice of tube degradation model could seriously affect the performance of the NNP models. Thus, it is important to minimize the uncertainties associated with the tube degradation models.

CHAPTER 4

STEAM GENERATOR TUBE WEAR MODEL

4.1 Introduction

Wear is defined as the removal of discrete particles from matting surfaces of components as a result of their relative movement with other components. It can be categorized by a variety of mechanisms depending upon the particular type of mechanical interaction and relative motion. In any particular situation, it is possible that more than one type of wear mechanism exists. The main mechanisms of wear may be classified as adhesive, abrasive, corrosive, and fretting. These mechanisms are described extensively in the literature [63,70-72]. However, it is necessary to give a brief description of these mechanisms to understand the underlying concepts of the wear mechanism of heat exchanger tubes.

Adhesive Wear is known as one of the most fundamental wear mechanisms. It remains active as long as the matting surface of two materials are in rubbing contact even if the other modes of wear mechanisms are eliminated. In adhesive wear, when two surfaces are pressed together, the contact load causes interactions between the roughness peaks (asperities) of the two surfaces. The contact area constituted by these asperities is much smaller than the nominal (apparent) contact area. Thus, the pressure in these small

contact sites can be extremely high, possibly exceeding the elastic yield strength of one or both materials and leading to possible cold welding of the asperity tips. The application of tangential loads resulting from relative sliding motions will break the cold-welded junctions and thus wear particles are generated.

Abrasive Wear occurs when asperities of the harder rubbing surface scratch or score the opposite softer surface. The wear mechanism is basically a cutting action which is accompanied by noticeable surface deformation. Wear particles can be removed as prows which form in front of a moving asperity due to plastic deformation.

Corrosive Wear causes the removal of material from a surface by both chemical reactions and rubbing. The chemical interaction of materials with environment or other material can result in the formation of corrosion products between contacting surfaces. Hard corrosion products could result in a high rate of wear. This is due to the fact that if the hard layer of corrosion products is broken off, it removes particles from material surface and then exposes the bare material to the corrosive environment and thus causes a new corrosive interaction process. Moreover, the broken layer may operate as the abrasive third body wear mechanism between two rubbing surfaces.

Fretting-Wear is common when a normal force acts on contacting surfaces of two bodies and thereby causes the two bodies undergo relative oscillatory sliding motion with very small amplitudes. It usually incorporates other wear mechanisms such as

abrasion, adhesion, corrosion, and fatigue. Fretting-wear mechanism is quite similar to adhesive wear since micro-coldwelding occurs on the contacting surfaces. It is sometimes considered as a stationary process since the particles formed during the wear process are retained at or near the wear location. However, in many cases such as heat exchanger tubes, it operates with slip and sliding motions. Fretting-wear is usually ensued by adhesive and abrasive wear mechanisms.

4.2 Tube Wear Model Development

Recent studies [15,18,24] on wear mechanism of heat exchanger tubes reveal that fretting-wear mechanism accompanied by rolling/sliding motions is responsible for the wear of tubes within their tube supports. Indeed, many researchers [15,16,18,24,37] in this field have found that shear force components developed during tube-to-support interaction correlate well with the wear rate of tubes. The shear forces and normal forces are often correlated by the coefficient of friction between two sliding surfaces (here tube and tube support). Therefore, the wear rate can be described as a function of normal forces as well.

The literature survey in Chapter 2 shows that most wear models of heat exchanger tubes correlate tube wear rate to normal forces and a few constant parameters obtained by experimental methods. Since the interest of this research study is in the estimation of service or remaining life of steam generator tubes as they degrade and age over time, a more detailed tube wear model is required. The model should incorporate factors or parameters that are affected by tube aging and degradation process. To develop such

a model, a more realistic understanding of the contact deformation mechanism of a heat exchanger tube within its tube support is required.

Experimental investigations [15,18,36] on the wear process of heat exchanger tubes within the tube supports have shown that considerable plastic deformation of a tube surface occurs during the wear of that component. To simply assume that an elastic contact exists between two surfaces (of the tube and tube support) would be insufficient. Therefore, an elastic-plastic contact deformation model is employed to derive a wear model of a heat exchanger tube.

4.2.1 Contact Deformation Model

If two bodies are loaded against each other, the stresses in rolling/sliding contact before yield are elastic and can be determined by Hertz's [59,63] contact theory. Further increase in load during the first pass will cause plastic deformation and introduce residual stresses in the interacting material. On subsequent passes over the same place, the material will experience a combination of contact and residual stresses. After several passes, an equilibrium condition could be achieved where the combined stresses are higher than the yield point of the material at that region (see Figure 4.1). Customarily this process is called work hardening or the state of shakedown [70,71] whereby the material behaves entirely in an elastic region subjected to the same existing load. This means that for further plastic deformation in that region a higher load is required. It should be noted that according to Hertz's contact theory, the maximum shear stress occurs beneath the contact layer while the maximum normal stress occurs

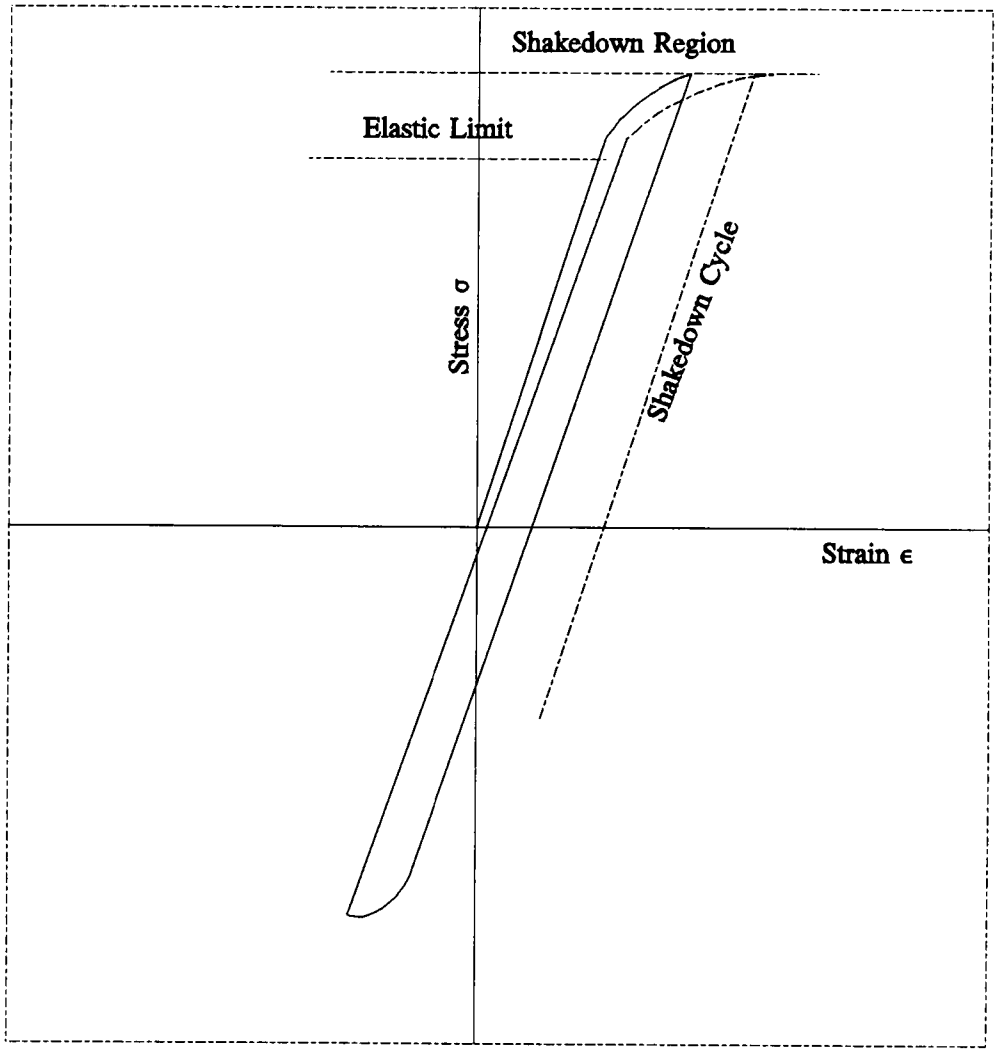


Figure 4.1: Shakedown process during the deformation of a rolling element.

on the contact layer.

Based on the shakedown theory, the following inference can be made:

- At the equilibrium condition, the geometry of the harder surface remains approximately constant while the geometry of the softer (mating) surface will deform in such a way that the maximum pressure at the interface does not exceed the

  shakedown pressure 'P_s' of the softer material.

To apply this to the wear model of a steam generator tube, the tube support is considered as the harder material and the tube as the mating surface with a softer and smoother material. The surface geometry of the tube support is assumed to contain spherically tipped asperities (indenters) which are pressed against the softer tube material. The high pressure induced by the spherical contacts could exceed the elastic point of the tube material and cause plastic deformation on the tube surface. During the deformation process, indentations are developed as the tube surface conforms to the geometry of the indenters. After a few cycles of deformation, the maximum stress at all points of contact between the indenters and the tube surface reaches P_s (shakedown pressure of the tube material). The shakedown pressure P_s can be considered as a new yield point of the tube material.

Figure 4.2 illustrates a typical contact geometry between an individual asperity (indenter) and an indentation. The contact area will appear as a circle with radius, r. The pressure distribution under the indenter can be assumed to be uniform as shown in Figure 4.2. Therefore, the total load applied by the indenter is determined as the

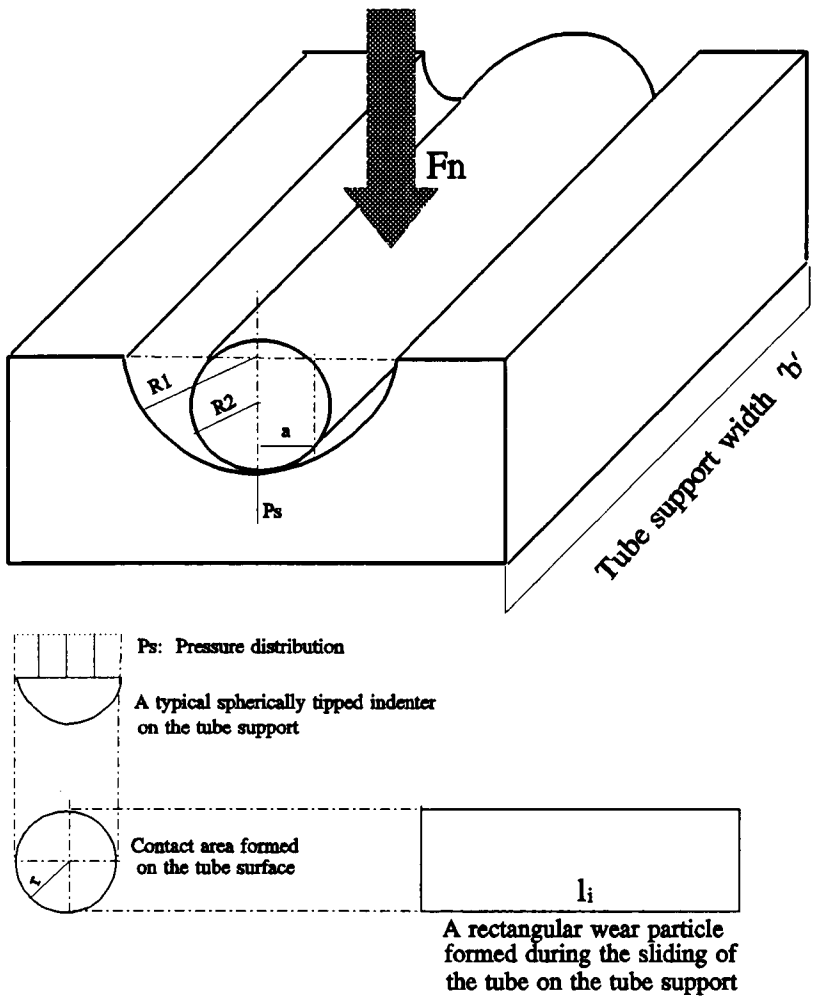


Figure 4.2: Schematic diagram of the interaction mechanism between a tube and tube support.

product of the shakedown pressure, P_s, and the contact area. Thus

$$F_i = P_s\left(\frac{\pi}{4} r^2\right) \tag{4.1}$$

Since the geometry of tube and tube support are cylindrical, the type of contact developed during the interaction of tube-to-support resembles a line contact. Using Hertz's contact theory for the case of line contact, the following relations hold for the pressure P_s and the contact width 2a:

$$a = \left(\frac{F_n E}{\pi R_e}\right)^{\frac{1}{2}} \tag{4.2}$$

$$P_s = \left(\frac{4 F_n R_e}{\pi E}\right)^{\frac{1}{2}} \tag{4.3}$$

where

$$\frac{1}{E} = \frac{1-\nu_1^2}{E_1} + \frac{1-\nu_2^2}{E_2} \tag{4.4}$$

and

$$\frac{1}{R_e} = \frac{1}{R_1} - \frac{1}{R_2} \tag{4.5}$$

F_n = Applied load developed during tube-to-support interaction

R_1 = Tube support radius

R_2 = Tube radius

E_1 = Tube support modulus of elasticity

E_2 = Tube modulus of elasticity

ν_1 = Poisson's ratio of tube support material

ν_2 = Poisson's ratio of tube material

The radius 'r' is proportional to the contact width a.

The preceding relations will allow us to calculate contact parameters for a plastically deforming tube surface. The contact parameters can then be applied to develop a wear model based on the concept of required frictional work and shear energy to form a wear particle. This will be explained in the following section.

Previously, it was shown that the geometry of an indentation can be estimated based on Hertz's elastic contact theory. It was also assumed that the softer material, tube, reaches the shakedown state during the deformation process. At the shakedown state, the maximum pressure at all points of contact area is equal to the shakedown pressure P_s. Therefore, the stress distribution in sublayer beneath the indentations will be identical at all points and so is the depth of maximum shear stress. This suggests that if the tube material wears along a sliding path, wear particles should have the same dimensions as the indentations with the depth of maximum shear stress. To form a wear particle of volume, V_s, with the indentation area, A_i, along the sliding distance of l_i, the required shear work, W_s, is the product of the shear force and the sliding distance. Thus:

$$\begin{aligned} W_s &= \tau A_i l_i \\ A_i &= 2rl_i \end{aligned} \qquad (4.6)$$

where τ is the shear stress at which plastic flow occurs. Since a portion of the

frictional energy developed during the sliding contact process goes into shearing off a wear particle, a work criterion can be developed to determine the amount of wear due to the frictional forces. Based on this criterion, the fraction of the frictional energy which goes into wear must be proportional to the work W_s required to form a wear particle of volume V_s. The frictional work W_f is the product of the load applied by the indenter, F_i, sliding distance, l_i, and friction coefficient μ. Therefore

$$W_f = \mu F_i l_i = \mu \left(\frac{\pi r^2 P_s}{4}\right) l_i \tag{4.7}$$

A portion of this work that goes into wear is αW_f where α is a constant for a given friction coefficient. Now, by using the proportionality law, if V_s is the amount of wear due to work W_s, the wear volume V_f due to work αW_f is

$$V_f = \frac{V_s \alpha W_f}{W_s} = \frac{\alpha \mu \pi r^2 d_i P_s}{4\tau} \tag{4.8}$$

$$V_s = 2 r l_i d_i$$

where d_i is the depth of maximum shear stress beneath the indentation. The above relationship gives the wear volume formed in a discrete contact as a result of the frictional work imparted to an individual asperity. To compute the overall wear volume, it is required to integrate V_f over the expected number of asperities in contact for all locations on the wearing tube surface. Relationships for the assessment of the expected number of contacts for engineering surfaces are given in the wear literature [70-72]. These relationships usually correlate the number of contacts to the probability distribution of those asperities whose heights are greater than d which is the separation

between the reference planes of the contacting surfaces (see Figure 4.3). The type of probability density considered for most engineering surfaces is the Gaussian function. However, in some cases an exponential distribution is more favorable. The mathematical representations of the expected number of contacts and the real area of contact for surfaces are expressed as follows [71]:

$$\begin{gathered} N = nAF_0(h) \\ A_e = \pi nAR\sigma F_1(h) \\ F_m(h) = \int_h^\infty (s-h)^m \phi(s)\, ds, \quad m=0,1,2,\ldots,k \\ h = \frac{d}{\sigma} \\ s = \frac{z}{\sigma} \end{gathered} \tag{4.9}$$

where

N = Expected number of contacts

n = Total number of asperities

R = Radius of spherically tipped asperity

A_e= Real area of contact

A = Nominal (apparent) area of contact

σ = Standard deviation of the height distribution of asperities

Function $F_m(h)$ represents a Guassian distribution of asperities and can also be expressed as a function of normalized compliance parameter $\delta = (z-d)/\sigma$. Thus

$$N = nA\int_0^\infty \phi(\delta)\, d\delta \tag{4.10}$$

This relationship allows us to determine the wear volume formed by the contacting

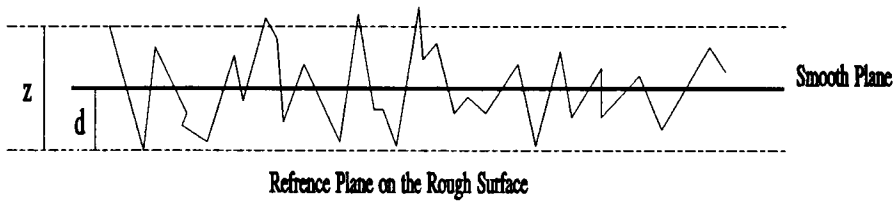


Figure 4.3: Penetration of asperities of one surface onto the opposing surface [71].

asperities in area A as follows:

$$V_t = NV_f = nA\int_0^{\infty}\phi(\delta)\,d\delta\,(\frac{\alpha\mu\pi r^2 d_i P_s}{4\tau}) \qquad (4.11)$$

$$A = 2ab$$

The apparent area, A, is considered as a product of the tube support width, b, and the nominal contact width 2a. Thus, the area A has length b and width 2a. The value of 'a' is determined based on Hertz's theory for a line contact interaction as shown in Equation (4.2). The wear volume obtained by Equation (4.11) is for a sliding distance, l_i, which indeed is the length of an individual indentation. This wear volume must be integrated over the circumference of the tube to give the overall wear volume for one cycle of contact.

$$V_t^o = (\frac{\int_{s_i}^{s_f} ds}{n_c 2a})\,V_t \qquad (4.12)$$

$$\int_{s_i}^{s_f} ds = \pi D_t$$

where

n_c = Number of asperities on the circumference of tube

D_t = Tube diameter

This is the wear volume formed during one cycle of contact between a tube and tube support. To obtain the amount of wear volume generated during the operating time t, the wear volume V_t must be multiplied by time 't' and divided by a time constant T during which a wear cycle is completed. Thus

$$V_t^{\circ} = t\left[\frac{\pi^2 b n \alpha \int_0^{\infty} \phi(\delta)\, d\delta}{4 T n_c}\right]\left(\frac{\mu r^2 D_t d_i P_s}{\tau}\right) \tag{4.13}$$

The term inside the square brackets in Equation (4.13) remains approximately constant as the wear process advances. The integral of $\phi(\delta)$ is fairly constant except for the severe case of wear [53-56]. This is also true for parameters n and n_c. The changes in α can be integrated with the variation of friction coefficient μ since this parameter depends heavily on μ. Denoting K_0 as the term inside the brackets and differentiating Equation (4.13) with respect to time will result in a relationship for the wear rate which is usually more desirable for practical applications. This results in Equation (4.14).

$$\dot{W} = K_0 D_t \left(\frac{\mu r^2 d_i P_s}{\tau}\right) \tag{4.14}$$

Parameters r, P_s, and d_i can be expressed as a function of applied load using Hertz's line contact theory. The following relationships show the general dependency of these parameters on the applied load F_n [59,63,71](see also Equations (4.2) and (4.3))

$$r = K_1 F_n^{\frac{1}{2}}$$
$$P_s = K_2 F_n^{\frac{1}{2}}$$
$$d_i = K_3 F_n^{\frac{1}{2}}$$

Note that K_1, K_2, and K_3 stay fairly constant as the tube and tube support age. This is due to the fact that the modulus of elasticity is basically a constant parameter for a given material and the changes in the radii of tube and tube support are negligible with respect to their sizes. Substitution of these relationships into Equation (4.14) gives:

$$\dot{W} = K\frac{\mu F_n^2}{\tau}$$
$$K = D_t K_0 K_1 K_2 K_3 \qquad (4.15)$$

Parameters μ, τ, and F_n can be changed as the tube and the tube support age. The changes in these parameters occur slowly as a function of time. Fortunately, field measurements and prior experience could identify the variations of these parameter either as a direct or an indirect function of time. For instance, the variation of the interaction force F_n over time is because of deposit build-up in the vicinity of tube/tube support or increased misalignment between the tube and its support during the operating time of a steam generator. The changes in the shear stress τ can be ensued due to thermal cycling or load cycling in the steam generator system. The friction coefficient could change with corrosion, oxidation, and deposit buildup over time.

4.3 Parameter Identification of Tube Wear Model

Some characteristic features of tube wear model parameters must be known before a tube wear model can be used. These characteristics of parameters include variation mechanisms in friction coefficient, shear stress yield point, and normal contact forces due to material aging and mechanical and/or environmental degradation processes.

4.3.1 Coefficient of Friction

The sliding/rolling motions between the surfaces of a heat exchanger tube and its tube support generate a kinetic friction force at the interface of the two surfaces. This friction force is correlated to a normal force and a kinetic friction coefficient. The

value of the friction coefficient depends on the tube/tube support surface texture conditions and the speed of sliding motion. Previous investigations [13,22,24] on the friction coefficient of heat exchanger tubes suggest that a typical value of the friction coefficient lies in a range of 0.1 to 0.4 for stainless steel material. However, this range of values is valid for clean and smooth surface conditions. The friction coefficient is subjected to change when the contacting surfaces are contaminated with corrosive material or corrupted with surface damage and flaws. In a steam generator, surface contamination of tubes and their tube supports can occur as a result of chemical interaction of surrounding fluid with the surface material. The importance of surface contamination for the tubes of Once-Through Steam Generators (OTSG) at Duke Power's Oconee Unit is reported in Reference [42]. The report gives the following observation on the tube surface near the 15th support plate :

"Substantial magnetite deposit buildups were present around the wear areas. On the wear surfaces the deposit were compacted. An electron microscope scan of the wear surfaces revealed scratch widths consistent with magnetite particle sizes and circumferential scratch lengths of about 0.003 inch (0.08mm)."

Thus, the presence of a contaminating film between the sliding surfaces operates as an environmental degradation process and may have a marked detrimental effect on the characteristics of coefficient of friction and consequently the wear of tubes. It should be noted that some contaminants are beneficial and can reduce friction and surface failure since they act as lubricants. Examples of such contaminants are certain oxides, sulfides, plated films, and any low-shear-strength material [70,71].

The coefficient of friction can also degrade due to an undesirable amount of surface roughness or indentation. In a wear process, the removal of materials from the contacting surfaces introduces tiny grooves and scars which damage the initial surface textures of the contacting bodies. Consequently, this causes the coefficient of friction to increase as the wear process advances. In the wear of steam generator tubes, where fretting also operates, the tube surface damage is even greater. The fretting damage in steam generators can accelerate the deterioration of the protective (corrosion and wear) films [69,70] coated on the tube surfaces through vibro-sliding/impacting of the tubes against their support plates. In addition, it can also introduce microstructural surface deformations and dents which results in a greater surface roughness and thus a larger friction factor. In fact, the experimental studies conducted by El-Sherbiny and Salem [69] for different coating materials indicate that the coefficient of friction increases with the number of fretting cycles and then approaches an asymptotic value ranging from 0.5 to 0.8. The friction behavior of Ion-plated material is illustrated in Figure 4.4. Similar behaviors have been also observed by other investigators [72] for uncoated metallic materials (such as stainless steel) in the absence of oxide particles at the interface of rubbing surfaces. In such situations, the coefficient of friction first usually tends to remain constant at the beginning of a fretting-wear process (equilibrium condition). Then, it starts to grow rapidly as the wear mechanism advances towards a severe wear stage over a long period of time. Finally, at the stage where the contacting surfaces reach their maximum roughness, it levels off to a certain value.

Based on the foregoing discussion, it is plausible to consider a time dependent

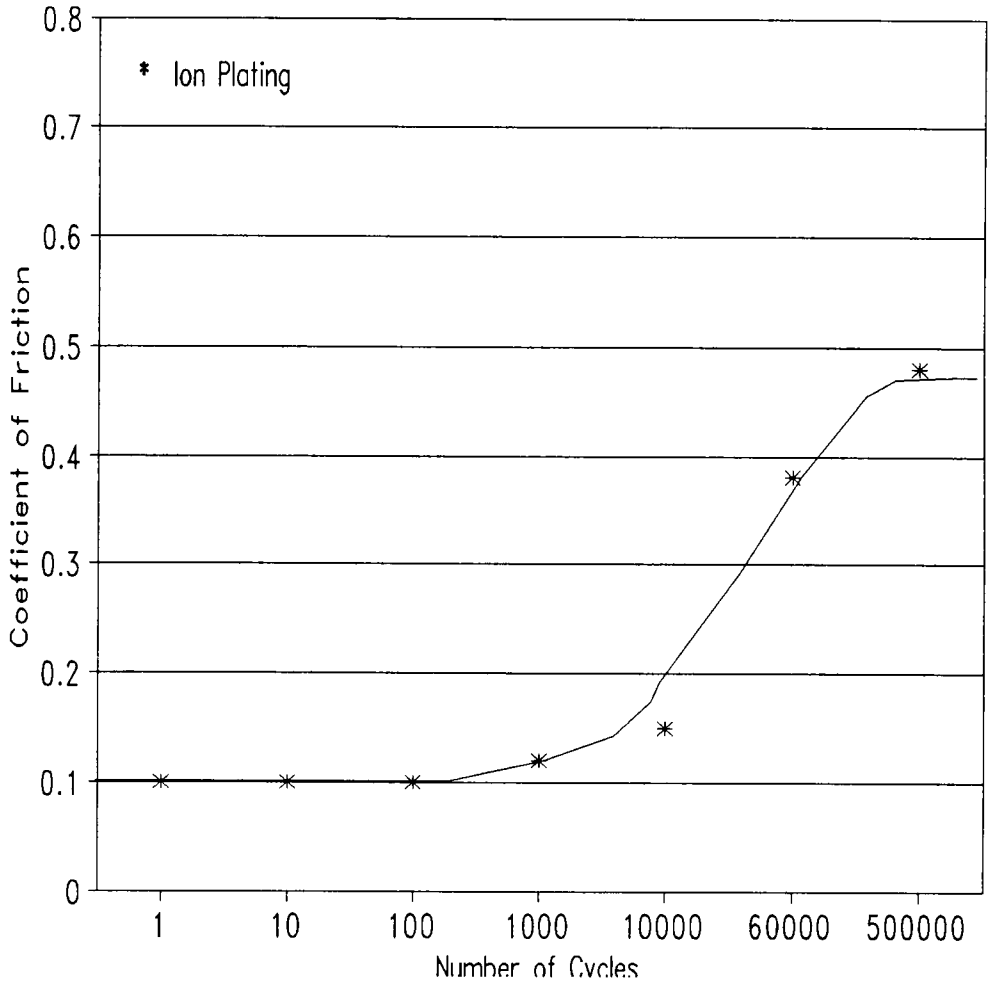


Figure 4.4: Frictional behavior of ion-coating test [66].

degradation model for the coefficient of friction between tubes and tube supports in an OTSG steam generator. The model considered in this research study is a power function of time as

$$\mu(t) = \mu_0 + a t^b \tag{4.16}$$

where μ_0 is the initial value (usually 0.1 for Inconel 600), t is time, and a and b are constant parameters which determine the rate that the coefficient of friction degrades. An upper value of 0.75 is considered in this study for the coefficient of friction. It should be noted that the degradation of the friction factor is typically a very slow and gradual process over time since the tubes are coated with a very resistive wear and corrosion material. However, on the other hand, scratches and surface flaws which sometimes occur during the fabrication of steam generator tubes can considerably increase friction forces between contacting surfaces of tubes and tube supports. In such cases, the rate of change in the coefficient of friction would no longer be slow and could grow rapidly (case of sever wear phase [70]). It should also be pointed out that the current knowledge about the characteristics of the coefficient of friction for different materials and different operating conditions are not well developed [63,70-72]. For example, the behavior of friction factor at different temperatures, speeds, frequencies, and surface conditions is still under investigation. Therefore, further developments in such areas are needed to identify a more accurate aging model of this parameters.

4.3.2 Shear Stress Yield Point

In a wear process, the shear strength of a material is considered as a measure of its

wear resistance characteristic. It is an important parameter in a wear process since it represents the resistance of the materials against a plastic flow that may ensue by high pressure indenters during a sliding motion. Thus, the degradation of the shear strength is accompanied by an increase in the wear rate [15,70].

This quantity is directly correlated with the surface hardness of a material. Consequently, any factor that affects the surface hardness will also influence the shear strength. In a steam generator (e.g; OTSG type) where the tube materials are Inconel 600, the tube surface hardness is approximately 250 Vicker [85]. This large number indicates that the tube materials are resistive enough to the forces that may shear off the tube surface. However, the tube surface hardness and shear strength yield point are subject to aging and degradation processes [17,67] resulting from service exposure. Thermal cycling, environmental degradations, and mechanical damage mechanisms are common causes of reduced shear strength and surface hardness in the tubes of OTSG units. Perhaps among all causes, mechanical types are the most damaging ones. For instance, during the wear of a steam generator tube the removal of material from tube surface introduces geometrical and microstructural discontinuities at the wearing location. The presence of discontinuities in the material is detrimental because these act as local stress-raisers (stress concentrations) which cause the tube materials rapidly reach their yield strength point. They also produce suitable points for the initiation of micro-surface and subsurface cracks which eventually result in the delamination of tube surface during fretting-wear of that component[9]. Therefore, it is expected that a

[9]This phenomenon is also known as fretting fatigue [63].

wearing tube surface gradually loses its yield strength and hardness over time and consequently the plastic flow of wear particles are facilitated. Environmental degradation and loading conditions can also weaken the tube strength. Prime examples are corrosion and thermal fatigue which can seriously damage the strength and hardness of the tube materials in a long period of time [17,68]. Indeed, nuclear steam generator tube pullout tests [17,68] have confirmed the occurrence of such phenomena and their effects on the mechanical strength of the tubes. Laboratory tests on the specimens of pulled tubes show that the strength of tube materials has reduced to some extent due to such degradation mechanisms [17].

From the foregoing evidence it is reasonable to adopt an aging model that describes the gradual variations of tube shear strength with time. In this study, an exponential model is considered to reflect the effects of material aging and degradation processes on the shear strength yield point. The model is selected based on two criteria: (1) surface hardness and fatigue stress[10] of metallic materials that age and degrade in a fashion resembling exponential functions [63,66], and (2) exponential functions have shown to be useful in a wide variety of aging mechanisms [62]. Hence, the mathematical description of the model is:

$$\tau(t) = \tau_0 \exp(\alpha t) \tag{4.17}$$

where τ_0 is the initial value of yield shear strength point and α is a constant parameter which represents the rate of aging. The value of α for slow and gradual aging

[10] In the presence of thermal and/or mechanical cyclic loading (which is the case for steam generator tubes).

processes such as those of steam generator tubes is typically a small negative number near zero (e.g; -0.01 1/year).

4.3.3 Normal Contact Forces

Wear rate of a steam generator tube is strongly correlated to normal contact forces. It is usually a power function of contact forces and thus any changes in these forces could cause a large variation in the wear rate.

There are a number of parameters associated with contact forces. These are: tube-to-tube support clearance, tube-to-support misalignment, tube support stiffness, excitation forces, and tube materials properties. Variation in contact forces is usually attributed to the changes of such parameters. A parametric study of tube-to-support interaction model can reveal the dependency of contact forces on these parameters.

In a steam generator system, the parameters will vary over the component's operating time because of aging and degradation processes. For instance, mechanical wear and chemical tube thinning increase the tube-to-support clearances which vary the behavior of the contact forces. Thermal and mechanical stresses and un-even wear rate may increase/cause tube-to-support misalignment. However, tube materials properties (such as modolus of elasticity and moment of inertia) and the excitation forces associated with the tube-to-support interaction mechanism remain fairly constant at steady-state conditions. A parametric evaluation of tube-to-support interaction mechanism can be used to develop a time dependent model for the variation of contact forces. This will be demonstrated in the next chapter.

4.4 Comments on the Wear Model

Verification of the mathematical models for physical and engineering systems is usually achieved by experimental investigations and testing. Such a verification for the wear model developed here is beyond the scope of this research work. However, it is possible to validate the wear model in a qualitative manner. Archard's [63,72] model for adhesive wear have been adopted for the wear of heat exchanger tubes by many investigators. Archard's model confirms the direct proportionality of wear volume generated between two rubbing surfaces to normal forces acting between two contacting surfaces, a sliding distance, and a wear coefficient. It also shows that the wear volume has an inverse proportionality with the Brinell Hardness of the softer material. Since the hardness of a material is directly related to its yield shear stress, the wear volume is also proportional to the inverse of the shear stress of the softer material. The wear model developed in this study shows the relational consistency of wear parameters to those of Archard's model. Also, recent studies [5,18,30] on the wearing of heat exchanger tubes show that the wear rate of heat exchanger tubes correlate well to a power function of contact forces and a wear coefficient which is a function of friction coefficient and tube material properties (see Chapter 1). For instance, Pettigrew [5] found (by experimental investigation) that the wear rate for heat exchanger tubes using Incoloy 800 for tubes and Inconel 600 for tube supports can be expressed as follows:

$$\dot{W} = 6.8\times10^{-16} F_n^{4.75} \tag{4.16}$$

where the wear rate is in mg/10^6 cycles. Therefore, the wear model developed here agrees qualitatively with the models proposed in the literature.

It is necessary to point out that despite several decades of research into wear mechanism and wear modeling, wear still defies an accurate quantification and even characterization. This is due to the fact that an elaborate analytical modeling requires a continuing integration of metallurgical, mechanical, and chemical engineering expertise on the subject, combined with experimental investigations and verifications. Therefore, it is not surprising that the existing tube wear models (which are mostly experimental) can not adequately describe the extremely complex phenomena that comprise most wear situations.

4.5 Mechanics and Patterns of Tube Wear in OTSG Systems

As described in Chapter 1, flow-induced tube vibration causes fretting wear of tubes in OTSG systems. The wear of tubes is attributed to vibrating motion of tubes and to clearances between tubes and tube support plates. The clearances, required for the thermal expansion and for the ease of construction, allow the vibrating tubes to interact dynamically with their support plates. The dynamic interactions of the tube within its support produce impact and tangential sliding of the tube against the tube support plate with consequent tube wear at that location. In OTSG units, this phenomenon is more important at the 15th tube support plate than at any other location. This is due to significant flow-induced tube vibrations in a region between the 15th tube support and the upper tube sheet. Indeed, the inspection of the pulled out tubes from OTSGs at Duke Power's Oconee Unit indicates a substantial metal loss at locations corresponding to the 15th tube support [42]. Figure 4.5 shows an affected tube with rectangular wear

scar patterns conforming to the shape of interfacing land areas of the 15th tube support plate. The reported reduction in the tube wall thickness of Figure 4.5 is approximately 0.01" (0.2 mm). This value is not considered as a typical value for the wear of OTSG tubes at this location. However, a rectangular wear scar geometry is regarded as a typical wear pattern at this location [42].

4.6 Summary

A heat exchanger tube wear model has been developed based on a plastic/elastic contact deformation model. The shake down theory of plasticity was utilized to define a maximum contact pressure equal to P_s that can be regarded as a new yield point of the tube material because of residual stresses combined with strain hardening introduced during several passes of the tube over the tube support. Following the shake down theory, the geometry of an indentation formed (on the tube surface) by a hard, sliding (spherically tipped) asperity of the tube support was predicted. Hertzian line contact formulae were employed to calculate the radius of indentation which corresponds to the half width of a wear particle. The amount of the wear particle was then determined by equating the frictional work input due to a sliding asperity with the energy required for fracture of a wear particle. This amount was integrated over the tube surface area within the tube support to derive a model for the wear of that component during one cycle of contact.

The wear model developed in this study clearly characterizes the dependency of the wear rate on the coefficient of friction, shear stress yield point, and normal forces. This

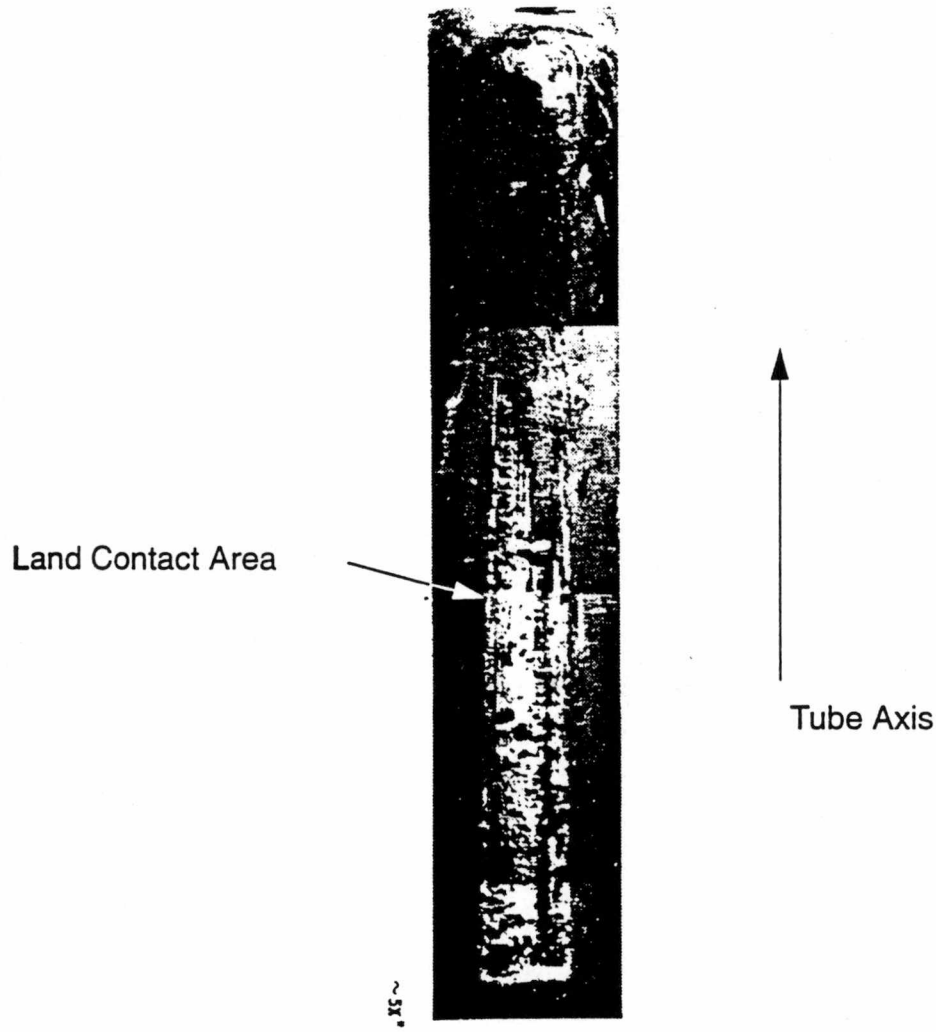


Figure 4.5: Pattern of wear scars on a pulled out tube from an OTSG of Duke Power's Oconee unit [76].

characterization is important for the wear estimation of tubes as they age and degrade over time. Aging and degradation processes in steam generators and heat exchangers can result in the variation of wear parameters such as friction coefficient, shear stress yield point, and contact forces.

Two time-dependent models were also suggested to describe the variation of the coefficient of friction and the shear yield strength point of tube materials due to aging and degradation mechanisms. The changes in these parameters will introduce behavioral changes in the wear of tubes. This is illustrated in Chapter 6.

CHAPTER 5

DEVELOPMENT OF A MATHEMATICAL MODEL FOR TUBE/SUPPORT INTERACTION IN MULTI-SPAN STEAM GENERATOR TUBES

In this chapter, the development of a vibration model for a Once-Through Steam Generator (OTSG) tube is presented. Prior to the model development, a brief description of an OTSG system is presented. A review of flow induced vibration mechanisms in OTSGs is also provided.

5.1 Once-Through Steam Generators

One type of steam generator used in Pressurized Water Reactors (PWRs) is the Once-Through Steam Generator (OTSG). It is installed in the primary side of a nuclear power plant which also contains a reactor vessel, reactor coolant pumps, and a pressurizer. The general arrangement of a typical OTSG is shown in Figure 5.1.

The OTSG system is a single-pass counter flow heat exchanger which is of the vertical straight tube-and-shell arrangement. The tubes in the bundle are attached to the upper and lower tube sheets and loosely supported by several uniformly spaced (only the spacing between the last support and the upper tube sheet may be different from the rest) broached supports (see Figure 5.1). The bundle is confined within a thin shell

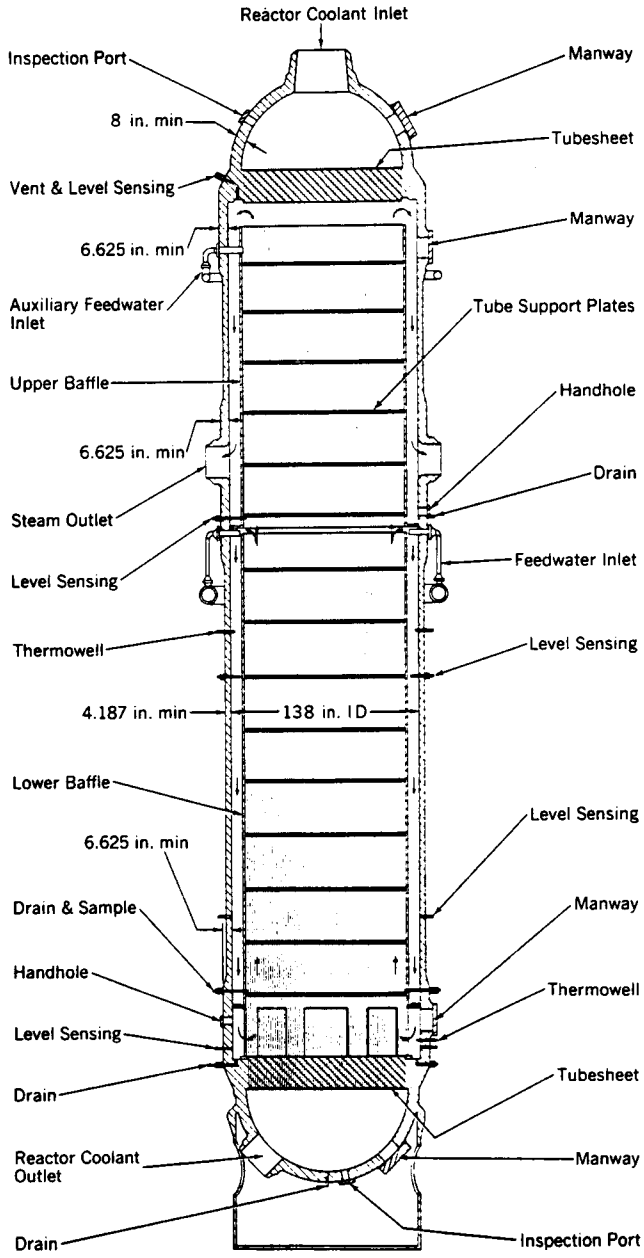


Figure 5.1: Schematic diagram of a typical Babcock & Wilcox Once-Through Steam Generator unit [74].

which is called the shroud. The function of an OTSG unit is to convert the secondary subcooled feedwater flow to a superheated steam for turbines.

The primary coolant flow from the reactor enters the steam generator via an inlet nozzle at the top head. It flows downward and thus transfers heat to the secondary fluid in the shell side of the steam generator. The primary flow leaves the steam generator at the bottom head.

A subcooled feedwater flow is introduced into the shell side of the steam generator via feedwater nozzles. It flows down through an annulus (downcomer) inside the shell where it is heated to the saturation temperature by mixing with a flow of steam bleeding from the tube bundle region. The saturated flow changes its direction and travels upward as it enters the tube bundle at the bottom. As the flow rises to the top, it is converted to a superheated steam which exits the steam generator through steam outlet nozzles.

The design data of a typical OTSG unit used in the Oconee nuclear power plant are given in Table 5.1. The data were extracted mainly from References [17 & 74].

5.2 Flow-Induced Vibration in an OTSG

Tube vibrations are produced in an OTSG by the flow pattern of the secondary fluid system. The secondary flow field is primarily axial until the 15th tube support (TS). However, between the 15th TS and the upper tube sheet the flow has to develop a radial component to exit the steam generator. The radial flow increases linearly from the center line of the tube bundle toward the steam generator shroud as it crosses over

Table 5.1: Design data for a typical Once-Through Steam Generator (OTSG) used in Oconee power plant [17,74].

DESIGN DATA	
Design Pressure, psi	1050
Design Temperature, °F	600
Steam Flow, million lb/hr	5.6
Steam Pressure, psi	910
Inside Diameter of Pressure Shell, ft-in	11-6
Inside Height of Pressure shell, ft-in	66-0
Number of Tubes	15530
Tube Outside Diameter, in.	0.625
Tube Wall Thickness, in.	0.034
Tube Materials	Inconel 600
Number of Tube Support Plates	15
Spacing between Two Support Plates, ft-in	3-3
Tube Support Plate Thickness, in.	1.5
Diameter of Drilled Holes in Support Plates, in	0.64
Tube Support Plate Material	Carbon Steel

the OTSG tubes [17]. This cross-flow is primarily responsible for the vibrations of the steam generator tubes. It possesses the strongest potential for exciting vibration in the outer tubes where the flow velocity is maximum.

There are five main vibration mechanisms which could be associated with a cross-flow [5,9,12]. These are vortex shedding, turbulent buffeting, fluid-elastic excitation, acoustic resonance and jet switching. These mechanisms have been investigated and published extensively in the literature [2-9,12]. However, based on the test and field vibration data, Davis and his colleagues [17] reported that the main mechanisms of flow-induced vibration in OTSG units are vortex shedding and random turbulent buffeting. They did not consider jet switching (see Reference [9]) as a major vibration mechanism in OTSG units, since the dimensionless velocity v/fd was less than 75 (they found a maximum of 48), where v is the flow velocity, f is tube vibration frequency, and d is tube diameter.

5.2.1 Vortex Shedding

When a uniform flow crosses a cylindrical object, pressure variation occurs around the cylinder (for Reynold's numbers greater than 5). As the flow velocity increases, the pressure variation around the cylinder also increases. The increasing pressure calls for the retardation of fluid boundary layer around both sides of the cylinder. This will eventually cause the boundary layer to slide from the cylinder. The sliding of the boundary layer is associated with the formation of vortices. These vortices will be alternately shed from the cylinder at discrete time intervals [9]. The frequency at which

the vortices are shed can be calculated by the following equation [9,12,17]:

$$F_s = S\frac{u}{d_o} \tag{5.1}$$

where S is Strouhal number, d_o is the cylinder diameter, and u is a uniform cross velocity.

A cylindrical object (such as a tube) responding to vortex shedding experiences vibratory forces at discrete frequencies, perpendicular to the direction of the flow. These forces are in fact dynamic lift force that can be modeled as follows:

$$F_l = \frac{1}{2}\rho U^2 D C_l \sin\omega t \tag{5.2}$$

where ρ is the density of the flowing medium, U is the flow velocity, D is the cylinder diameter, C_l is a lift coefficient, and ω is the frequency of oscillation. The lift force, F_l, in the above equation is per unit length and it is proportional to the local dynamic pressure represented as $1/2\rho U^2$. The lift coefficient C_l is a function of Reynold's number and its value decreases as the Reynold's number increases. A wealth of data on this quantity for various geometrical objects has been published in many fluid mechanics books and literature. Its value for the tubes of an OTSG system, as suggested in Reference [17], is approximately 0.08 (corresponding to a Reynold's number of 7.8×10^4) at the steam generator full power conditions.

5.2.2 Random Turbulent Buffeting

The flow patterns in most tubular heat exchangers and steam generators are

basically turbulent. In a turbulent flow the velocity fluctuates in both magnitude and direction randomly [9,17]. As a consequence, small eddies and vortices are created. These vortices grow in size and then disappear by merging into nearby eddies. As a result, a transfer of momentum occurs in this process. A tube in the path of such flow experiences a steady drag force which is associated with the transfer of momentum. In an OTSG, where a bundle of tubes exists, a greater flow turbulence gives rise to a series of random forces exerted on the tubes. These forces are usually modeled as a Gaussian white noise [17]. Since the nature of such forces is random, the power spectral density of the forces can characterize their behavior. For instance, it can show the frequency at which the maximum tube response occurs due to random turbulence forces.

5.3 Simulation of Impact Forces

Flow-induced tube vibrations can cause dynamic impact forces between tubes and tube support plates in heat exchangers and steam generators. The dynamic characterizations of these forces are central to the wear rate estimation of tubes as described in Chapter 4. Since it is not practical to measure such forces in industrial heat exchangers or steam generators, mathematical simulations are needed to estimate them from flow and vibration information.

Complex nonlinear boundary conditions at the tube-to-support clearances and sophisticated loading conditions of the excitation forces restrict the use of analytical solutions only to simple tube-to-support configurations (e.g; single tube support). On

the other hand, the application of finite element techniques and high speed computers permits numerical simulation of complex tube and support geometries.

A one-dimensional beam finite element technique [58-61] is employed in this study to simulate the underlying physics of the impact forces in a multi-span tube. The construction technique of the finite element vibration model of a multi-span tube is well documented in the literature [5, 19-25]. In brief, the tube is considered to be an assembly of beam elements, each having 4 degrees of freedom[11] (translational and rotational displacements at each end). If these elements have known mass and stiffness properties (see Appendix B) then it is possible to construct mass and stiffness matrices which represent the whole structure. Using the structural mass, damping and stiffness matrices and removing the rigidly constrained degrees of freedom, the equations of motion for the tube are written as

$$[M]\ddot{X} + [C]\dot{X} + [K]X = F_{exc} \tag{5.3}$$

where [M], [C] and [K] are structural mass, damping, and stiffness matrices, respectively, and x is the tube position vector. F_{exc} denotes excitation forces. The added mass of surrounding fluid is included in the lumped mass matrix [M]. The above equation is valid when there is no contact between the tube and the tube supports.

The matrix development of mass, stiffness, and damping have been explored extensively in the literature [57-61]. The mass and the stiffness matrices are obtained by applying both kinetic energy and bending strain energy to a beam element subjected

---

[11] For a three dimensional model, there are 12 degrees of freedom.

to a transverse force distribution [23,61] (see Appendix B). The damping matrix is usually considered as a linear combination of mass and stiffness matrices, and it is modeled as follows:

$$C = \alpha M + \beta K$$

where the values of α and β are obtained based on beam structural damping values [57,60].

For the case where contact exists between the tube and its support plates, the preceding tube vibration equation [Equation (5.3)] is changed as follows:

$$[M]\ddot{X} + [C]\dot{X} + [K]X = F_{exc} - F_{sp} - F_{dmp} \qquad (5.4)$$

where F_{sp} and F_{dmp} are the forces produced by the spring and damping action of the supports on the tube, respectively. These forces are generated when the tube displacement within the support exceeds the clearance between tube and support. The summation of these forces is considered to be the impact forces acting between the tube and the tube supports.

The excitation force, F_{exc}, is determined based on the characteristics of vortex shedding and turbulent buffeting mechanisms in an OTSG. Equation (5.2) can be used to estimate typical excitation forces experienced by a tube due to the vortex shedding mechanism. This equation requires an average value of cross flow velocity in the tube bundle area. In an OTSG unit, the excitation forces are determined based on an estimated cross flow velocity profile between the 15th support and the upper tube sheet. Davis and co-workers [17] presented a cross-flow velocity profile in a region between

the 15th tube support and the upper tube sheet. The profile was obtained based on three assumptions. These assumptions are (1) flow velocity components (both radial and tangential) are zero at the upper tube sheet; (2) the flow profile can be estimated as a triangular distribution starting at 18 inches below the tube sheet (see Figure 5.2); (3) continuity equation holds between axial flow rate coming to the 15th support area and the radial flow rate leaving the OTSG system. Based on these assumptions, the maximum cross flow velocities were 25.75 m/sec (84.5 ft/sec) in the tube bundle area and 41.45 m/sec (136 ft/sec) in the open lane (near the outlet nozzle). Using this velocity profile, an average cross flow velocity of 12.87 m/sec (42.25 ft/sec) was obtained between the 15th tube support and upper tube sheet. The average velocity was used in conjunction with Equation (5.2) to estimate the excitation forces.

The excitation forces due to turbulent buffeting can be modeled as a wide-band Gaussian white noise. The variance of the noise may be chosen to be in the range of 10% to 40% of one Newton. They could be added to the deterministic forces resulting from vortex shedding and thereby providing the overall excitation forces.

In this research, a uniform distributed force (which is constant with respect to tube axial direction) is assumed to act on the tube from the 15th tube support to the upper tube sheet. This represents the deterministic excitation force resulting from vortex shedding in this region. The frequency of the force is taken to be 55 Hz and its amplitude 2.8 N/m. The force amplitude has been determined based on Equation (5.2) and an average cross-flow velocity of 12.87 m/sec (42.25 ft/sec). The proposed oscillation frequency given by previous investigators [17,23,24] is in the range of 40

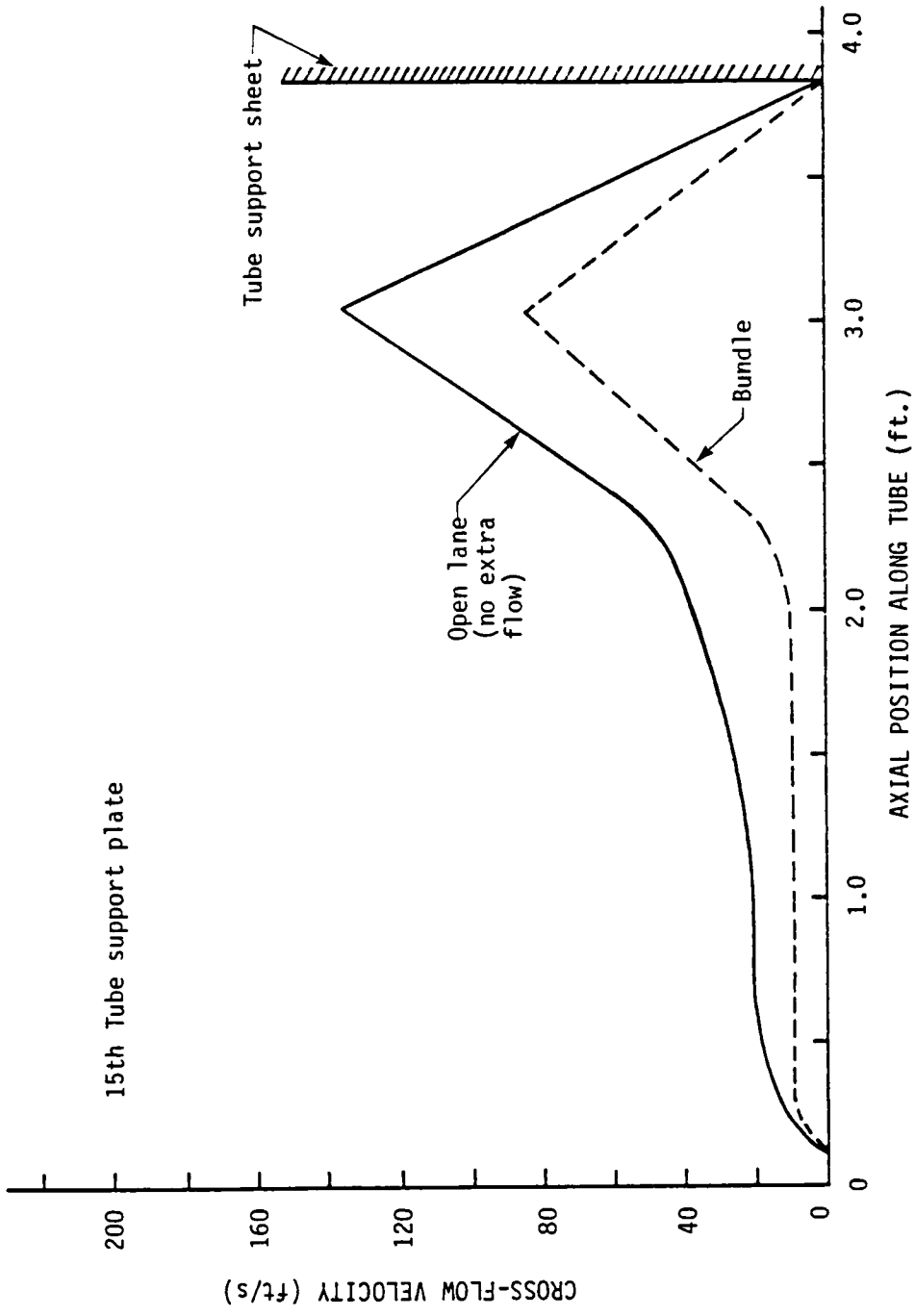


Figure 5.2: Cross-flow velocity profile between the 15th support tube and the upper tube sheet in an OTSG unit [17].

Hz to 60 Hz.

A random force with a Guassian distribution with mean zero and variance 0.1 N/m is also added to the deterministic force to simulate the overall excitation forces which may act on the tube during normal operation of an OTSG unit. This random force represents the effects of turbulent buffeting in an OTSG.

The spring force, F_{sp}, is produced when a contact between a tube and its tube support plate occurs. Because of this contact, both the tube wall and the tube support plate deform radially and the normal contact force F_{sp} develops. This contact force is simulated as a product of tube support stiffness coefficient and a contact deflection, δ. The contact deflection is defined as

$$\delta = |X_{sp}| - C_r \tag{5.5}$$

where X_{sp} is the tube displacement within the support and C_r is the tube-to-support clearance. Note that $|X_{sp}|$ must be always greater than C_r to produce a contact deflection. Thus, the contact spring force bears the following relationship

$$F_{sp} = K_{sp}\delta \tag{5.6}$$

where K_{sp} is the spring coefficient of tube support. The suggested value of K_{sp} for carbon steel plates is 5×10^6 N/m [22].

The support material damping force, F_{dmp}, generated during the contact is calculated by using the following relationship [23].

$$F_{dmp} = 1.5\alpha F_{sp}\dot{X} \tag{5.7}$$

where α is the material damping constant and $\dot{x}$ is the tube velocity at the time of

contact. The above equation is developed based on the concept of hysteresis energy loss of a moving body during a single impact [28]. The suggested value of α for carbon steel is 0.25 s/m [23].

As stated earlier, the summation of the contact spring force and the contact damping force results in an overall tube-to-support contact force. It follows from the above equations that the magnitude of a contact force depends strongly on the amount of deflection at the tube support and the velocity of tube at the time of contact. The time duration of each contact force typically lies in a range of 200 to 500 μsec [30] for most industrial heat exchangers and steam generators. This short time duration indicates that these forces operate in an impulsive fashion.

5.3.1 Solution Procedure

The numerical solution of the equations of motion [described by Equation (5.4)] is rather involved and cumbersome, because the time derivatives are coupled in the mass and damping matrices. It becomes even more complex when a large number of equations is involved or when the excitation forces are non-periodic [61]. In such cases, in order to ease the computational efforts, it is suitable to uncouple the equations of motion by using modal analysis method. In this technique, the expansion theorem is used to express the displacement of the masses as a linear combination of the normal modes of the system. This linear transformation arranges the equations of the motion in a set of uncoupled differential equations of second order. The solution of these equations, which is equivalent to those of single degree freedom systems, can be readily determined. The complete description of the modal analysis and the construction

techniques of modal matrices are available in many books and literature [57,60,61] (this will not be elaborated here). Thus by using the method of modal analysis , Equation (5.4) is changed to

$$[\ddot{q}] + [2\zeta_i \omega_i \dot{q}] + [\omega_i^2 q] = [\phi]^T [F_{exc} - F_{sp} - F_{dmp}] \qquad (5.8)$$

where

$[\phi]$ = Modal matrix

q = Generalized coordinate ($x=[\phi]q$)

ω_i = The i-th natural frequency of tubes

ξ_i = Overall damping ratio

The matrices indicated by [] on the left hand side of Equation (5.8) are all diagonal. The suggested damping ratio in an OTSG unit is 0.01 [17]. It should be noted that both numerical stability and accuracy of Equation (5.8) depends strongly on the integration time step. As a rule of thumb the time step should be less than one-tenth of the time period corresponding to the highest natural frequency of the system.

5.3.2 Simulation of Tube-to-Support Contact Forces for an OTSG Tube

The tubes of Once-Through Steam Generators (OTSG) are subject to flow-induced vibration excitations which occur all along the tubes. However, as stated earlier, lift and drag cross-flow excitation in the upper span, where high flow rate steam leaves the steam generator toward the outlet port, is responsible for most of the tube vibration. Because the excitation forces mainly act between the 15th tube support and the upper tube sheet, the dynamic interaction at the 15th tube support is of primary interest. It

should be noted that since the tubes inside an OTSG usually have 15 supports or 16 spans, the excitation forces have very little effect on the vibration of tubes below the 12th supports due to considerable amount of fluid and structural damping. Based on the same analysis, the motion of the tube far from the 15th support has negligible effect on the motion at the 15th support[12]. Therefore, a four-span tube model can simulate the vibro-dynamic interaction of a typical OTSG tube at the 15th tube support with an adequate accuracy.

Figure 5.3 schematically shows the four-span model of an OTSG tube. The tube is assumed to be clamped both at the upper tube sheet and at the 12th support. The clearance between the tube and the supports is approximately 0.19 mm (identical for all three supports). The supports are equally spaced and the distance between two consecutive supports is approximately 1 m. The distance between the 15th support and the upper tube sheet is approximately 1.15 meter.

A computer code written in the FORTRAN language embodies the construction techniques of finite element vibration model of the four-span OTSG tube. Using a specified number of finite elements, the code generates the tube equations of motion according to Equation (5.4). Then, it employs the modal analysis to perform numerical calculations of the tube model according to Equation (5.8). The overall number of finite elements used for the tube model is 20 (5 elements per span). The required number of finite elements is obtained based on sufficient accuracy and economics of

[12] This has also been supported by the theoretical investigations of Fisher et al [30] and field reports from nuclear OTSG service inspections [17].

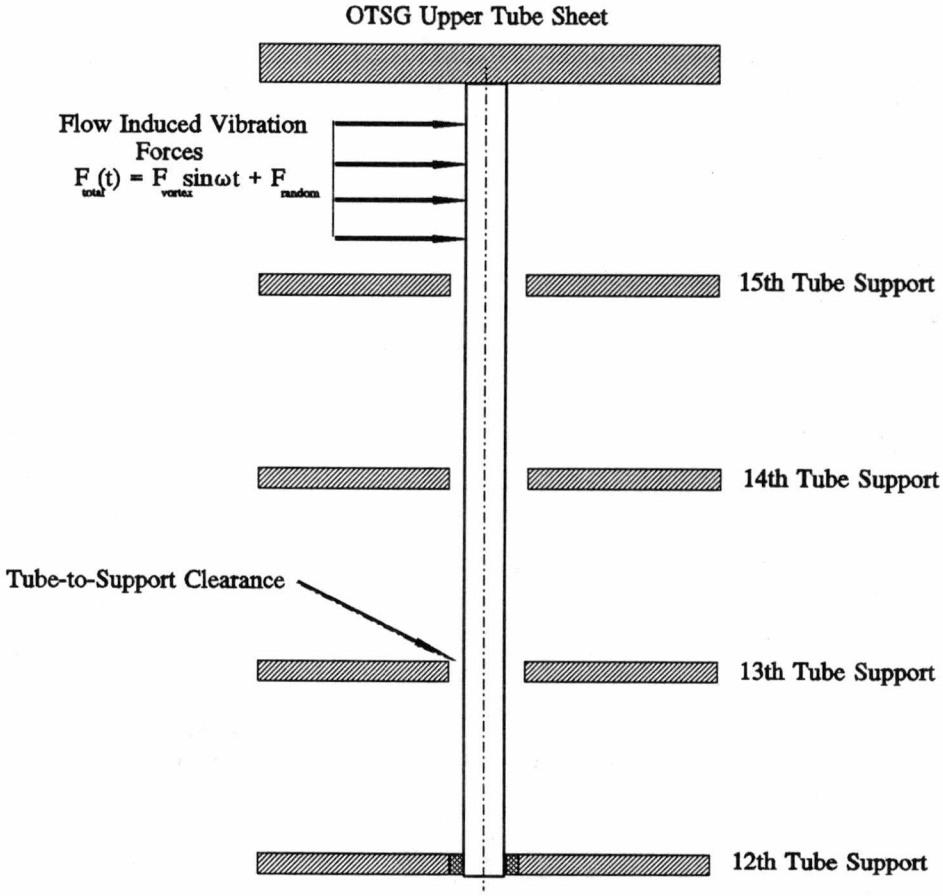


Figure 5.3: Schematic diagram of the four-span model of an OTSG tube.

computation. The code can be executed in a VAX mainframe or a workstation. It can also be run on Personal Computers (PCs) equipped with IMSL software package [87] with minor modifications.

To determine the number of finite elements required to adequately represent the tube responses at the 15th tube support, initial simulations were conducted with the tube vibration model using sixteen, twenty, and twenty four finite elements (equally divided among all four spans). The excitation forces used in these simulations are uniformly distributed between the 15th tube support and the upper tube sheet. They incorporate two components (1) a deterministic oscillatory force with amplitude 2.8 N/m and frequency 55 Hz and (2) a random force[13] with mean zero and variance 0.1 N/m. Therefore,

$$F_{exc} = 2.8\sin 55t + 0.1f(t) \tag{5.9}$$

where F_{exc} is the total excitation forces per meter and f(t) is a white noise with mean zero and variance one. The simulation time is four seconds[14] and the integration time step size is 4×10^{-4}. This small time step size is required for both accuracy and stability of calculations. The simulation results are presented in Table 5.2 in terms of rate of change of RMS value of contact forces and rate of increase in CPU computation time. As seen in Table 5.2, when the number of finite elements increases from 20 to 24, the rate of changes in contact forces does not vary significantly (approximately 3%)

---

[13] This is the typical excitation force considered in this research.

[14] This is the time duration of excitation forces.

Table 5.2: Computational efficiency of the finite element model of OTSG tube vibrations.

# of Finite Elements	RMS Values of Forces (N)	CPU Time (sec)	Rate of Change in RMS Values[1]	Rate of Increase in CPU Time
16	31.29	185.74	-------	-------
20	26.20	252.04	19.4 %	35.7 %
24	27.05	368.64	3.14 %	46.3 %

1: The absolute difference between the RMS values of forces with N and M number of finite elements over the RMS values of forces with N number of finite elements.

whereas the CPU time increases by a factor of 1.46. This indicates that the contact forces are converging to their limiting value and thus future increase in the number of finite elements does not significantly improve the accuracy of the computation but it considerably increases the CPU time of calculations. Based on this study, a tube vibration model with twenty finite elements (5 elements per span) is used in subsequent simulations because it provides sufficient accuracy with a reasonable computation time. The simulation time and the integration time step size remain same as before.

Typical dynamic response characteristics of the tube vibration model with 20 finite elements (due to the ecitiation forces of Equation (5.9)) are shown in Figures 5.4 and 5.5, respectively. The simulation of the tube displacement in Figure 5.4 indicates that the tube instantly impacts the support plate when the displacement goes beyond the tube-to-support clearance. As the consequence of these impacts, contact forces are developed at the tube/support interface locations (see Figure 5.5). They act in an impulsive manner with different magnitudes but with similar contact duration times. A typical duration time of 350 μsec and the RMS values of 26.2 N are calculated for the impact forces. Figure 5.5 also indicates that only a small fraction of the tube life is spent in contact. In this case, the overall contact time to the simulation time is only 0.012.

The frequency responses of the tube displacement and contact forces are also shown in Figures 5.6 and 5.7, respectively. The frequency responses indicate that the highest peaks for both the contact forces and the displacement occur at a frequency of 55 Hz which is same as the excitation frequency. Other frequencies do not show important

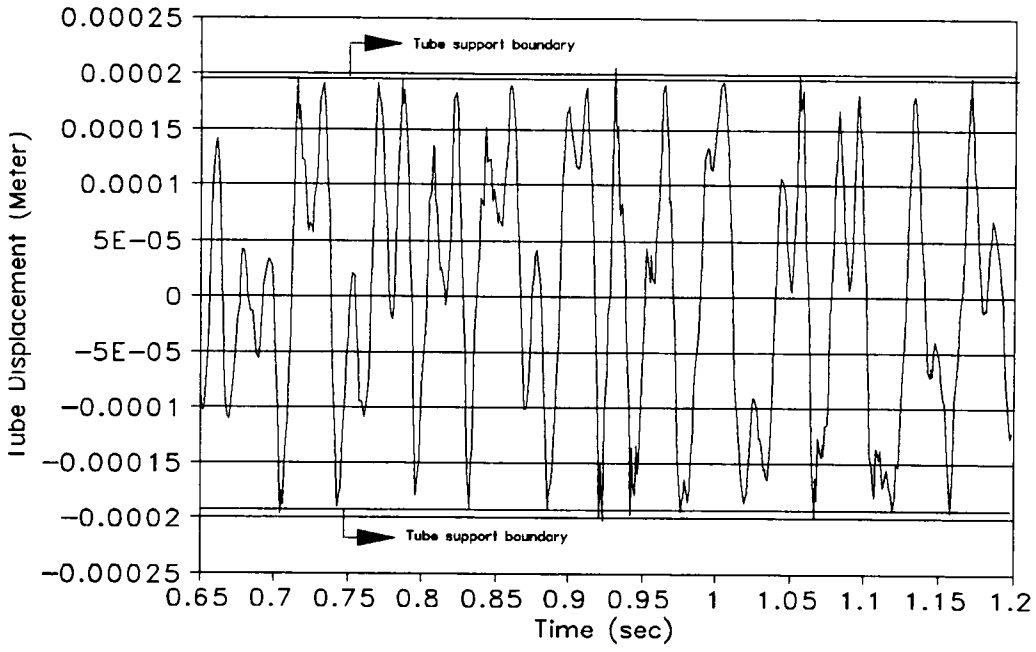


Figure 5.4: Simulation of tube displacement at the 15th tube support of an OTSG system due to the excitation forces of Equation (5.9).

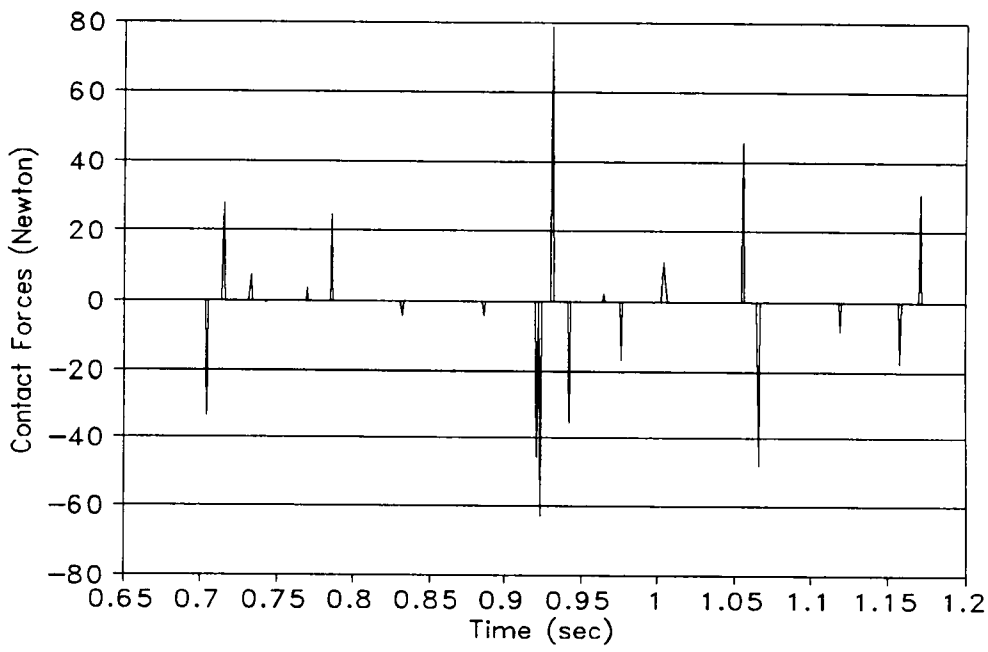


Figure 5.5: Simulation of contact force history at the 15th tube support of an OTSG system due to the excitation forces of Equation (5.9).

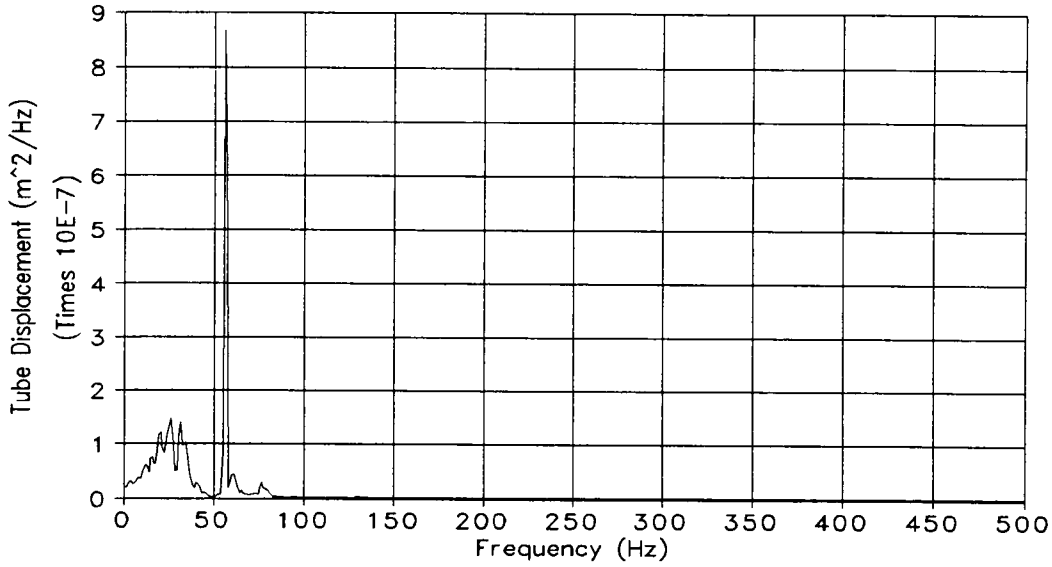


Figure 5.6: Frequency response of the tube displacement at the 15th tube support due to the excitation forces of Equation (5.9).

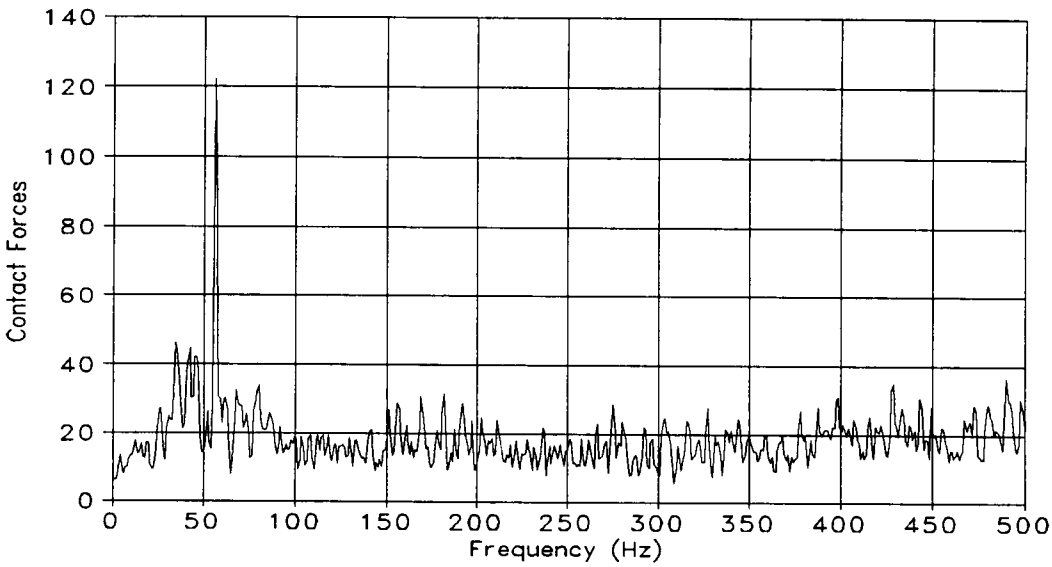


Figure 5.7: Frequency response of the contact forces at the 15th tube support due to the excitation forces of Equation (5.9).

changes in the dynamic characteristics of the tube.

As stated earlier, the analyses of the tube contact parameters were carried out only for the 15th tube support. This is due to the fact that reports from nuclear power plants using OTSG systems indicate that the most wear damage on the tubes occur in the vicinity of the 15th support [17].

5.4 Parametric Study of Contact Forces and Contact Duration Time

The computer code developed for the tube vibration was used to perform a parametric study. In accordance with step 2 of the proposed life assessment methodology, a parametric evaluation of contact forces was necessary to identify the trends of changes in contact forces and contact duration time as a function of factors associated with aging and degradation mechanisms. In an OTSG, these factors could be tube-to-support clearance, misalignment between tube and tube support, and tube support stiffness coefficient. Among all these factors tube-to-support clearance is the most important, since it is directly affected by the tube wear process. The wear of tube increases the clearance which in turn changes the contact forces and the contact time and consequently the tube wear rate. This means that the clearance and the tube wear process are inter-correlated quantities so that variation in one introduces changes in the other in a mutual manner. The clearance may also change due to environmental degradation such as deposit buildup and chemical corrosion tube thinning. Steam generator cleaning may also introduce variations in the clearance.

Tube misalignment or eccentricity is a factor which certainly changes the dynamics

of tube-to-support interaction [30]. Usually, every tubular heat exchanger or steam generator has a certain amount of tube misalignment which occurs due to manufacturing error and tube fabrication process. However, it is not well known how aging or environmental degradation may vary a pre-existing eccentricity or cause a tube misalignment. Perhaps, one possible cause could be an uneven wear of tube at the two opposite sides of the support plates. The other factor, stiffness coefficient, remains fairly constant during the life of an OTSG unit. Variation in the support material composition does affect the stiffness coefficient. This may occur because of nuclear radiation effects. However, the significance of these variations is not quite known yet. Therefore, this factor is not considered in this research study.

A parametric evaluation was carried out to determine the trends of the contact forces and contact duration time because of changes in tube-to-support clearance. Figures 5.8 and 5.9 show the variations of these parameters due to changes in the clearance. As shown in Figure 5.8, the RMS values of the contact forces increase nearly linearly with the clearance. Therefore, a linear model was used to describe the variation of such forces with the clearance. The linear variation was also confirmed by the benchmark studies performed by Ko and Roger [16], Fisher et al [30], and Sauve and Teper [23]. Figure 5.9 indicates that the contact duration time decreases nearly in an exponential manner with the clearance. Thus, an exponential fit was used to describe the changes of this parameter as a function of the clearance. These models will be later combined with the tube wear model to estimate fretting-wear rates and eventually the service life of tubes as described in the proposed life assessment

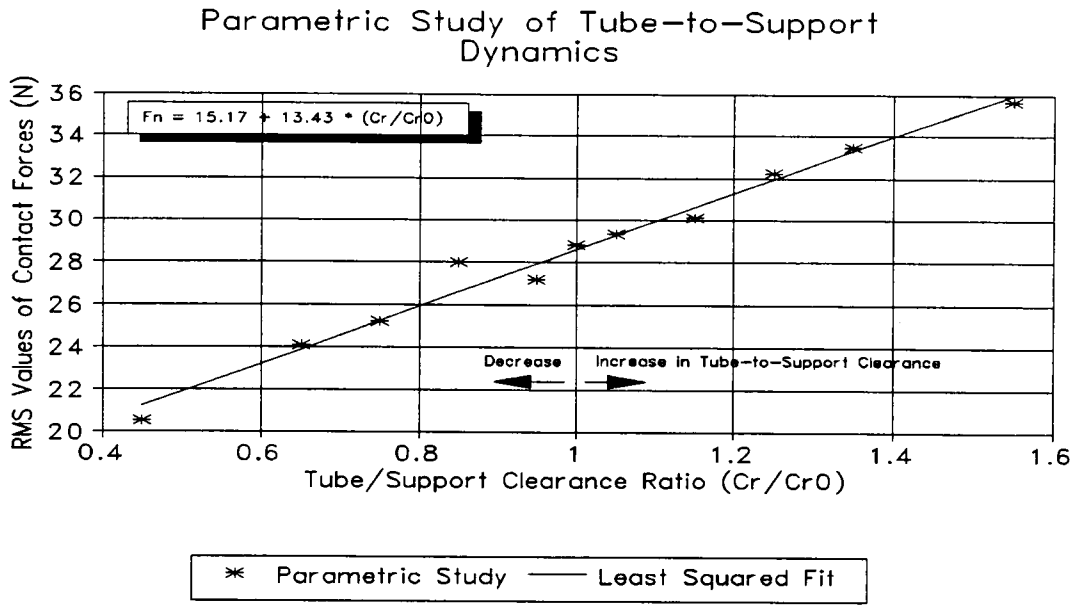


Figure 5.8: Variations of the contact forces at the 15th tube support with clearance.

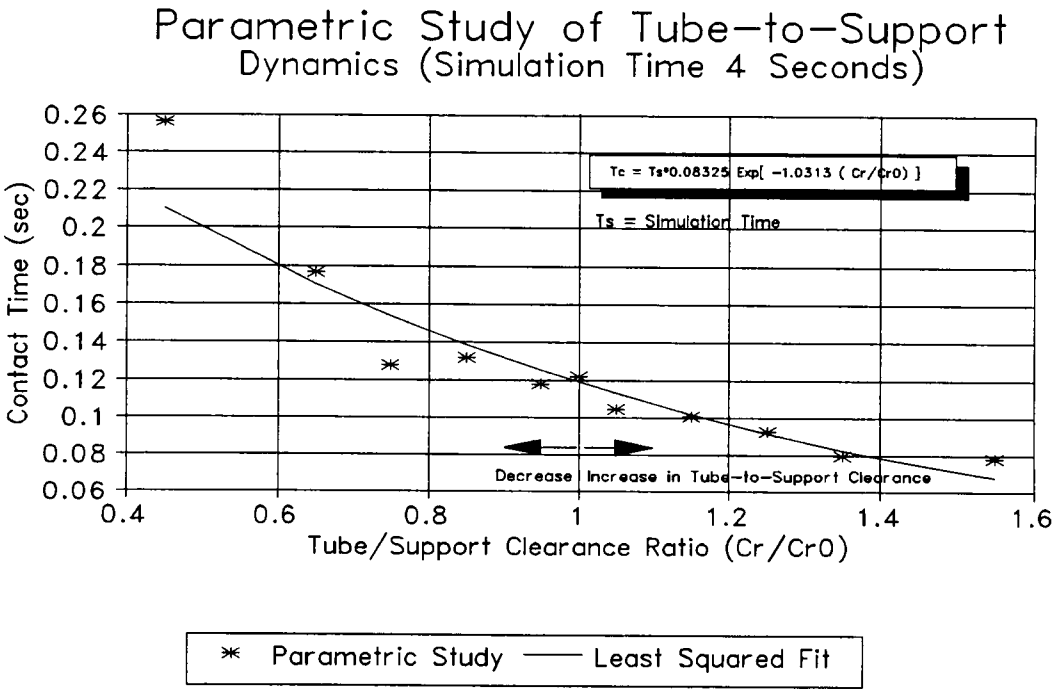


Figure 5.9: Variations of the contact duration time at the 15th tube support with clearance.

methodology.

Simulations were also conducted to understand the effects of tube misalignment on tube wear. The misalignment is considered to be the amount of tube eccentricity with respect to the tube support plate. The impact of misalignment on the contact forces and the contact time are shown in Figures 5.10 and 5.11, respectively. The figures indicate that the trends of both contact parameters increase approximately linearly with the misalignment. This means that a tube with a large misalignment is worn out more rapidly because of increases in the contact parameters.

5.5 Summary

A brief description of a typical OTSG system and its secondary flow pattern are given. Two major flow-induced vibration mechanisms that operate in such a system were identified and described. They are vortex shedding and turbulent buffeting. The excitation forces caused by these mechanisms were calculated at full power conditions of the OTSG system. They include two force components: (1) a deterministic sinusoidal force with a typical frequency of 55 Hz and an average amplitude of 2.8 N/m (representing the vortex shedding effects) and (2) a Guassian random force with mean zero and variance 0.1 N/m (representing the turbulent buffeting effects). These forces were uniformly distributed with respect to the tube axis between the 15th tube support and the upper tube sheet where the secondary flow possesses the strongest potential for the vibrations of tubes.

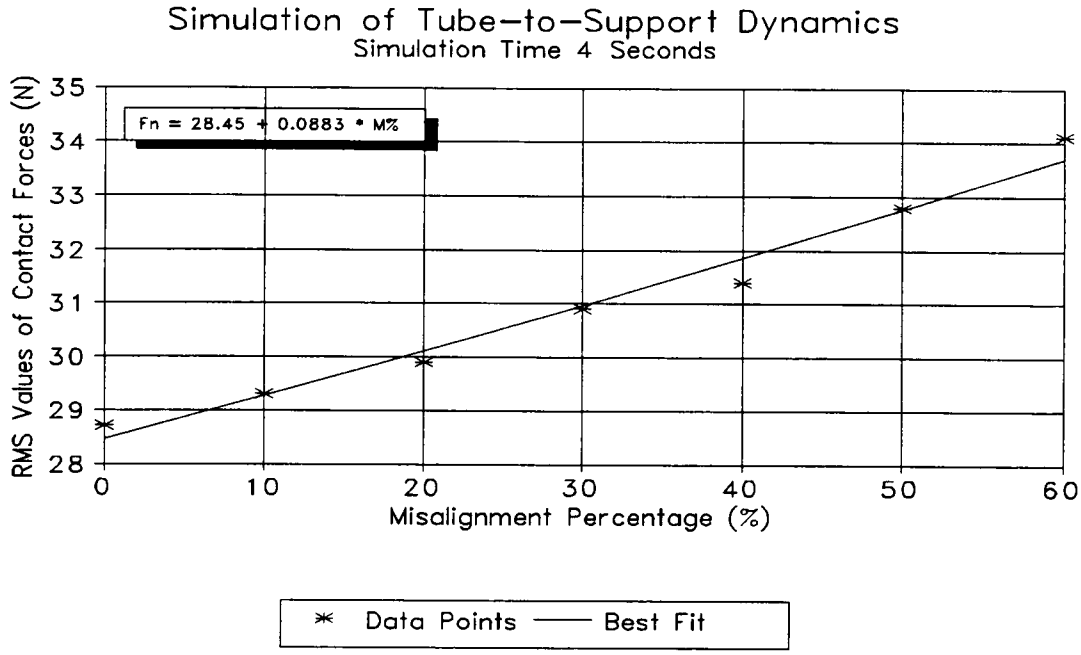


Figure 5.10: Variations of the contact forces with tube-to-support misalignment at the 15th tube support.

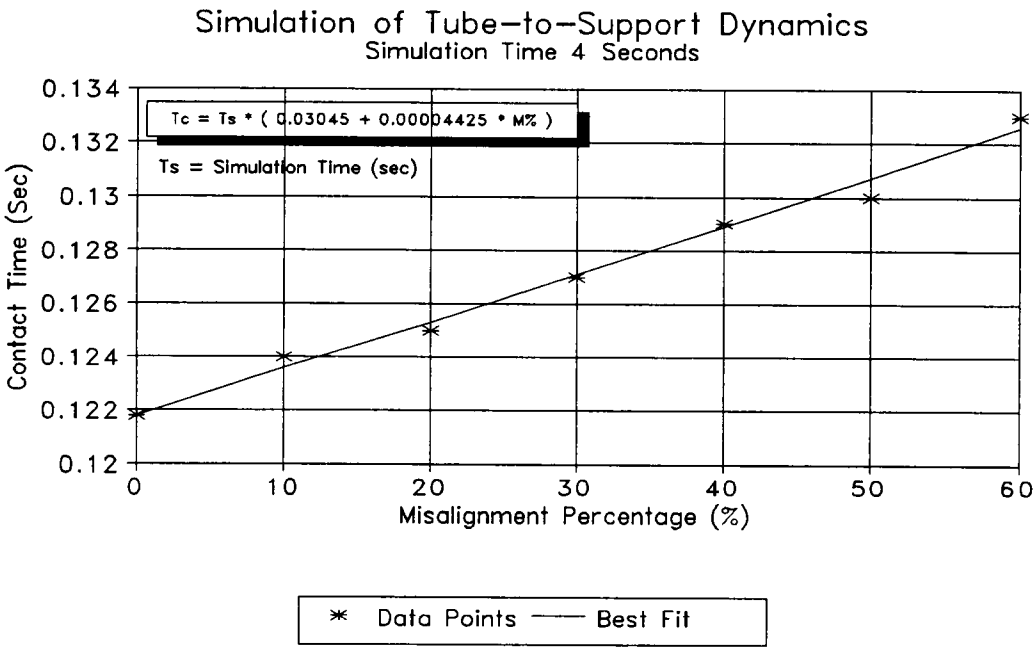


Figure 5.11: Variations of the contact duration time tube-to-support misalignment at the 15th tube support.

A computer code was developed to incorporate a one-dimensional finite element vibration model of a four-span OTSG tube. The forcing function for the model is the excitation forces produced by the flow-induced vibration between the 15th tube support and the upper tube sheet. The code was used to predict vibratory response and tube-to-support contact forces at the 15th tube support where most tube failures occur. It was also used to conduct a parametric study of the contact forces and the contact duration time because of variations in the tube-to-support clearance and in the tube misalignment. The results show that the contact forces increase linearly with the clearance but the contact duration time decreases exponentially with the clearance. They also indicate that tube misalignment can have detrimental effects since both the contact forces and the contact duration time increase with the misalignment.

CHAPTER 6

IMPLEMENTATION OF THE LIFE ESTIMATION METHODOLOGY TO THE WEAR OF STEAM GENERATOR TUBING

This chapter presents the implementation of the life assessment methodology, described in Chapter 3, for forecasting the trends of tube wear degradation processes in an OTSG system. The wear model developed in Chapter 4 was used in conjunction with the results of the parametric study of Chapter 5 to develop a computer code for the wear estimation of the OTSG tubes over a period of 30 years. The computer code generates synthetic wear data used for the construction of suitable empirical prediction models. The prediction models were established in both parametric and non-parametric forms. The parametric models employ regression analyses while the non-parametric models utilize artificial neural network methods. After building the prediction models, the (remaining) life of the tubes may be estimated with respect to an alarm level or a value for the maximum allowable wear amount. The performance of the prediction models was also evaluated to provide guidelines for selecting a correct prediction model.

This chapter also briefly describes methods and measurements used in identifying the wear mechanism of nuclear steam generator tubes.

6.1 Tube Wear Data Acquisition Methods

Steam generator tubing inspections utilize non-destructive methods to detect incipient failures and to monitor tube degradation processes. A number of non-destructive tests such as eddy current, ultrasonic, and radiographic methods are available for detecting anomalies and damage mechanisms that may develop at various tube locations [77,79]. Among all these tests, the eddy current technique is probably the most reliable, the most widely used, and in many respects the most convenient method for in-service inspection of tube integrity in heat exchangers and steam generators. This method employs a bobbin type probe that embodies one or two AC coils which induce electric current (or magnetic field) around the tube. The presence of flaws, material discontinuity, and dimension variations will cause changes in the coil impedance that are sensed by eddy current signals such as the coil current and voltages. The signals are then conditioned, processed, and recorded (or displayed) by a variety of electronic instruments for later analysis.

The phase angles and amplitudes of eddy current signals can be used to determine various anomalies and information about the changes. The analysis of these quantities can provide the information necessary to classify the types of flaws, to estimate the size of variations, and ultimately to identify the status of tube integrity. The accuracy and reliability of the analysis depend partly on the sensitivity of the probes in detecting small changes. Probes with different coil configurations (such as rotating pancake and multi-frequency coils) can enhance specific detection or sizing capabilities. This is particularly important for the estimation of the tube wear amount since the wear scars

typically initiate with tiny and small sizes on the tube surface. EPRI investigations [42] on the accuracy of the wear measurement using eddy current testing in conjunction with ASME eddy current standards and guidelines indicate that the measurement tends to be a little more conservative than that of metalographic tests. The results of the investigations show that an average discrepancy of 8% exists for different wear shapes and sizes. However, Ko [15] stated that eddy current tests can provide sufficient accuracy for the estimation of tube wear. In his experimental studies of the tube wear process, the test was able to detect metal loss from the tube surface equivalent to a uniform wear with depth 5μm. Future developments and advances both in eddy current technology and in data processing methods are expected to markedly improve the accuracy of this test.

It should be noted that in nuclear steam generators, eddy current testing can produce a gigantic amount of data due to the number of tubes to inspect and the number of signals (for each tube) to process. Thus, an in-depth and elaborate analysis of such a huge database for detecting small variations is extremely hard especially with difficulty in data interpretation. Over the past years, this has presented a stumbling block to systematically collect historic data and information for trend analysis of the tube degradation mechanisms. In the past, the way that most power utilities had used eddy current tests was mainly based on comparing the tube test patterns with some reference patterns or the previous patterns of the same tube in conjunction with certain guidelines (such as ASME) to make decisions about the fate of suspected tubes. In addition, they normally performed the tests for random samples of the tubes in sensitive locations of

a steam generator [17] to reduce the amount of data to be processed.

This shows that more automation is required for both signal processing and signal classification in such tests. In fact, recent developments in the applications of artificial neural networks and expert systems to data processing and pattern recognition of eddy current signals have produced encouraging results for detecting small anomalies, defects, and abnormalities [78].

6.2 Experimental Studies of Tube Wear Mechanisms in Heat Exchangers

The number of experimental studies on the wear of heat exchanger and steam generator tubes is small but growing. Ko [15] has perhaps performed the most detailed experimental studies of wear mechanisms of heat exchanger and steam generator tubing. He developed testing equipment to investigate fretting-wear between tube and tube support. The test apparatus included a vibration generator, tube and tube support specimens, transducer platform, and top and bottom support plates. It was designed to provide a simple unidirectional tube motion, or a combined impact and sliding motion. The device was used to conduct several tests to correlate tube wear rate with material combination, support reaction force, tube/support clearance and test duration time. The major findings of these tests are as follows:

1. The wear rate of Inconel 600 tubing increases with increasing clearance for a carbon steel tube support.

2. Tube materials of Incoloy 800 of the Incoloy 800/Inconel 600 pair show severe surface damage of the adhesive type which is attributed to the fretting-wear resulting from impact and sliding motions.

3. For long duration tests in a range of 1000 to 5000 hr, the wear rate trends of tubes with Incoloy 800 and Monel 400 increase with time under moderate excitation forces with a time exponent greater than one. This is shown in Figure 6.1.

The author also concluded that tube fretting-wear seems to include the following stages: the dispersion of surface film by oscillating movement, adhesion, plastic deformation, and metal transform.

Although this experimental study did not exactly simulate the real-world tube wear mechanisms which take place in steam generators and heat exchangers, it did provide qualitative information about the changes in the wear process with regard to time and other parameters influencing tube fretting-wear. This study also demonstrated that the general trends of the tube wear rate could increase with time in a nonlinear manner.

6.3 Simulation Procedure for Tube Wear Degradation

In Chapters 4 and 5, the basic models required to determine the wear amount of a typical OTSG tube are derived and described. These models are: tube wear process, degradation and aging of the friction coefficient and shear yield strength point, and parametric study of contact forces and contact duration time. In this section, a procedure or an algorithm for simulating the tube wear amount using the above models is presented. The algorithm generates a sequence of steps to calculate the wear amount according to the flow chart of Chapter 3 (Figure 3.5). As it will be shown later, when the models are combined together the resulting relationship for the wear calculation will take an implicit closed form with respect to time which requires a numerical solution.

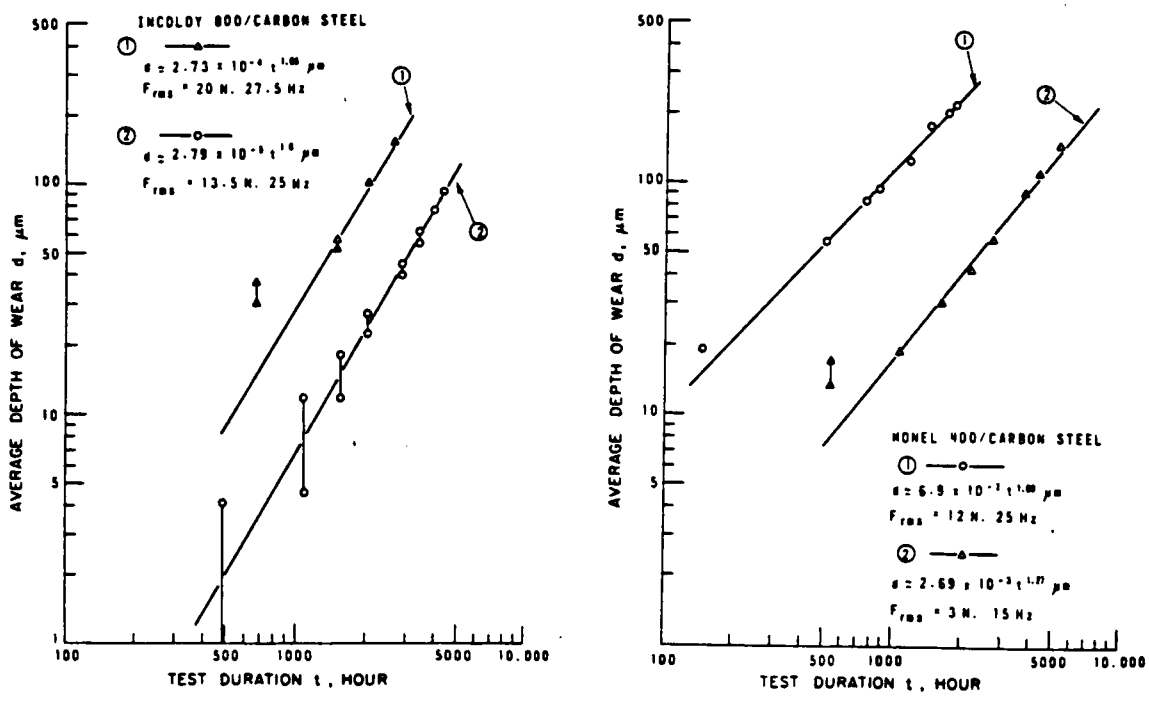


Figure 6.1: Variation of the wear mechanism with time for tubes with Incoloy 800 and Monel 400 materials (carbon steel is the tube support material) [15].

The first step in developing the solution procedure is to organize all necessary models and relations required to solve the problem in proper forms. Starting from the tube wear model of Chapter 4, the integral form of the model for a time interval of dt = t_{i+1}-t_i is

$$W\Big|_{t_i}^{t_{i+1}} = K\int_{t_i}^{t_{i+1}} \frac{\mu(t)\,F_n^{\,k}(t)}{\tau(t)}\,dt_c \tag{6.1}$$

where W corresponds to a uniform metal loss from the surface of tube within its tube support. It can also be expressed as the difference between tube-to-support clearance between time t_i and t_{i+1}.

$$W = Cr(t_{i+1}) - Cr(t_i) \tag{6.2}$$

The normal contact force, F_n, and the contact duration time, t_c, are time varying quantities since the wear process continuously changes the clearance with time. From the parametric study of Chapter 5, these variables take the following forms at time t_{i+1}:

$$\begin{aligned} F_n(t_{i+1}) &= a_1 + a_2\left(\frac{Cr(t_{i+1})}{Cr_0}\right) \\ &\text{and} \\ t_c(t_{i+1}) &= a_3\, t_{i+1} \exp^{\left(a_4 \frac{Cr(t_{i+1})}{Cr_0}\right)} \end{aligned} \tag{6.3}$$

where a_1 to a_4 are the constant parameters of the models as calculated in Chapter 5. Finally, as suggested in Chapter 4, the aging relations for the coefficient of friction and the shear strength yield point have the following forms:

To obtain a relationship for the calculation of the tube wear amount as a function

$$\mu(t_{i+1}) = \mu_0 + a_5 (t_{i+1})^{a_6}$$
$$\text{and} \qquad (6.4)$$
$$\tau(t_{i+1}) = \tau_0 \exp^{(\alpha t_{i+1})}$$

of time, Equations (6.2) through (6.4) should be combined with Equation (6.1). However, a quick review of these equations reveals that the combined equation will be in an implicit form since both the contact force and the contact duration time are interdependent and are correlated with the tube-to-support clearance which is directly proportional to the wear amount (see Equation (6.2)). Therefore, a recursive method is required to solve the problem.

A computing algorithm is devised to solve the above problem as shown in Figure 6.2. The algorithm treats the integrand of Equation (6.1) as a summation for a sufficiently small value of $dt \approx \Delta t = t_{i+1}-t_i$. It also calculates the variables of Equation (6.3) with $Cr(t_i)$ instead of $Cr(t_{i+1})$. This will result in an explicit solution of Equation (6.1) in a sequential fashion as shown in Figure 6.2. To ensure a good approximation, the time interval Δt is set to one hour[15] in this study. This means that during one hour of operation, the variables related to the wear process remain constant. For all practical purposes, this value is small enough to yield an accurate estimation of the tube wear. Indeed, the changes in the variables from one hour to another can be only detected by double precision digits. Also, physically, there will be insignificant changes in the wear process during one hour of operation. In fact, the suggested design value for the wear

[15] A larger time interval may also be used if the integrand is estimated by the Trapezoidal rule or the Simpsons's rule. However, a larger time interval may introduce errors in the calculation of contact forces and contact time which are performed in a recursive fashion.

INPUT model parameters

Step 1

For i = 0,1,...,n do steps 2-7
Set $\Delta t = t_{i+1}-t_i$ ***Equal time step size; 1 hr***

Step 2: Contact forces:

Set $F_n(t_{i+1}) = a_1 + a_2(C_r(t_i)/Cr_0)$ ***Recursion***

Step 3: Contact time duration:

Set $\Delta t_c = a_3\ (t_{i+1}-t_i)\ \exp(\ a_4 Cr(t_i)/Cr_0\ )$

Step 4: Calculate the coefficient of friction and shear yield strength point:

$$\mu(t_{i+1}) = \mu_0 + a_5(t_{i+1})^{a6}$$

$$\tau(t_{i+1}) = \tau_0\ \exp(\alpha t_{i+1})$$

Step 5: Compute tube-to-support variation due to the wear

$$Cr(t_{i+1}) = Cr(t_i) + K\Delta t_c \mu(t_{i+1})(F_n(t_{i+1}))^m\ /\ \tau(t_{i+1})$$

Step 6: Compute the total reduction in the tube wall thickness

$$W = \sum \{Cr(t_{i+1}) - Cr(t_i)\};\quad i = 1,2,3,...,n$$

Step 7: Output t, W, F_n, t_c, μ, τ into a data file with time interval of 1 year.

Step 9: Stop

Figure 6.2: A computer algorithm for the estimation of tube wear amount.

rate of heat exchanger and steam generator tube (during one hour) is in the order of 1.0 $\times 10^{-6}$ mm/hr, for a tube wall thickness of approximately 1 mm and a design life of 30 years [15].

The constant parameters of the wear model, namely K and m, are chosen from the experimental wear model developed by Pettigrew [5] (see Chapter 4 section 4.4) for Incoloy 800 and Inconel 600 as tube and tube support materials. The model parameter K was modified by a correction factor to take into account the frequency of vibration, conversion of metal losses to equivalent tube diameter changes (from grams to millimeter), normalization with respect to the coefficient of friction and shear yield strength point, and a proper unit (mm/hr). Table 6.1 shows a list of numerical values of all constant parameters used in the simulation.

A computer code written in FORTRAN language, called WEAR, embodies the described algorithm in order to calculate the wear amount. The simulation time is considered to be 30 years which approximately corresponds to the design life of steam generators [15]. The code generates a data file to store the calculated (cumulative) wear amount during each year of operation. The time interval of one year is analogous to the time interval that may occur in the real-world historic data of steam generators[16]. Appendix C presents the source program of the tube wear model.

Figure 6.3 represents typical simulations of the OTSG tube wear process due to variations in the coefficient of friction. When the coefficient of friction is constant, the

---

[16] As noted in Chapter 1, service inspections of nuclear steam generators are performed approximately once a year. This results in a time interval of approximately one year in the collected tube data.

Table 6.1: Values of constant parameters of the tube wear process model.

Constant Parameters of the Tube Wear Model	
Tube Diameter	15.875 mm
K	1.2×10^{-6} (mm/hr)
m	4.75 (---)
a_1	15.17 (N)
a_2	13.43 (N)
a_3	0.08325 (---)
a_4	-1.0313 (---)
a_5	0.005 (---)
a_6	1 to 2.5 (---)
Cr_0	0.1905 (mm)
μ_0	0.1 (---)
α	0 to -0.03 (1/year)

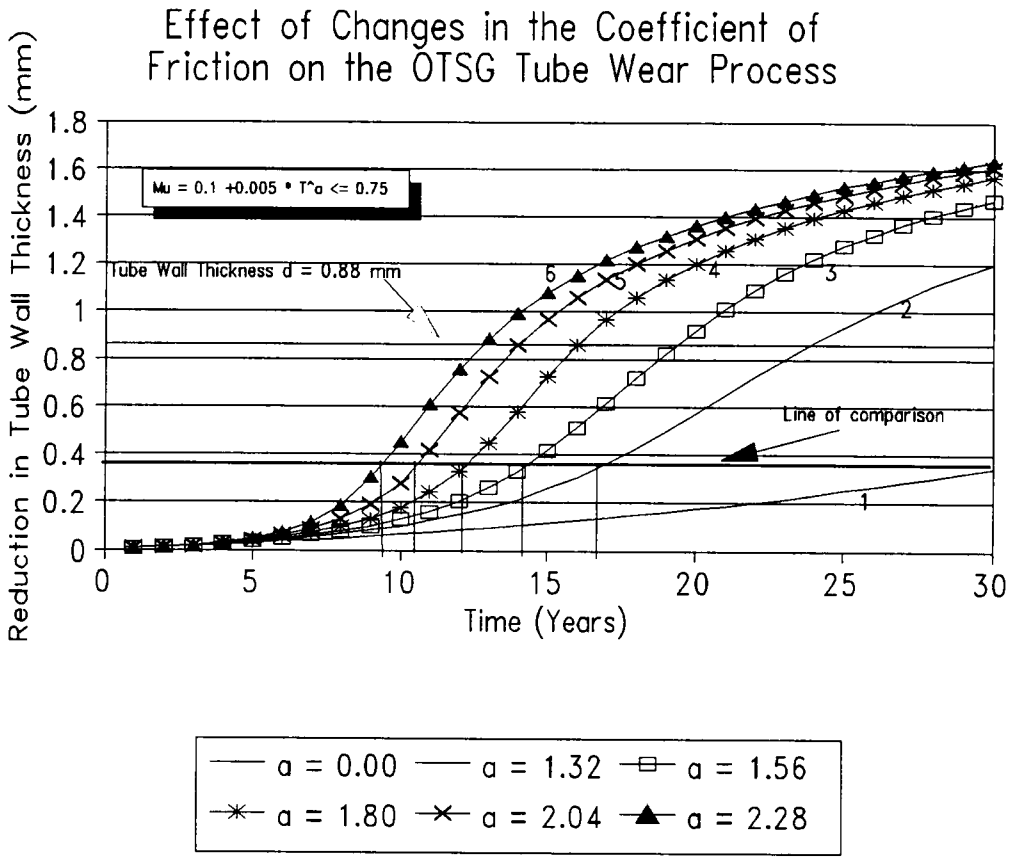


Figure 6.3: Simulation of the tube wear process using a time varying friction coefficient.

trend of wear process appears to be moderately non-linear with time. This nonlinearity is due to the fact that the wear process increases tube-to-support clearance which in turn changes the contact forces and the contact duration time. This is a typical wear trend that is expected to occur for the majority of the tubes according to the design calculations. However, if aging and degradation mechanisms influence the process, the trends can abruptly change. Figure 6.3 indicates that as the coefficient of friction degrades with time, the rate of tube wear first increases rapidly (up to 0.4 mm reduction in the tube wall thickness) and then decreases gradually with time. The figure also shows that when the exponent in the model for the coefficient of friction changes from 1.32 to 2.28 the corresponding tube life, with regard to the case of constant friction factor (a=0 in the figure), reduces approximately from 17 to 8.5 years. This demonstrates that how certain degradation or aging mechanisms can effectively reduce the useful life of a component. Although in practice there may be just a very small fraction of tubes that experiences such severe case of degradation, their impact could be extremely important from the standpoint of safety and accident related issues for industries such as nuclear power plants and chemical processing units.

A careful examination of the plots of tube wear simulation in Figure 6.3, indicates that the rate of changes in the wear trends start gradually decreasing after the tube wall thickness is reduced by 0.4 mm. This is due to the fact that generally, when the tube-to-support clearance increases beyond a certain point, the effect of reduction in the contact time becomes more dominant than the influence of increases in the contact forces. Therefore, the wear rate starts decreasing toward a zero rate which corresponds

to the loss of contact between the tube and its tube support plate. This can also be perceived conceptually from the mathematical description of the tube wear model presented earlier in this section. Ko [15] has also observed the occurrence of such phenomenon in his experimental studies.

The tube wear data generated in this fashion will be used in the next sections to establish semi-empirical prediction models as explained in Chapter 3.

6.4 Development of Parametric Prediction Models

As described in Chapter 3, one way to predict the future trend of a given degradation process is through a parametric regression model in which the process trend has a relationship that depends explicitly upon time as the regression variable. A first problem encountered when dealing with parametric models is that of assessing an approximate nature of the relationship between the degradation process under study and time. In the case of tube wear degradation, when the process model is not an explicit function of time, the type of model should be chosen so that it produces trends similar to those of the process model. The choice of a model should be frequently made on the basis of considerations such as (1) the compatibility of the model with the physics of the process, (2) the degree of model complexity, (3) the ease of mathematically handling the model, and (4) the amount of available data for a reliable estimation of model parameters. These are important issues especially when a model is applied to the trend prediction of real-world data which may be ill-conditioned. Based on the above considerations, two parametric models were established to extrapolate the future

trends of the tube wear process for two cases of tube wear degradation with three different block sizes of data.

6.4.1 Case Study #1: Normal Tube Wear Degradation

In this case study, it is desirable to construct models that adequately describe the trends of the tube wear process when the effects of aging or degradation of process variables, namely the coefficient of friction and shear yield strength point, are negligible. This is the situation that majority of OTSG tubes may experience during their life time based on design calculations. For such a case, two types of models are considered. They are

$$W(t) = a t^{b} \tag{6.5}$$

$$W(t) = a t^{b} \exp(ct) \tag{6.6}$$

where W is the cumulative wear amount and a, b and c are contact parameters to be estimated from available data.

The reason for choosing model of Equation (6.5) is that it has exhibited a relatively good agreement with the trends of experimental data as reported by Ko [15]. It is also the simplest type of model (includes only two parameters) that can explain to some extent the nonlinearities associated with the wear process trends. This model is customarily called as a Power-Law model [62].

The model of Equation (6.6) is derived from an approximation of the wear process model. In a process model if Cr(t) (tube-to-support clearance) presumably varies in a

manner proportional to time, then this model will result. The model includes both exponential and power terms which correspond to the physics of the contact duration time and the contact forces. In this study, it is called as Power-Exponential model.

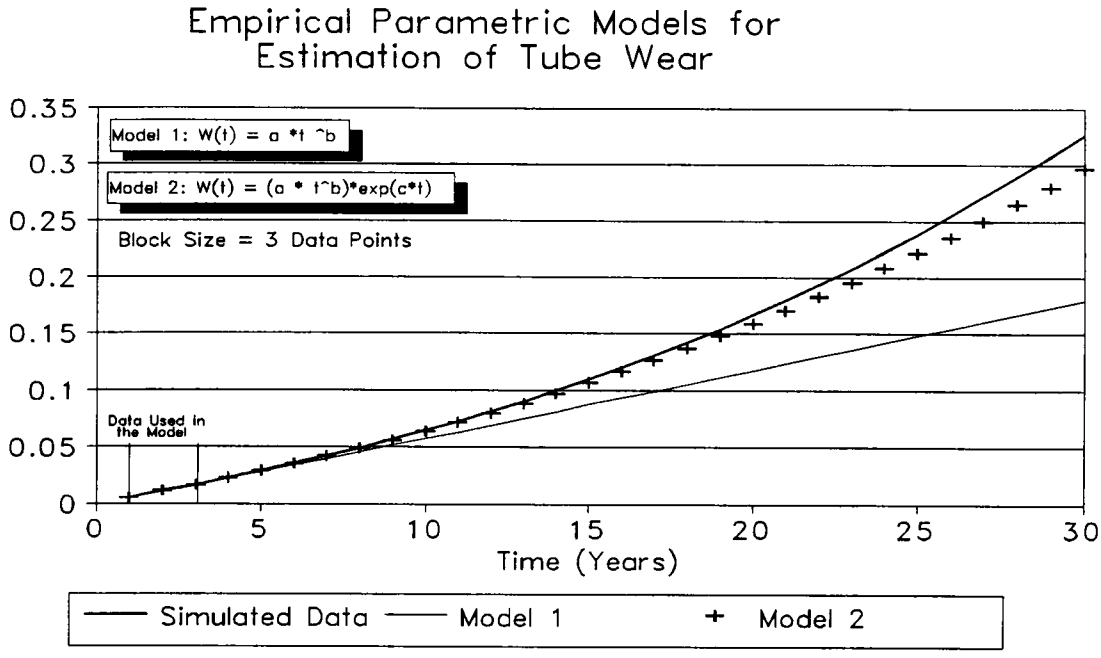
Both models satisfy the condition of zero degradation at time zero and the four considerations stated earlier for the construction of parametric models.

The process model was used to generate data in order to examine the performance of the suggested regression models. The models were fit to three data sets each containing 3, 5, and 10 data points, respectively. The time interval between two successive data points was 1 year corresponding to the time interval that usually occurs in real-world data. For each fit, the model parameters were estimated and the goodness of fit was analyzed using the SAS software system [86]. Table 6.2 shows the results of the analysis along with the parameters of the models.

The models were then used to predict the future trends of the wear process. Figure 6.4 shows the predictions of the models in comparison with the actual process trends. As seen in the figure, the Power-Exponential model (M2) follows closely the process trend whereas the Power-Law model (M1) tends to diverge as time increases. This implies that model M2 is more compatible with the physics of the process than that of model M1. The figure, however, indicates that model M1 provides a good prediction for a few points after the last data point used in the model construction. For instance, when 3 data points are utilized to construct the model, the model prediction matches very closely (with an RMS error of less than 0.005) with the process trend for the next 7 points (corresponding to a time of 10 years). This suggests that model M1 may be

Table 6.2: Estimated values of the parameters of the prediction models for the case of smooth wear data.

Model Type	# of Data points	Model Parameters			RMS Error of fitting	RMS Error of Prediction
		a	b	c		
1	3	5.272e-3	1.0371	--------	0.0	0.0645
at^b	5	5.242e-3	1.0514	--------	0.00157	0.0626
	10	5.106e-3	1.0867	--------	0.0065	0.0587
2	3	5.166e-3	0.9982	0.0218	0.00001	0.0124
at^b* exp(ct)	5	5.164e-3	0.9975	0.0222	0.000013	0.0115
	10	5.159e-3	0.9939	0.0236	0.000016	0.0087



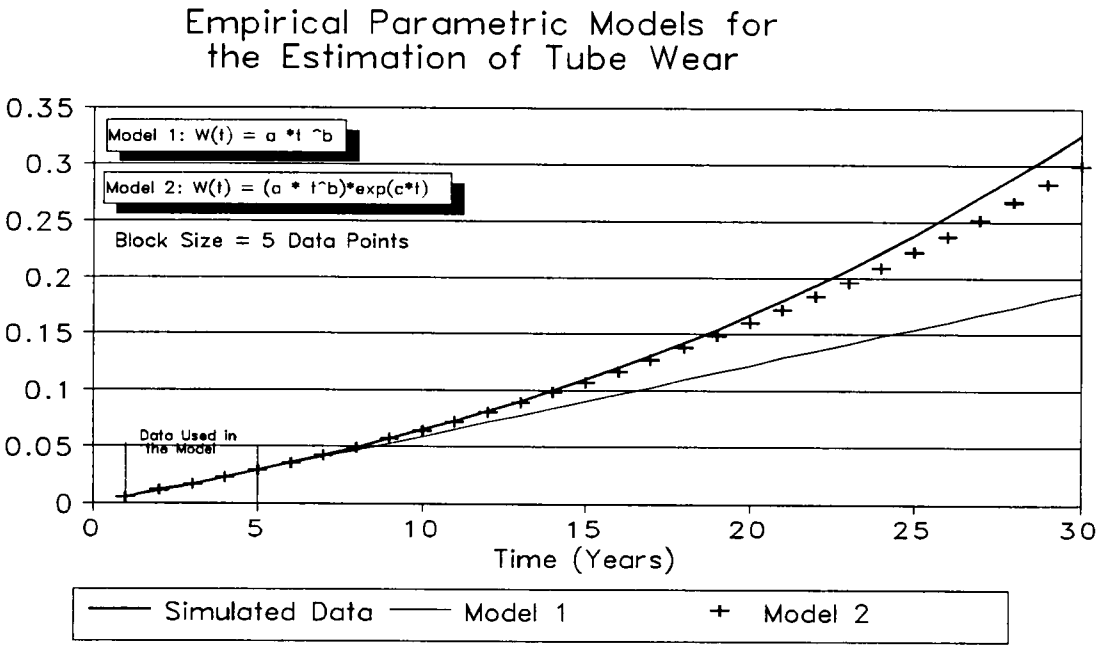


Figure 6.4: Trend prediction of a normal tube wear degradation using semi-empirical parametric models with three different block sizes of data.

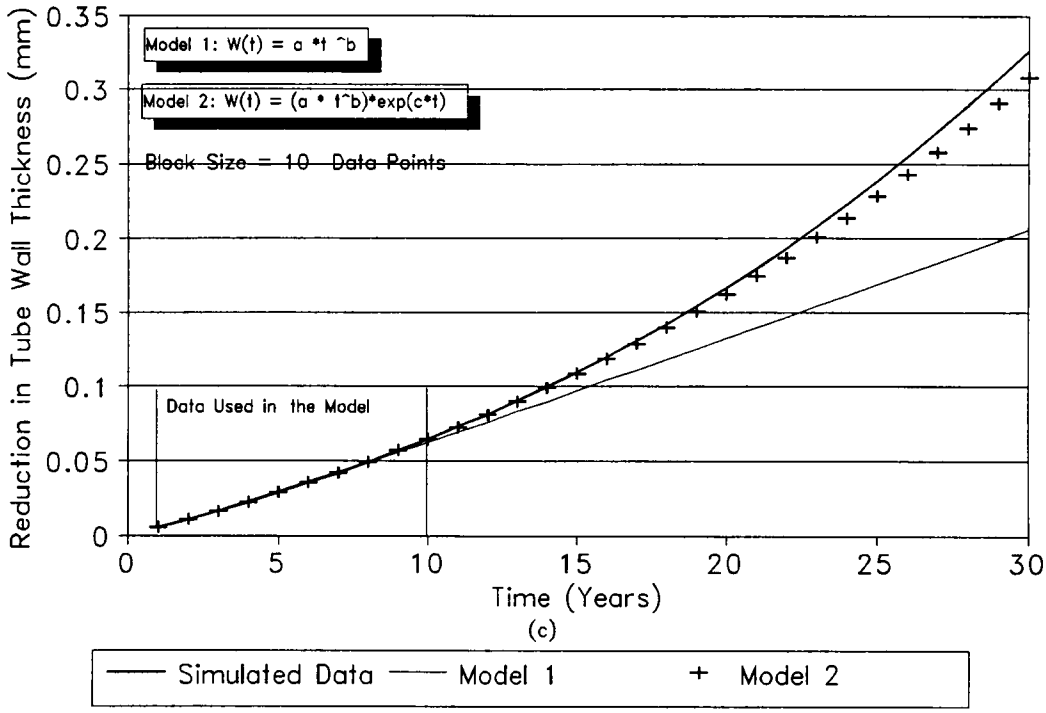


Figure 6.4 (continued)

suitable for short term predictions when sufficient data are not available to use a more detailed model. The only advantage of model M1 over model M2 is that M1 has a fewer parameters to estimate.

For the real-world data, the estimation of model parameters becomes an important issue if the available process data are limited and contaminated with measurement noise. The measurement noise can bias the estimation of the parameters if the sample size is not large enough to diminish its effects. For example, when the sample size contains 3 data points, it just provides the minimum number of required data to estimate the parameters of the model M2. Thus, it is expected that any fluctuations in the data points biases the estimation of the parameters. The effect of measurement noise on the stability of model parameters has been investigated here to provide some guidelines for applying these models to real-world data which usually include some level of measurement noise.

In this research, the measurement noise is simulated as a white noise with mean zero and variance one. The noise is then added to the simulated wear data according to the following relationship

$$W_n(t) = W(t)\,[1+\alpha\, n(t)] \tag{6.7}$$

where

$W_n(t)$ = Noisy wear data

$W(t)$ = Simulated wear data

$n(t)$ = Simulated white noise

α = Noise percentage (fraction)

Noise levels of 2%, 4% and 6% were added to the simulated wear data of the previous cases. Then, they were used to re-estimate the parameters of models M1 and M2 in order to understand the influence of noise on the estimation. Table 6.3 presents the results of the estimation with three sample sizes of 3, 5, and 10 data points for each case.

As shown in the table, for the sample size of 3 data points the parameters of model M2 vary noticeably with the amount of noise level. This is expected since a minimum number of data points, three, has been used to estimate the three model parameters. Therefore, although model M2 provides a better approximation of the wear process trend, its performance degrades in the presence of noise in the data. This means that at the beginning of a wear degradation process, if sufficient data are not be available a simpler model should be used so that measurement noise does not affect its performance drastically. For the model M1, however, there are minor variations in the model parameters for the same amount of noise level. This indicates that this type of model is more suitable for the cases that sufficient when data are limited.

Table 6.3 also indicates that the model parameters become more stable against the measurement noise if more data are employed for the estimation. For instance, the variations in the parameters of both models become negligible when 5 and 10 data points are used. This study clearly demonstrates that the choice of using a prediction model should also be based on the amount of required data in order to perform a sound estimation of model parameters.

Table 6.3: Estimated values of the parameters of the prediction models for the case of noisy wear data.

Model Type	# of Data points	Model Parameters for Data with 2% Measurement Noise			Variations in Model Parameters with Respect to 0% Noise (Table 6.2)
		a	b	c	a b c
1 at^b	3	5.3268e-3	1.0266	--------	1.04% 2.35% ---
	5	5.2922e-3	1.0449	--------	1.0% 0.60% ---
	10	5.1565e-3	1.0790	--------	0.9% 0.70% ---
2 at^b* exp(ct)	3	5.053e-3	0.9263	0.0563	2.1% 7.20% 158%
	5	5.206e-3	0.9867	0.0234	0.8% 1.06% 8.0%
	10	5.21e-3	0.9867	0.0234	0.9% 0.72% 0.5%
Model Parameters for Data with 4% Measurement Noise					
1	3	5.388e-3	1.0162	-------	2.2% 2.01% ---
	5	5.341e-3	1.0386	-------	1.9% 1.22% ---
	10	5.207e-3	1.0710	-------	1.9% 1.43% ---
2	3	4.942e-3	0.8549	0.0906	4.3% 14.3% 315%
	5	5.249e-3	0.9766	0.0239	1.6% 2.10% 15%
	10	5.260e-3	0.9795	0.0232	1.9% 1.44% 1.3%
Model Parameters for Data with 6% Measurement Noise					
1	3	5.434e-3	1.006	-------	3.1% 3.02% ---
	5	5.390e-3	1.032	-------	2.8% 1.81% ---
	10	5.258e-3	1.062	-------	2.9% 2.10% ---
2	3	4.834e-3	0.784	0.1248	6.4% 21.4% 472%
	5	5.292e-3	0.966	0.0271	2.4% 3.15% 22%
	10	5.312e-3	0.972	0.0230	2.9% 2.21% 2.2%

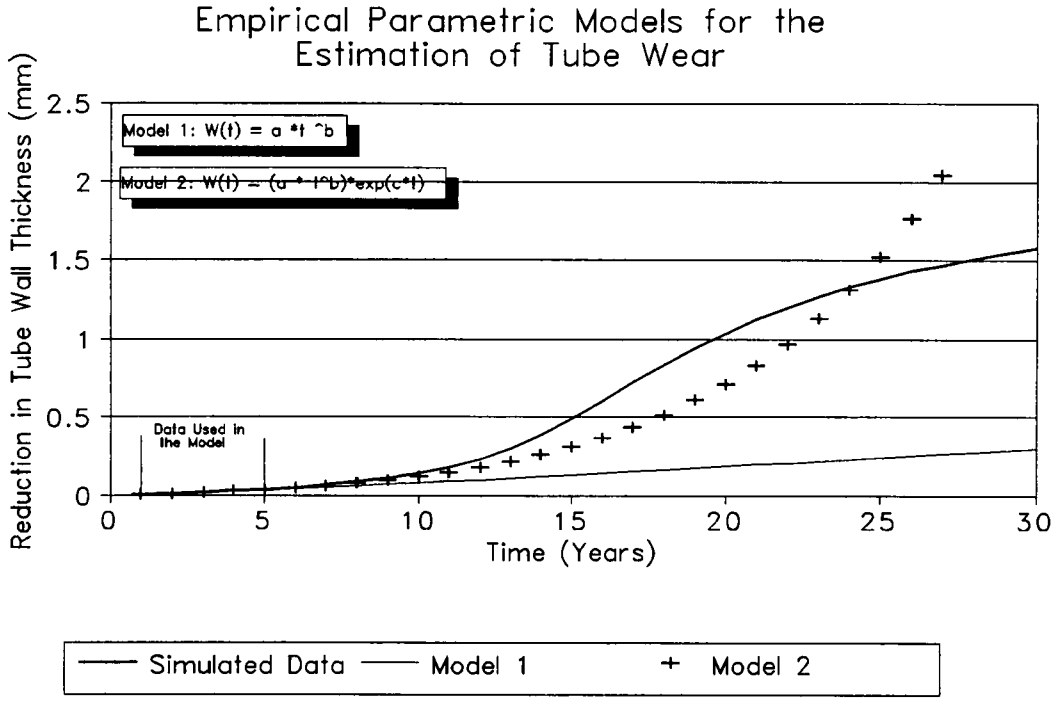
6.4.2 Case study #2: Rapid Tube Wear Degradation

The wear degradation could accelerate rapidly as the process variables such as the coefficient of friction and shear yield strength point start degrading with time. As explained in Chapter 4, this is a situation which may be experienced by some tubes in a steam generator.

Similar to the previous case study, the wear process model was employed to generate data for developing suitable prediction models. The data were generated with a time exponent of 1.5 for the friction model and an aging factor of α = -0.01 (1/year) for the shear yield strength point.

Models M1 and M2 were again used to approximate the trends in the process. There are three reasons for using the same models. First, the coefficient of friction is a power function of time and the shear yield strength point is an exponential function of time. Therefore, they can be represented by model M2 without any further modifications. Second, the parameter estimation of these models do not require extensive data. Third, if the models are suitable for the trend prediction of both rapid and normal degradation processes, this will allow us to specify prediction models in a more generic sense. A more complex model will be also examined later in this section.

Two sets of data, each containing 5 and 10 data points, were used to estimate model parameters. The structure of the data sets is similar to that of the previous case. As shown in Figure 6.5, when a block size of 5 data points is utilized, Model M2 provides a good approximation of the process trend up to 8 points beyond the last point used in the model construction. However, model M1 tends to underestimate the trends after



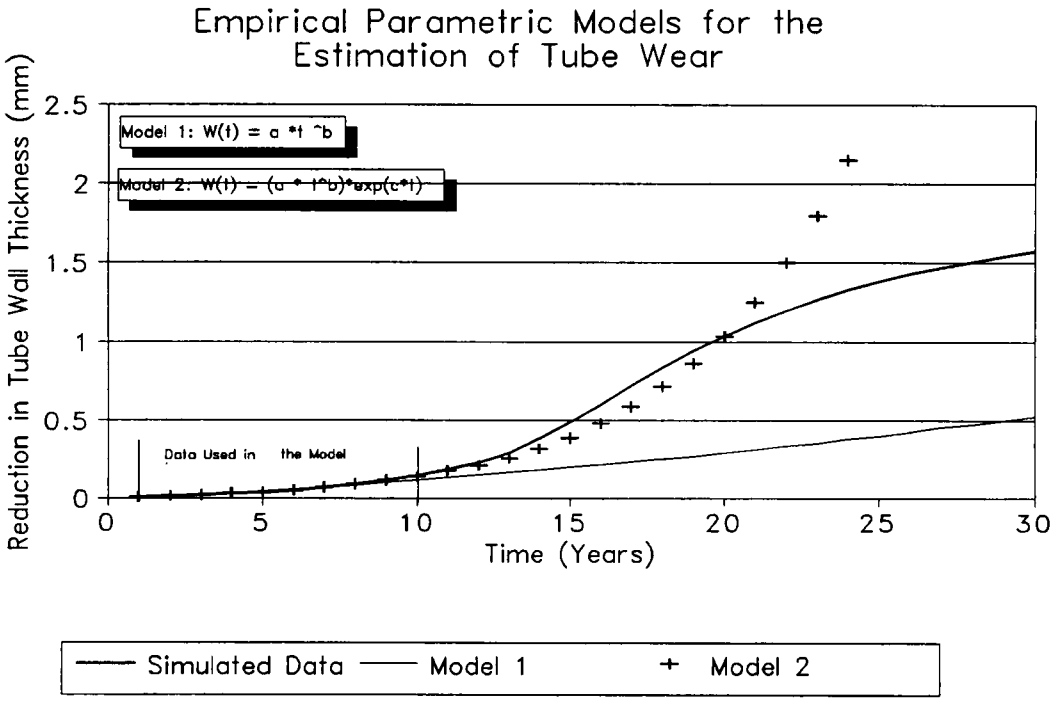
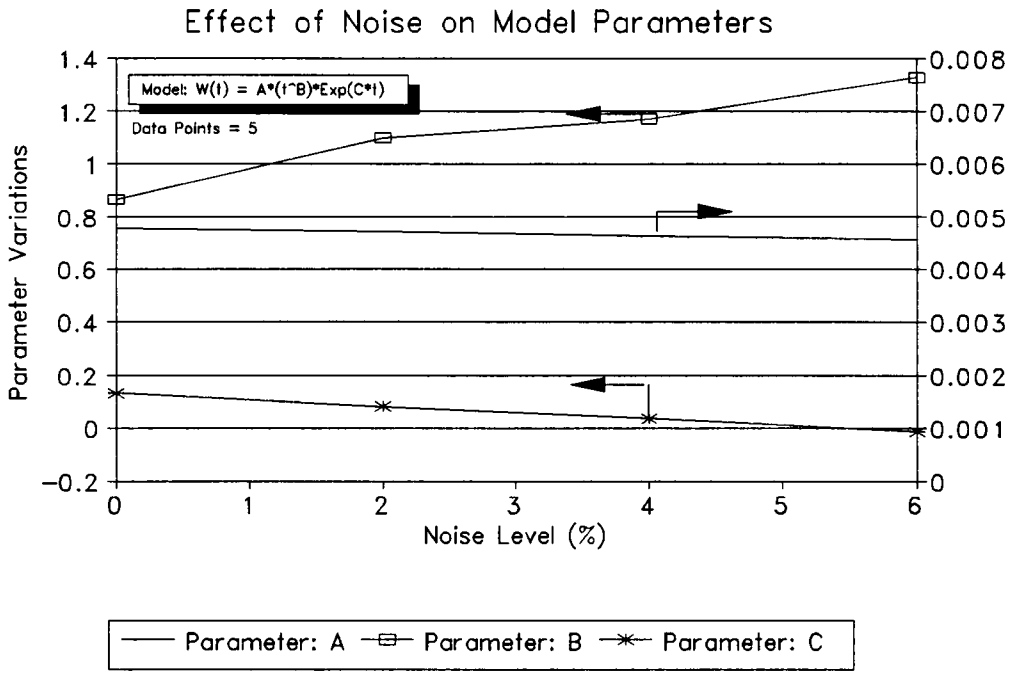


Figure 6.5: Trend prediction of a rapid tube wear degradation using semi-empirical parametric models with two different block sizes of data.

showing a good prediction for only four points. The figure also indicates that the predictions of both models improve as more data become available. However, model M2 exhibits a better improvement in its predictions than that of model M1 when 10 data points were used. This is again due to the fact that model M2 approximates the physics of the process more accurately than model M1.

The performance of model M2 was also examined against different measurement noise levels. As seen in Figure 6.6, as the noise level goes beyond 1%, the model parameters considerably fluctuate for the case of 5 data points. However, they exhibit a good stability against the measurement noise when 10 points are used (see the figure). Figure 6.7 shows the effect of noise on the model predictions for the case of 5 data points. It clearly indicates that the prediction collapses when the noise level reaches 6%. The noise analysis suggests that model M2 may not be suitable for fitting to a small sample size of real-world data. As a rule of thumb, a minimum of 2 data points per model parameter should be utilized for the parameter estimation process. A simpler model such as M1 may provide a more reliable short-term prediction, for the case of insufficient or ill-conditioned data, since the measurement noise does not affect its performance as much as model M2.

It should be note that the difference between the noise analysis of this case and the previous case is that in the previous case the parameters of the model were fairly stable for a 6% additive noise in the sample size of 5 data points. However, this was not true for this case since the rate degradation was faster. Thus, the inferences based on a normal degradation process may not be extrapolated for the case of rapid degradation.



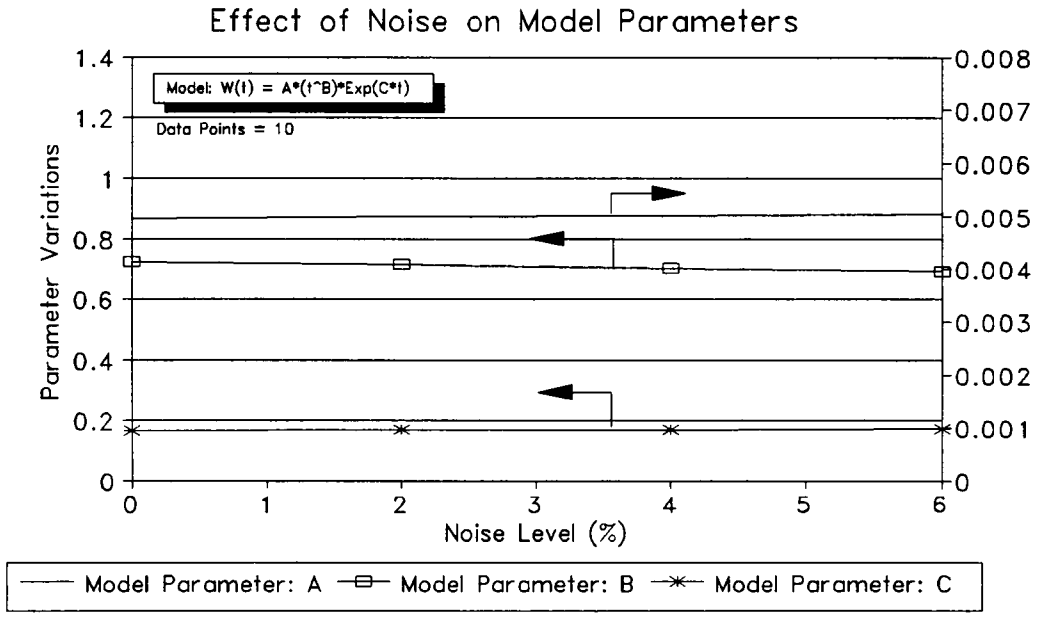


Figure 6.6: Effect of noise on the estimation of parameters of the Power-Exponential model for two block sizes of data each having 5 and 10 data points, respectively.

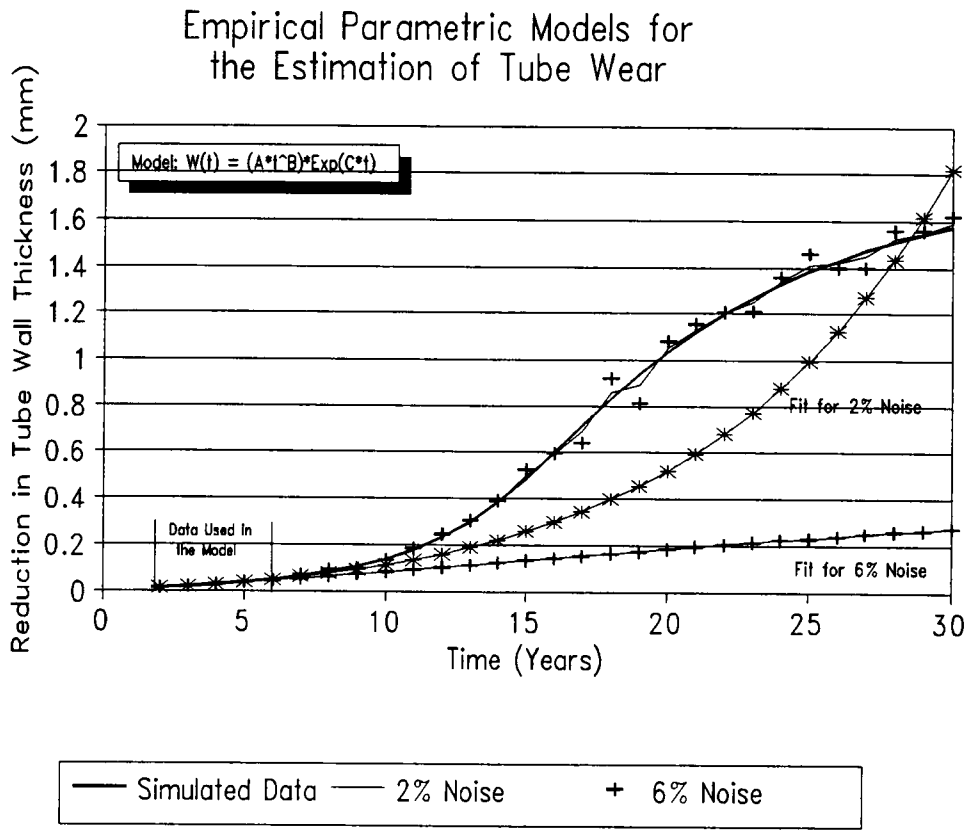


Figure 6.7: Effect of noise on the prediction of the Power-Exponential model.

In the presence of sufficient data, it is possible to construct a more sophisticated prediction model that can accurately approximate the trend in the process. In this study, it is realized that a model as described by Equation (6.8) is capable of providing such an approximation.

$$W(t) = (at + bt^2 + ct^3)\exp(dt) \tag{6.8}$$

where a, b, c, and d are to be estimated from the data using a nonlinear regression technique.

The above model was fit to ten data points of the process using the nonlinear regression analysis of the SAS package [86]. As shown in Figure 6.8, the model almost perfectly fits the process trend (the RMS value of error is 0.032 for the prediction).

However, the drawbacks associated with these types of models can out-weigh their advantages. For instance, a nonlinear regression technique does not always give a unique solution to the estimation of parameters [86]. The uniqueness of the results is central to the model prediction since wrong parameters produce faulty trends. In addition, nonlinear regression is cumbersome to apply since the convergence of the estimation depends to some extent on the initial guesses of the parameters. In practice, therefore, these models may not offer significant advantages due to their complexity and inconvenience.

In the case of tube wear process, the interest in the process prediction is at most up to the tube wall thickness. Thus, any trend analysis beyond the point of tube failure does not carry any physical meaning or significance. As seen in Figure 6.8, both the complex model of Equation (6.8) and model M2 produce almost identical trends up to

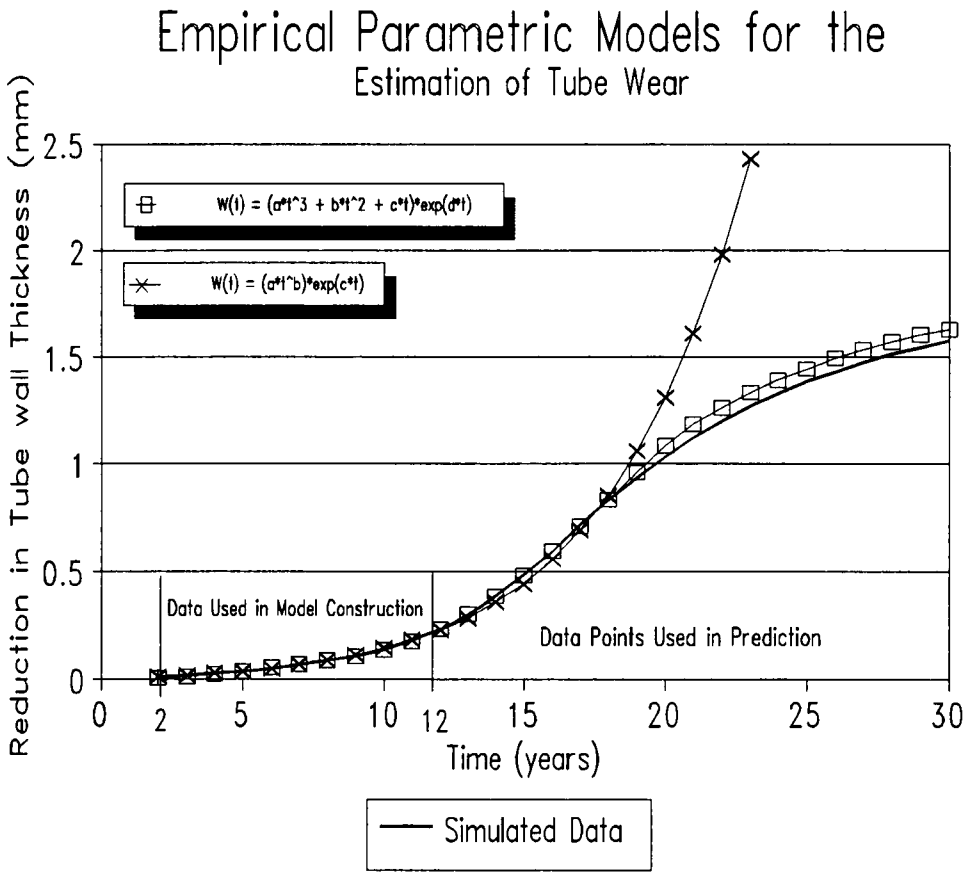


Figure 6.8: Trend prediction of a rapid tube wear degradation using a high order parametric model.

the tube wall thickness. However, model M2 is much easier to handle computationally. Therefore, in practical situations it is more advantageous to use a model like M2 over a complex model (Equation (6.8)) even when a large amount of data is available.

6.4.3 Dynamic Parametric Models

Several types of dynamic models were used to estimate the wear process trend of the previous case study (rapid degradation). The models were constructed according to the guidelines of section 3.2. They were obtained by combining models M1 and M2 with the wear process history in a dynamic manner. A simple dynamic model was also established. The models the following forms.

$$W(t) = a t^{b} + a_1 W(t-1) \tag{6.9}$$

$$W(t) = a t^{b} + a_1 W(t-1) + a_2 W(t-2) \tag{6.10}$$

$$W(t) = a t^{b} \exp(ct) + a_1 W(t-1) \tag{6.11}$$

$$W(t) = a t^{b} \exp(ct) + a_1 W(t-1) + a_2 W(t-2) \tag{6.12}$$

$$W(t) = a t + b + a_1 W(t-1) \tag{6.13}$$

The estimations of model parameters of Equation (6.9) through (6.12) require a nonlinear regression method since the equations are nonlinear in the parameters. This was performed by fitting the models to a block size of 10 data points using the nonlinear regression analysis of the SAS software system. A successful estimation of model parameters was obtained only for the model of Equation (6.9). The estimation

of parameters for the other models failed to converge. Two factors could have contributed to this problem: (1) poor initial guesses (2) overfitting. Overfitting appears to be a more convincing reason since these models with no dynamic terms [W(t-1) and W(t-2)] fit nearly perfect (see Figure 6.5). This is especially the case for the model M2.

For the model of Equation (6.9), the prediction of the future values was performed in a recursive fashion at equal time intervals as shown below.

$$\hat{W}(k+1) = a\,t^{b}(k+1) + a_1\,\hat{W}(k)$$

where k corresponds to time, t. Figure 6.9 displays the results of the prediction by this model in comparison with the model M1 and the actual wear process trend. The figure indicates that the dynamic model provides a much better estimation of the process trend than using a simple power-law model (at^b). This shows that the model is able to capture those dynamic variations of the data that are not explained by the simple model.

The linear dynamic model of Equation (6.13) was also fit to the same data set. The analysis of the model parameters and their correlation matrix suggests that there exists a strong linear correlation between the model response and its previous histories. This implies that a model which incorporates a linear combination (or a time series) of past wear data may serve as a good prediction model. To substantiate this deduction, the model was employed to forecast the future trends of the wear process. The plots of Figure 6.10 demonstrate that the model prediction is superior to that of simple linear model, and it is very similar to that of the Power-Exponential model (M2). This suggests that even a linear dynamic model is able to capture the process dynamics and

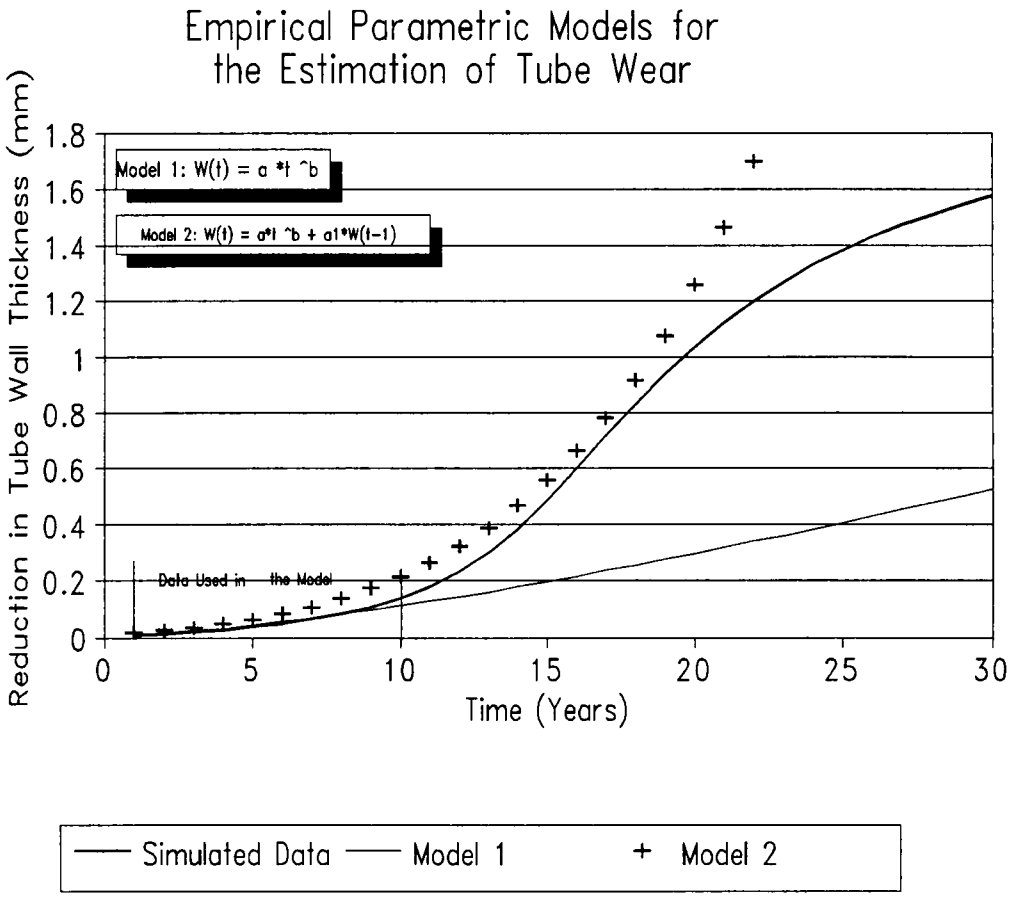


Figure 6.9: Trend prediction of a rapid tube wear degradation using a nonlinear dynamic regression model.

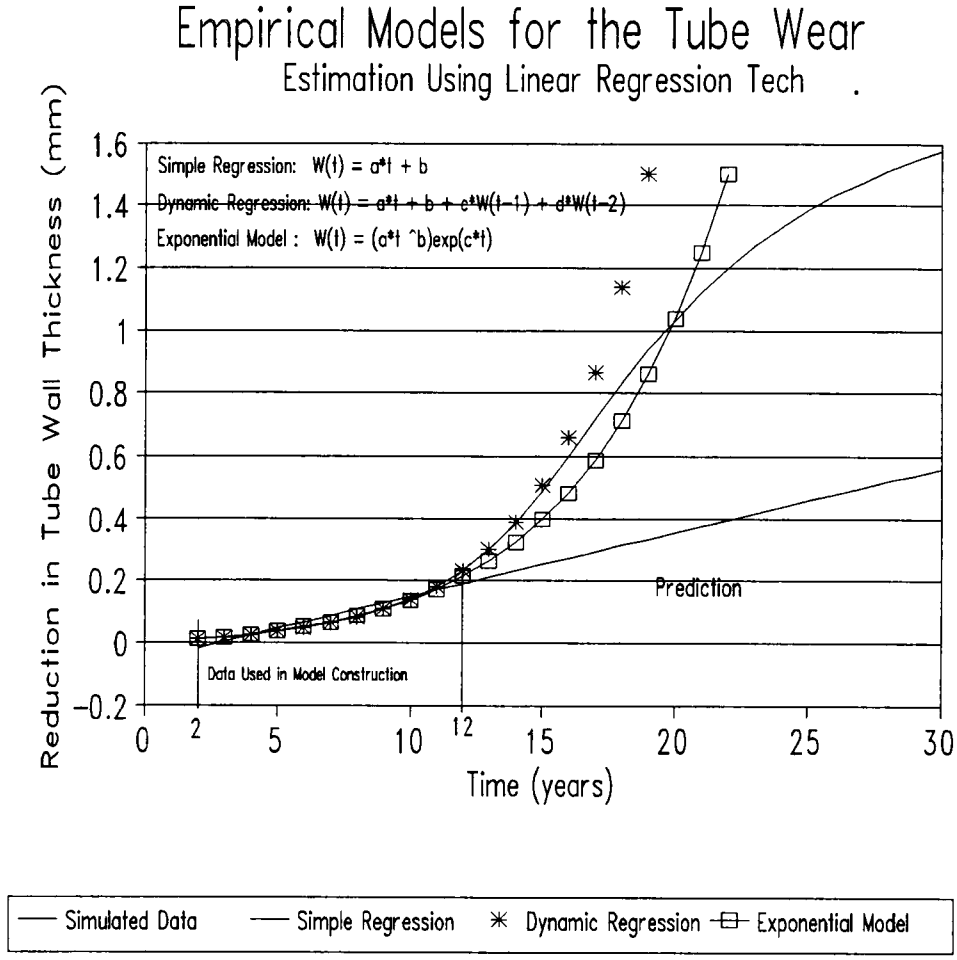


Figure 6.10: Trend prediction of a rapid tube wear degradation using a simple linear dynamic regression model.

nonlinearities. The performance of the model remains also satisfactory even in the presence of noise in the data as shown in Figure 6.11.

The results of the dynamic models indicate that these models are able to improve and enhance the prediction over classical regression models. However, they usually require more data for the estimation of parameters and for the recognition of data characteristics. For the situations where the identification of a process model is not possible, simple linear dynamic models should be seriously considered as possible alternatives to empirical models. These models have simple mathematics and can be easily established and implemented for a given application. For the tube wear process, they clearly demonstrated a superior performance over simple classical regression models.

6.5 Non-Parametric Prediction Models Using Artificial Neural Networks

To apply artificial Neural Networks Prediction (NNP) models to the trend analysis of the tube wear degradation (described in Chapter 3), first it is necessary to construct a domain of all possible tube degradation trajectories. To accomplish this task, the wear process model was used to generate a wide range of degradation paths that a tube could experience during its life time. This was accomplished by varying the model parameters within a certain range. In this study, the time exponent of the friction model [a_6 of Equation (6.4)] was perturbed from 0.0 to 2.4 with a step size of 0.4. Also the aging factor of shear yield strength point [α in Equation (6.4)] was changed form 0.0 to -0.03 (1/year) with a step size of -0.005 (1/year). The variations in these parameters

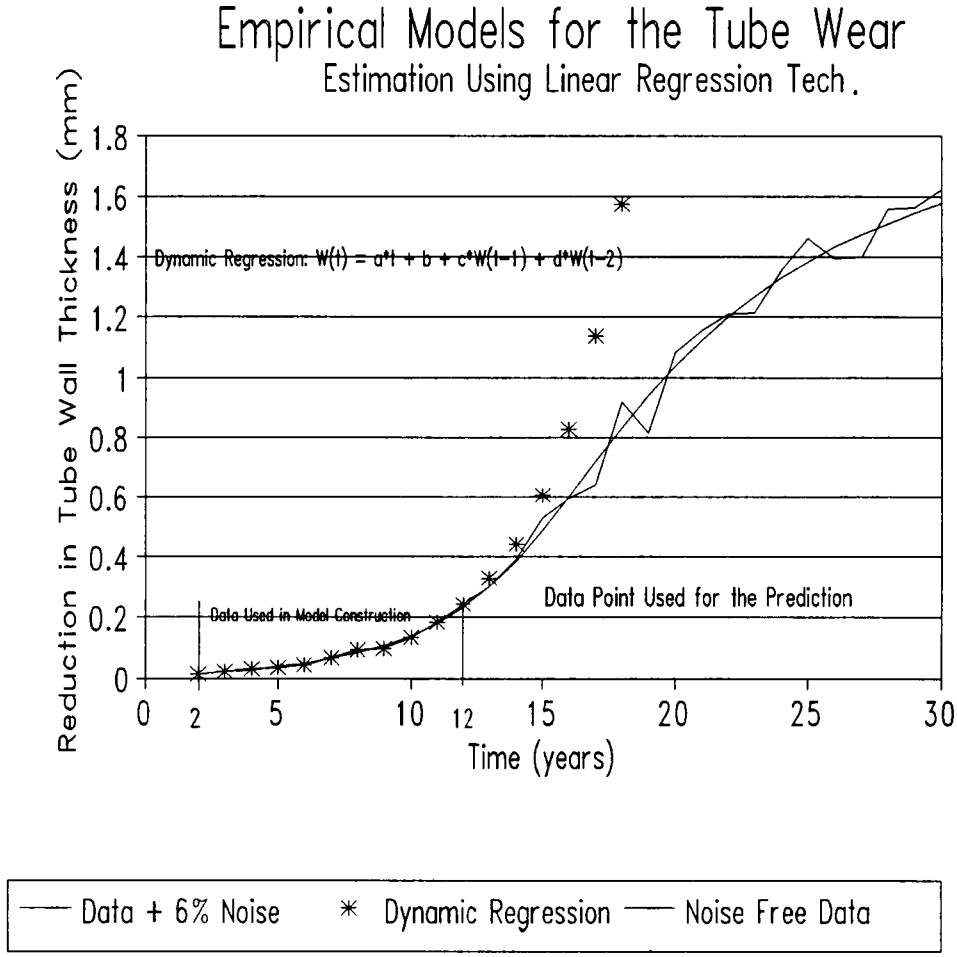


Figure 6.11: Effect of noise on the prediction of the linear dynamic model.

resulted in 18 distinct degradation paths[17]. The data generated from 12 degradation trajectories were processed to construct suitable training patterns for 3 types of NNP models as explained in Chapter 3. The data from other six paths were retained to produce testing patterns in order to evaluate the performance of the models.

The training patterns were prepared for 3, 5 and 10-point NNP models. Analogous to the parametric models, 3, 5 and 10-point NNP models correspond to short-term, intermediate-term, and long-term prediction models, respectively.

For the 3-point NNP model, the input vector of each pattern included 3 historic values of the wear degradation (with time interval of one year) and 2 data properties (features). The data properties were the difference between the first and third data points (indicating the rate of changes) and the value of the area under the data points. The output vector incorporated the 3 predicted values with a time interval of one year (see Chapter 3). Using this type of pattern structure, each degradation path produced 9 distinct patterns. This means that the input vectors of two consecutive patterns from the same the degradation path did not overlap. Thus, a total of 111 training patterns were produced to train the 3-point NNP model. A similar procedure was followed to construct the training patterns for the 5- and 10-point NNP prediction models. Figure 6.12 illustrates the structure of the training patterns for the 3 types of NNP models. It is obvious that the testing patterns will also have the same structure.

The backpropagation algorithm of the NeuralWare software Package [84] was used

---

[17]Redundant trajectories that did not provide any additional information over the other trajectories were discarded.

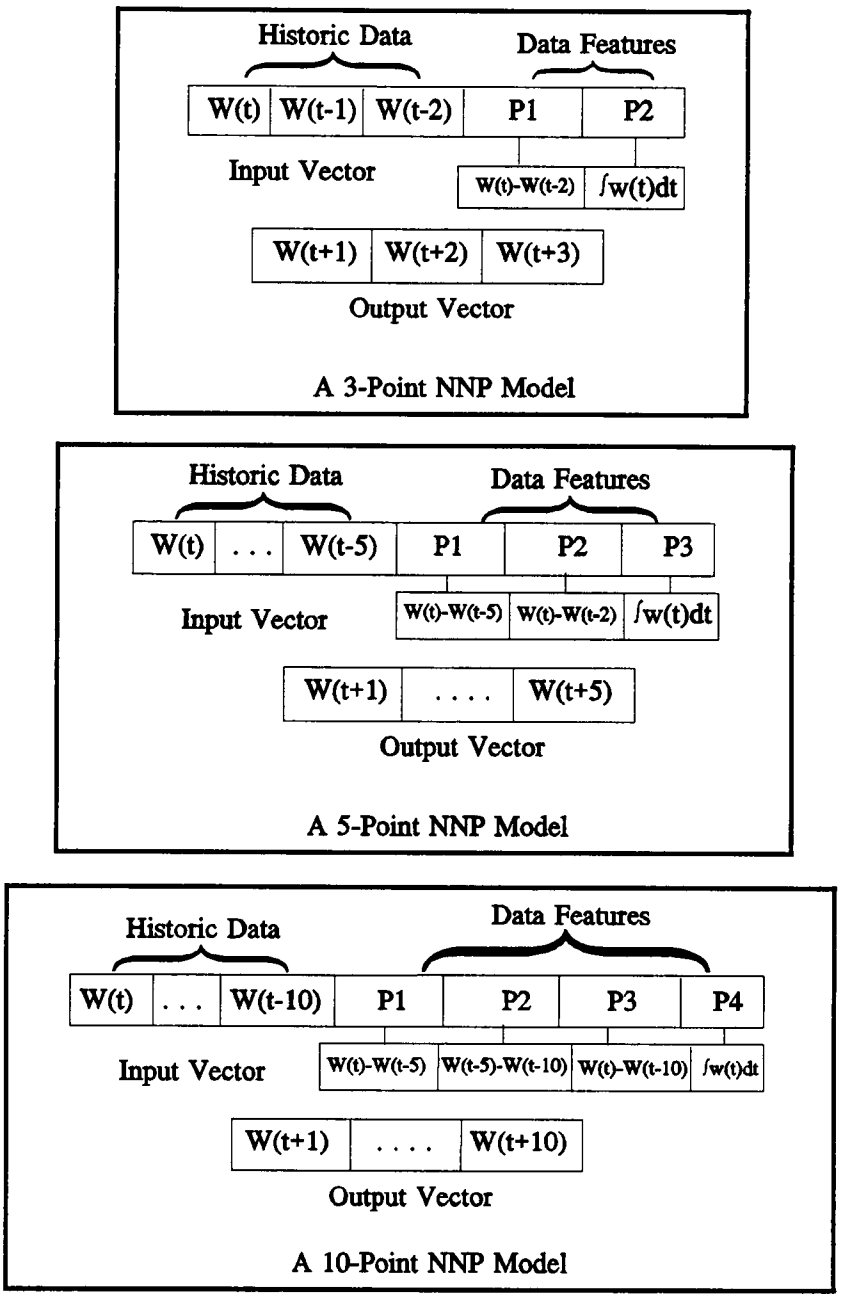


Figure 6.12: Data structure of the training patterns of the NNP models.

to build and train the neural network prediction models. This software offers several options for both training rule and the type of transform function [82-84]. It is found that a normalized cumulative delta rule and a hyperbolic transfer function [84] provide the best results for the applications of this research. A trial and error procedure was employed to obtain a suitable number of hidden layers and hidden nodes so that the networks produce satisfactory results. Table 6.4 presents the results of training phase along with necessary information regarding the structure of the models. The convergence of all three NNP models towards the desired outputs were extremely good as indicated by the RMS values of the training errors and the number of training cycles (Table 6.4).

The performance of the NNP models were examined with the patterns not used in training. Figure 6.13 shows the prediction of the NNP models in comparison with the process trends. As seen in the figure, all three NNP models were able to approximate the process trends with a good accuracy. Even for the extrapolated degradation path which was not inside the training domain, the NNP models produced satisfactory results (see Figure 6.13). This indicates that the models have learned the physics and the nature of changes in the tube wear process from the training data.

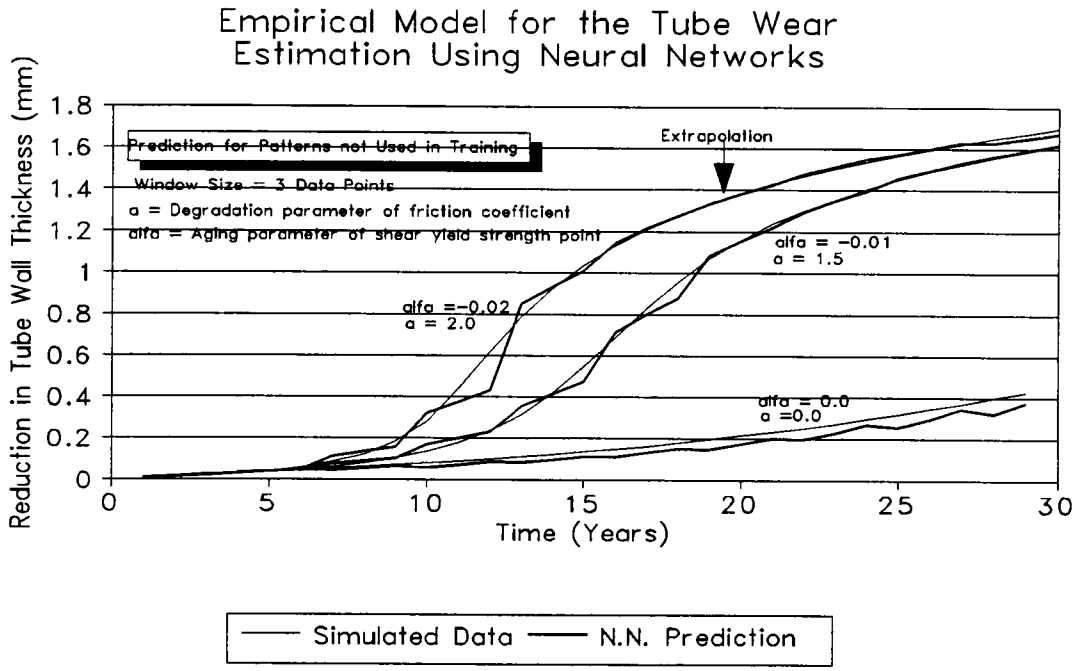
The influence of the measurement noise on the performance of the NNP models were also evaluated. Four and six percent white noise were added to the process data in a fashion similar to that of parametric models. Unlike the parametric models, the performance of NNP models against measurement noise remained satisfactory as shown in Figure 6.14. The noise level could not confuse the models in identifying the correct

Table 6.4: Structural and training information of the NNP models.

Model Type	# of Layers			# of PEs			# of Training Patterns	# of Training Cycles	RMS of Error	
	I	H	O	I	H	O			Learning	Testing
3-Point NNP	1	2	1	5	6	3	111	45600	0.018	0.0284
5-point NNP	1	1	1	8	7	5	72	50250	0.024	0.0352
10-point NNP	1	1	1	14	10	10	36	35000	0.005	0.0181

I = Input Layers, H = Hidden Layer, O = Output Layer, PE = Processing Element

RMS = Average Root-Mean-Squared Error for the Training and Testing Data Sets



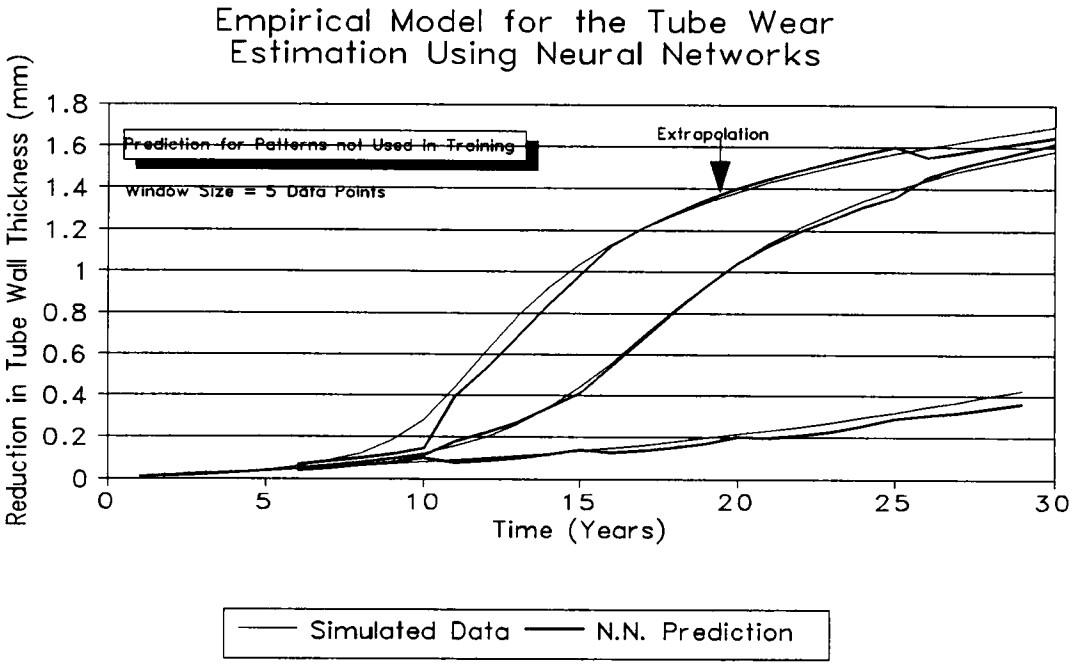


Figure 6.13: Trend prediction of various tube wear degradation trajectories using NNP models with 3 different block sizes of data.

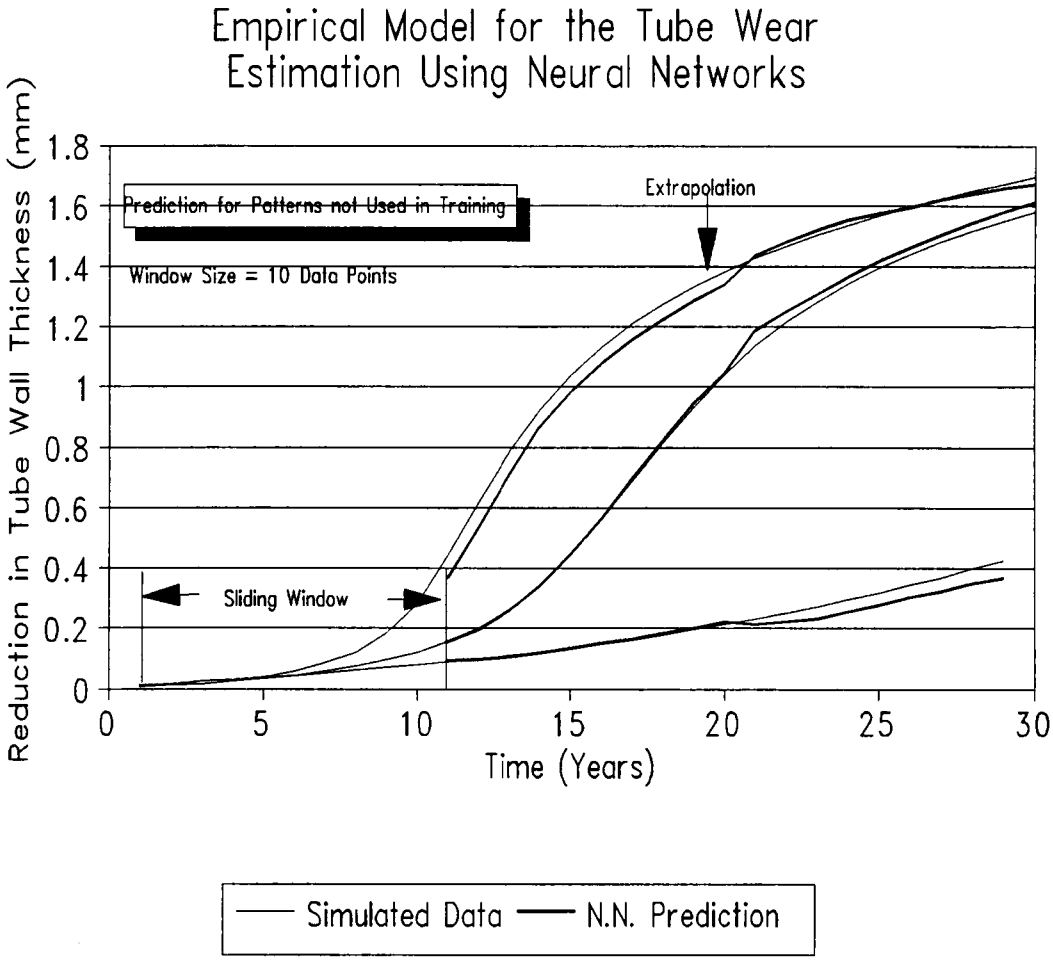
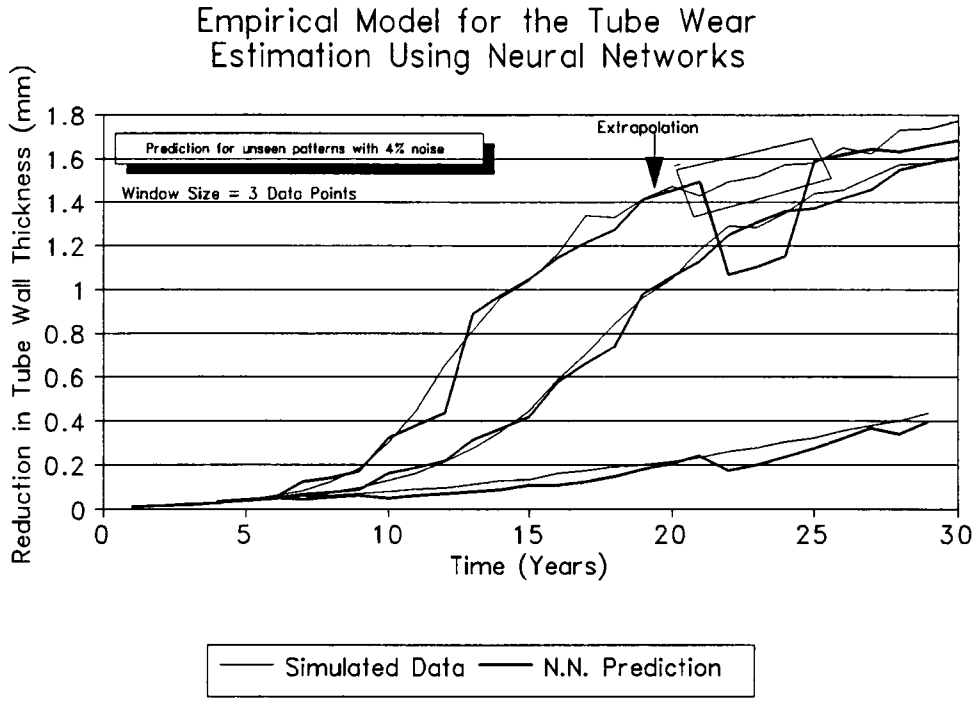


Figure 6.13 (continued)



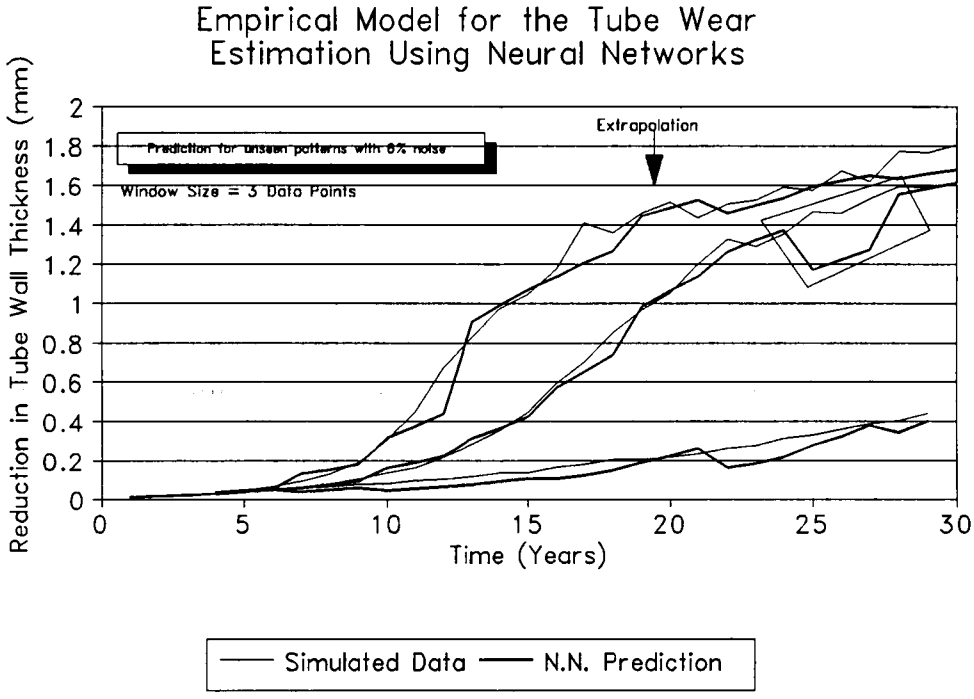
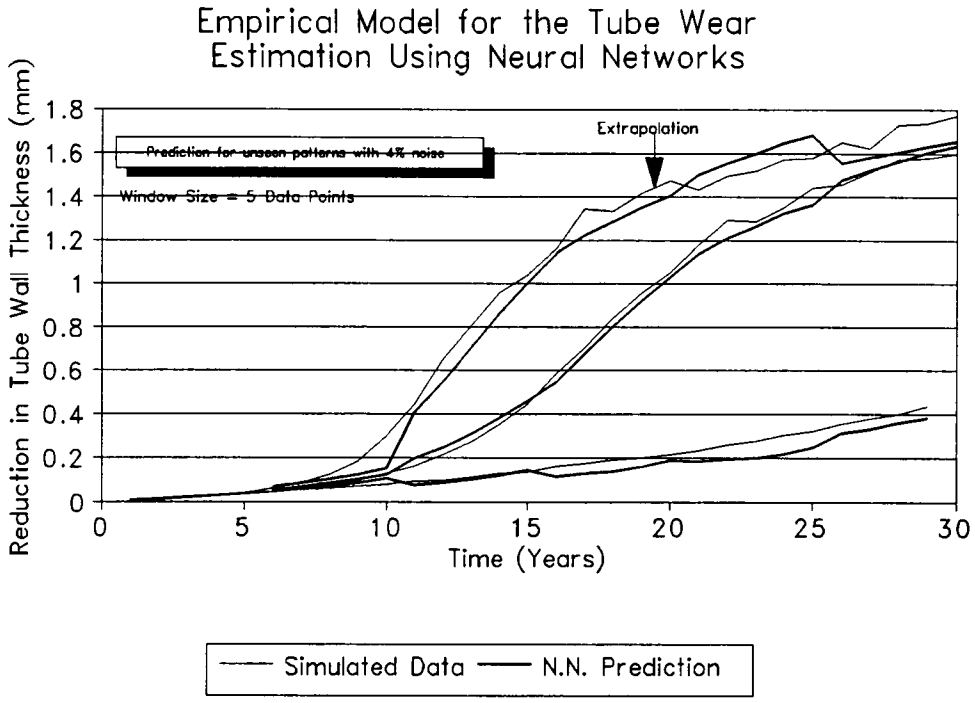


Figure 6.14: Effects of 4% and 6% noise levels on the prediction of a 3-point NNP model.

trends of the process especially up to the tube wall thickness (0.88 mm). However, as seen in the boxed area of Figure 6.14, the prediction of the 3-point NNP model was affected by the noise level when the rate of changes in the process trend with time became very slow. The measurement noise caused the previous values of the wear process to become larger than the future values. In such a small window size of data, this appeared as a decreasing trend which mislead the network in identifying the true process trend. As seen in the figure, this phenomenon occurred only after the wear amount exceeded the tube wall thickness (0.88 mm).

However, in real world applications the above problem is not realistic since first a tube always fails when the wear reaches a value close to the tubes wall thickness. In addition, the real-world wear data are always monotonically ascending with time since physically it is not possible that the wear of tube at the present or at a future time to be smaller than that at a previous time. Nevertheless, to ensure that this anomaly does not occur under any circumstances, it is possible to circumvent the problem by training the neural network with data contaminated with noise. This may prevent the network from confusion since it encounters such problems during the training phase. It should be noted that this abnormality occurred only for a three-point NNP model and it was not observed for the other models (see Figure 6.15).

The results of the NNP models demonstrate that the networks are capable of forecasting the process trends of a tube wear mechanism in a very efficient manner. They are far less noise-sensitive than parametric models, and is important for practical applications.



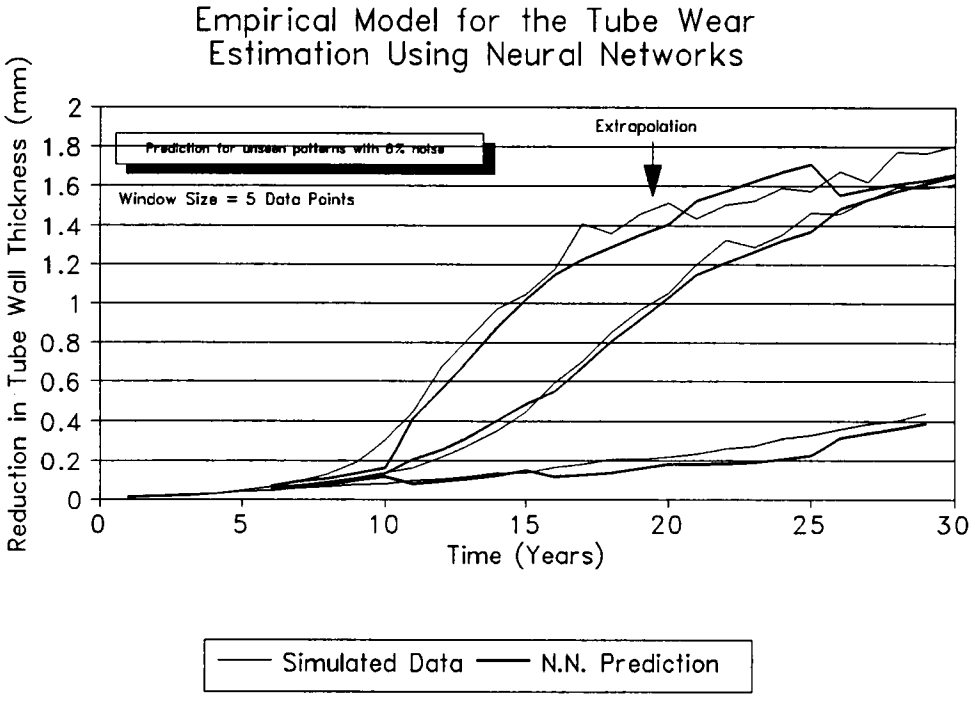


Figure 6.15: Effects of 4% and 6% noise levels on the prediction of a 5-point NNP model.

6.6 Residual Life Estimation

The overall scheme of the life prediction methodology was presented in Chapter 3. According to the methodology, two key components of any life estimation are: (1) a suitable technique for the trend forecasting of a damage process and (2) a value for the maximum allowable degradation (or alarm) level. The procedures for developing prediction models to trend a damage process have been described and investigated throughout this research study. However, such prediction models by themselves can not present an estimation of the component life if a value for the allowable degradation level is not given or known. Unfortunately, there is no global agreement on how to define this quantity for a certain degradation process. Laboratory experimentation can usually specify a value for a given damage mechanism that results in the failure of the component. Usually, this value is associated with a safety factor that depends on the sensitivity of the component to a plant operation and/or safety considerations. Thus, it is not surprising that individuals or industries using an identical equipment comprise different criteria for setting failure levels. For example, nuclear power industries tend to be more conservative in selecting values of failure levels for their components since safety and accident-free operation are important issues. Hence, the life estimation of a component with respect to a given failure level does not always represent the actual life of that component.

From the foregoing discussion, it is clear that defining a permissible value for any damage or degradation process plays an important role in the life estimation of a component. Certainly, the subject of defining accurate and reliable degradation levels

deserves a rigorous experimental and theoretical investigations which should be carried out in the future in order to complement the life assessment methodology.

Once a degradation level is defined (or given), the prediction models of the process under study are employed to calculate the overall life of the component by extrapolating the process trends to the degradation level. Having determined the overall life, the actual time of operation is subtracted to obtain the remaining life estimation. Figures 6.16 and 6.17 illustrate this concept for both parametric and NNP models.

For the wear of nuclear steam generator tubes, the maximum allowable limits are usually 25% to 32% of the tube wall thickness [42]. They approximately correspond to 0.22 mm to 0.274 mm for OTSG tubes with a wall thickness of 0.88 mm. Using these values in conjunction with parametric or NNP models, the useful life of the tubes can be estimated as described in the above. For instance, when the parametric model of M2 is applied for the case of normal tube wear mechanism, the extrapolation of the model trend up to 0.274 mm gives an overall life of 29 years, as shown in Figure 6.18. Since the model uses the first 5 data points (indicating an operating time of five years), the residual life would be 29-5 = 24 years. The true value of the residual life calculated from the simulated process trend is 22 years. Thus, the error of the prediction is approximately 2 years.

It is customary to provide a confidence interval with a forecast since any statistical point estimation includes some degree of uncertainty. A confidence interval is in fact a measure of how close the point estimation is likely to be to the true value. In other words, it represents an interval of plausible values for the estimation. The degree of

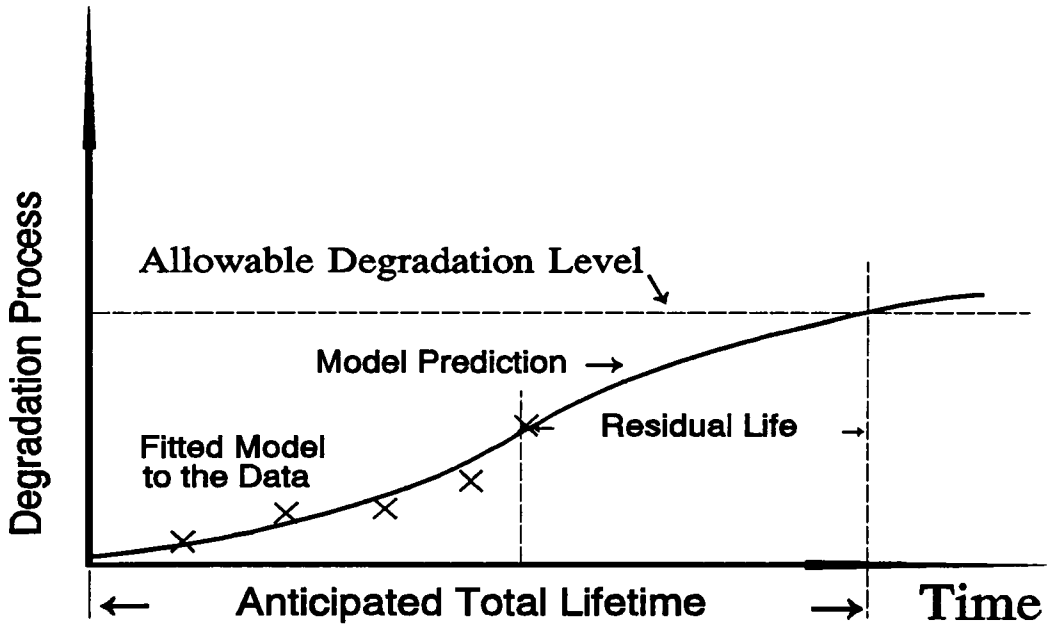


Figure 6.16: Schematic diagram of residual life estimation using parametric prediction models.

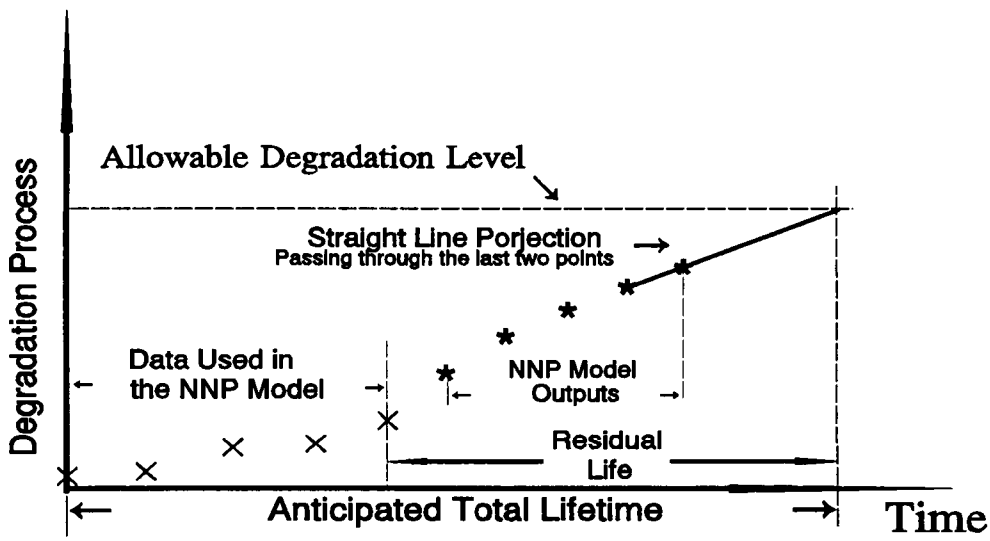


Figure 6.17: Schematic diagram of residual life estimation using NNP models.

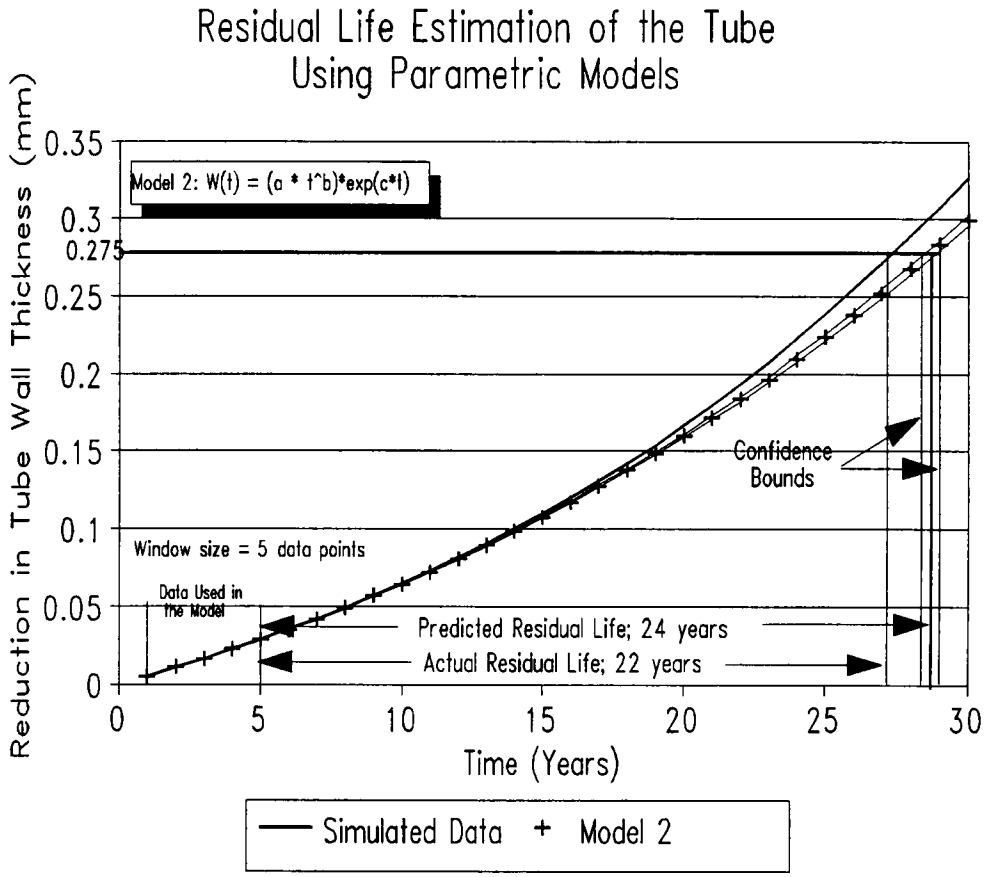


Figure 6.18: Residual life estimation of a typical OTSG tube when a parametric model is used for the trend prediction of a normal tube wear degradation.

plausibility will be specified by a confidence level which measures how conservative the estimation is required to be. A confidence level of 95% is very common and somewhat standard for many applications. The statistical software system SAS [86] provides this confidence level as one of its standard features. The theory of the confidence intervals are well documented in various statistical books [51,52,62].

Using a 95% confidence level for the above example, the interval of plausible values for the estimated residual life is from 21.7 years to 22.3 years (see Figure 6.18). This small confidence interval is due to an almost zero variance fit and a small block size of data used in the model construction (only 5 data points). Since the true value of the residual life does not lie in this interval, this may suggest that a tighter confidence level (for example 99%) is required for the cases with small block sizes of data. It should be note that in general the use of confidence intervals does not always warrant that the interval will include the true value.

For the case of NNP model, it may not be possible to extrapolate the process trend to the degradation level, since the model basically gives numerical values of the wear process within a specified time-frame. If the degradation level falls into that time frame, a simple interpolation will give the overall life and thereby the residual life is easily followed. However, if it does not fall into the time frame, the only certain inference that can be made is that the component will not fail during that time frame. In such situations, as a rule of thumb, one may make a projection by passing a straight line through the last two points of the predictions and by extending it toward the degradation level. For example, as shown in Figure 6.19, the 5-point NNP model for

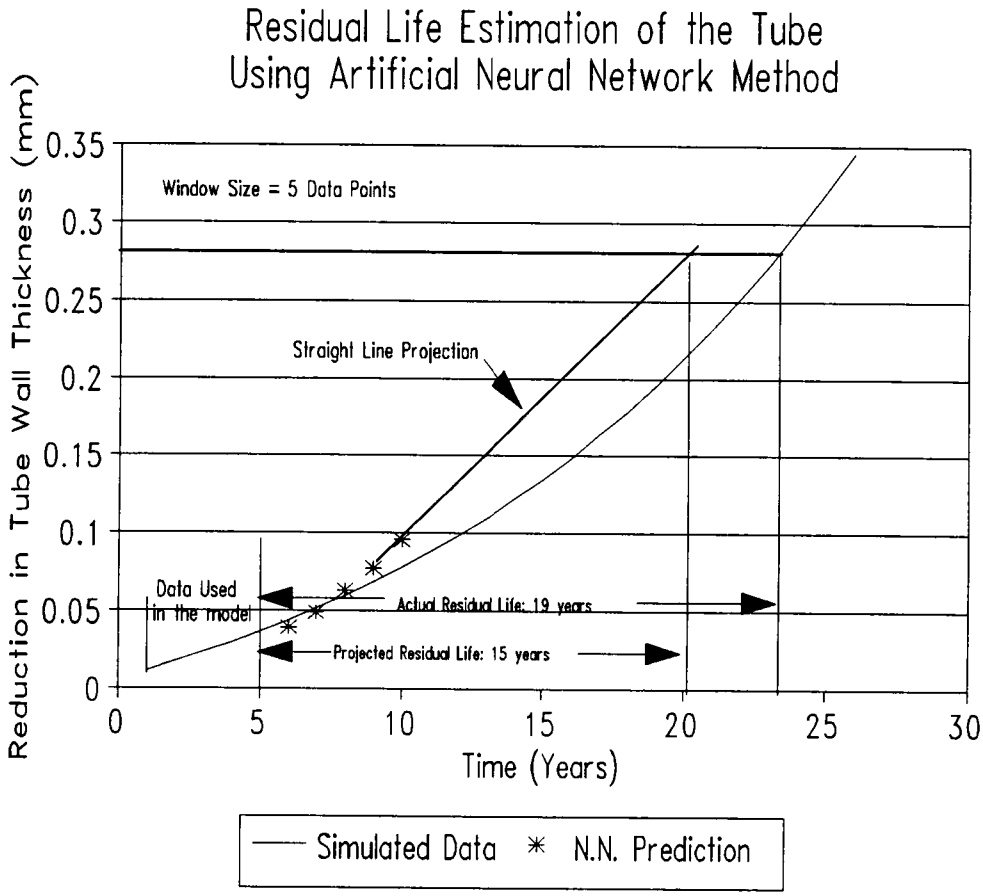


Figure 6.19: Residual life estimation of a typical OTSG tube when a NNP model is used for the trend prediction of a normal tube wear degradation.

the case of normal tube wear degradation forecasts a maximum wear amount of 0.1 mm during the next five years (when the first five data points were used as input to the model). This number is smaller than 0.274 mm (the allowable degradation level), thus the only certain conclusion is that the tube will last another five years. However, using the straight line projection the anticipated total life and residual life would be 20 and 15 years, respectively. It is necessary to point out that the residual life obtained in this fashion is only an approximation.

It is also possible to associate a failure probability with the forecasts of the NNP models. The failure probability, F_{prob}, may be defined as

$$F_{prob} = \frac{Predicted\ degradation\ value}{Allowable\ degradation\ level} \tag{6.15}$$

Thus, for each point of prediction the failure probability will change. A maximum failure probability of one corresponds to a zero residual life. This brings about the definition of a survival probability which is simply

$$S_{prob} = 1 - F_{prob} \tag{6.16}$$

These probabilities can be used to measure the reliability of a component. In the previous example, the failure probabilities for the predicted values lie in a range of 0.145 to 0.363 during the next five years of the operation. The corresponding survival probabilities are in a range of 0.855 to 0.637.

6.7 Parametric Sensitivity Analysis

A degradation process, in general, is subjected to a changing environment, aging,

and variations in its operating conditions such as temperature, pressure, load, etc. These changes result in the variations of the process parameters which in turn change the process trends and characteristics. Thus, the sensitivity of a degradation process to parametric variations is of prime importance since the trend analysis of any degradation process relies to some extent on a knowledge of the parameters representing the process.

The determination of the degree of sensitivity as a function of process variables can be carried out relatively easily. Sensitivity of a process, W, to a parameter, a, is normally defined as a measure of the percentage change in W to a percentage in the parameter, a. One such definition is

$$Sensitivity \approx \frac{\Delta W/W}{\Delta a/a} = \frac{\Delta W}{\Delta a}\frac{a}{W} \tag{6.17}$$

For the case of tube wear process, the variation of the wear amount with respect to the changes of the process parameters is regarded as a measure of sensitivity. The parameters considered for the sensitivity analysis are the exponent of the friction factor model, aging parameter of shear yield strength point, and rate coefficients of the contact time duration and the contact forces. Since the wear process model is in a closed form, it is not possible to derive explicit mathematical relationships that correlate the changes in the wear process with the changes in these parameters. Therefore, computer simulations were conducted to perform the sensitivity analysis. In all simulations, the parameters were perturbed one at time from their nominal values. The results of the simulations are presented in Figures 6.20 through 6.23.

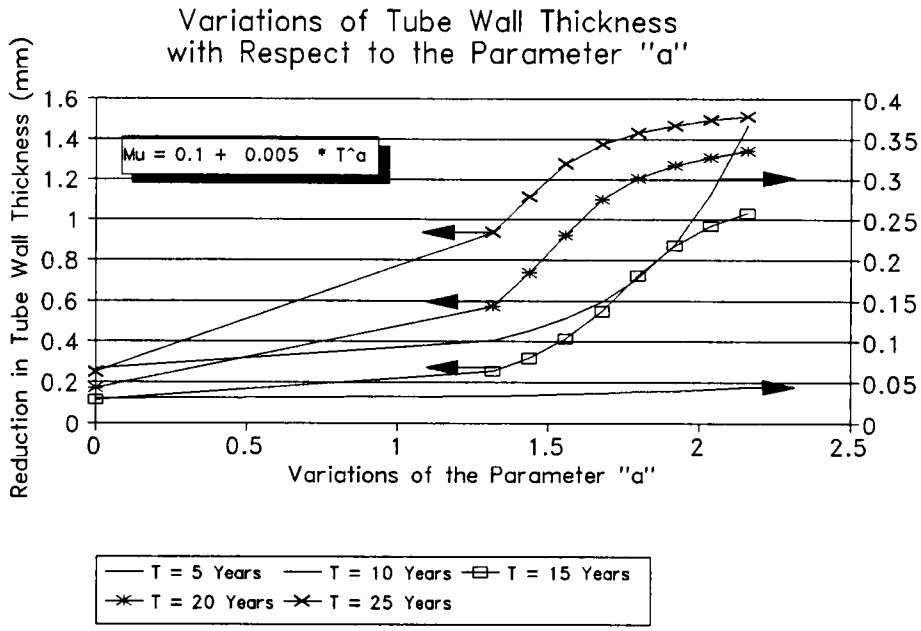


Figure 6.20: Variation of tube wear with the exponent parameter of the coefficient of friction.

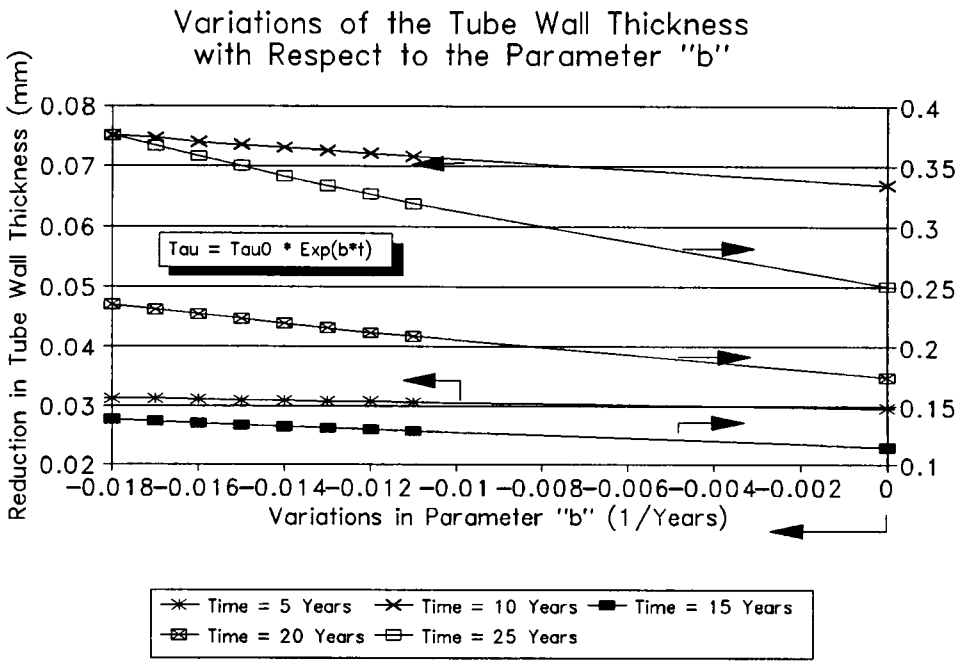


Figure 6.21: Variation of tube wear with the aging factor of the shear yield stress point.

The simulation results in Figure 6.20 indicate that the rate of tube wear with parameter a_6 (the exponent of the friction coefficient) is nearly linear at the beginning of the tube life and then becomes nonlinear towards the end of life. The steepest changes occur during the first ten years when the tube-to-support clearance is small enough to produce adequate contacts between the tube and the tube support. During this time, a 33% (from 1.5 to 2) increase in the exponent parameter causes the tube wall thickness to reduce by a factor of 2.8 (from 0.1 to 0.28). However, towards the end of tube life (20 or 25 years) when the clearance becomes too large, insufficient contacts reduce the rate of changes rather significantly. For example, at time 25 years when the exponent parameter changes from 1.5 to 2, a 33% variation, the tube thickness reduces from 1.3 mm to 1.5 mm, a 15% variations[18]. This indicates if the contact is small, the variation in the friction factor does not notably influence the wear process.

Figure 6.21 (see the previous page) shows that the wear of tube varies approximately linearly with the aging parameter of shear yield strength point. The rate of wear is slow at the beginning of the tube life but becomes fast towards the end of life. This is rather an interesting phenomenon since towards the end of the tube life when the clearance becomes sufficiently large (in a range of 0.2 mm to 0.4 mm), stronger contact forces are produced. Consequently, the combined effects of a lower shear yield strength and larger contact forces will ensue a faster tube wear rate.

Figure 6.22 displays the effects of variations in the rate parameter of the contact

---

[18] These numbers do not have a physical meaning since the tube fails when the wear amount reaches 0.88 mm; however, mathematically they indicate the effect of contact time duration on the wear rate.

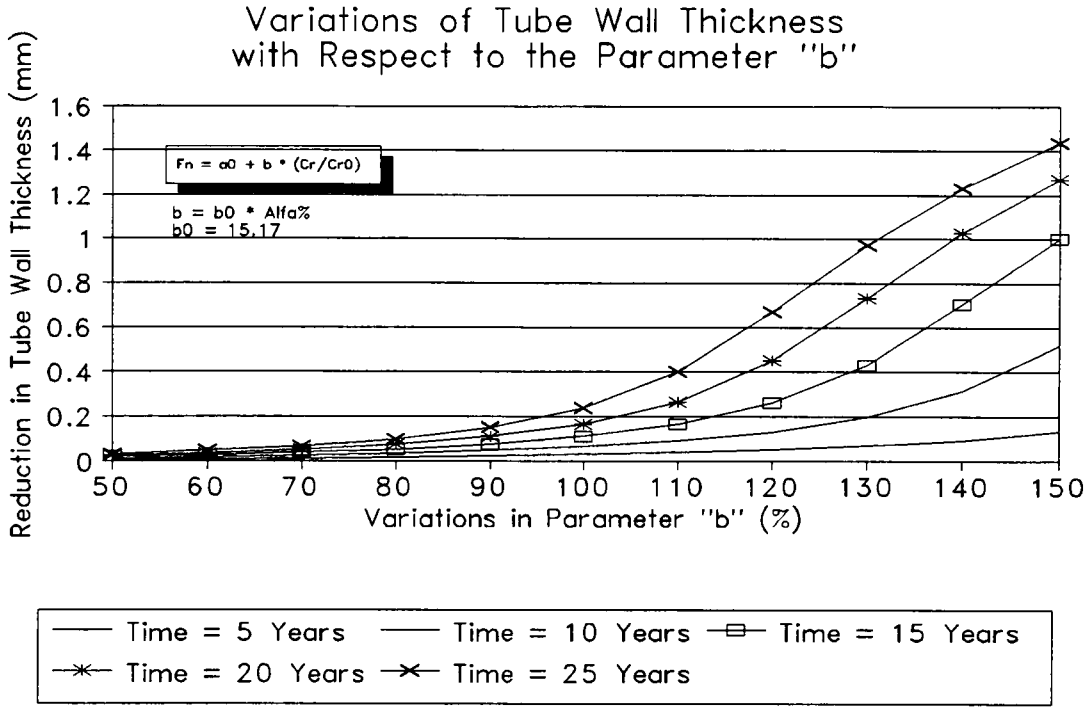


Figure 6.22: Variation of tube wear with the rate parameter of the contact forces.

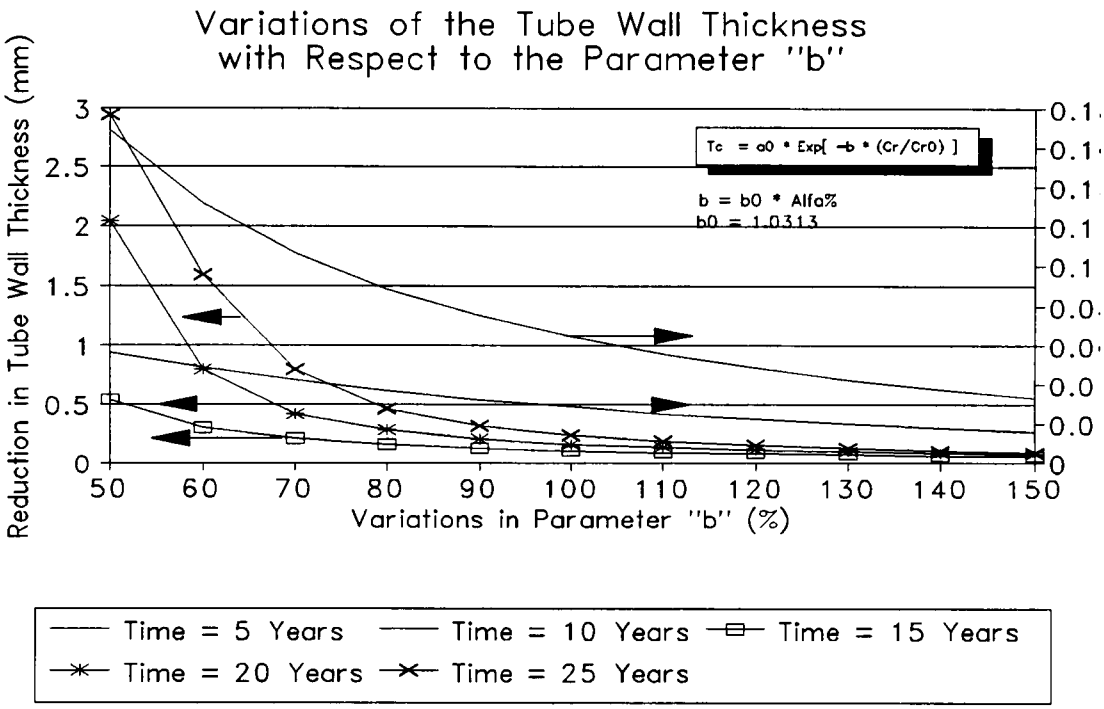


Figure 6.23: Variation of tube wear with the rate parameter of the contact duration time.

forces. As the rate parameter increases from its nominal value of 100% to 150%, the wear rate increases in a nonlinear fashion. The wear rate appears to increase rapidly as time increases. However, when the parameter decreases from 100% to 50%, the wear rate appears to reduce asymptotically towards a small value. The reduction in the wear rate for any operation time remains approximately constant as the rate parameter decreases from 100% to 50%. This is attributed to an inter-dependent correlation among the contact forces, the tube wear amount, and the tube clearance (see the wear process model in section 6.3). Raises in the rate parameter increases the tube clearance which in turn increases the contact forces (a mutual effect). However, its reduction initially reduces the contact forces nonetheless it still increases the clearance (but with a slower rate) which tends to raise the contact forces. These two effects to some extent cancel each other out and thus the contact forces and the wear rate remain fairly constant as the rate parameter decreases.

Variations in the rate parameter of the contact time duration change the wear amount in an exponential manner as shown in Figure 6.23 (see the previous page). The rate of change increases as time increases. This is fairly obvious since the contact duration model is an exponential function of the clearance which increases with time. The figure indicates that a 50% increase in the rate parameter (from its nominal value) causes a reduction of 60% in the wear amount. In general, a larger tube clearance corresponds to fewer contacts between the tube and the tube support.

In summary, the analysis of the above results indicates that the tube wear rate can vary significantly as the parameters of the wear process change. This is quite evident

for the case of coefficient of friction and the contact forces that can change the wear rate by several factors from its design (nominal) value. These parameters can also change the characteristics of the wear process trends since the degree of nonlinearity in the process depends strongly on the values of such parameters. For instance, higher values of friction factor and contact forces can introduce significant nonlinearity in the process trend (see Figure 6.3). Generally speaking, it is always desirable to control the variation of the parameters in order to have a satisfactory operation and a correct prediction of the process.

6.8 Simulation of Uncertainties

Since the tube wear process is a power function of the contact forces, any uncertainties in the characterization of such forces may considerably influence the process trends. In the previous section, the parametric sensitivity analysis showed that variations in the rate parameter of the contact force model can markedly affect the wear of tubes. In this section, variations in the characteristics of the contact forces are considered as potential uncertainties. They are simulated as (1) random variations in the contact forces from their calculated RMS values and (2) bias in the contact forces.

As shown in Chapter 5, the variations in the contact forces with time are generally random in nature due to the presence of random excitation forces and nonlinear boundary conditions at the tube-to-support clearances. Thus, it is plausible to associate a certain degree of randomness with the magnitude of such forces. This is performed by adding a normal Guassian random variations to the deterministic model of the

contact forces. This means that statistically the mean RMS values of the forces remain unchanged but their magnitudes vary randomly with time. The effects of 1 to 8 percent (corresponding to a variance of 1 to 4 N) random force variations on the wear of tube are shown in Figure 6.24. The results demonstrate that the random force fluctuations slightly increase the wear amount (maximum 15%), but they do not cause characteristic changes in the process trend. Therefore, this type of uncertainty does not introduce significant or systematic errors either in the wear calculation or the process trend prediction.

The force biasing is simulated as a step increase or decrease in the mean value of contact forces. Figure 6.25 shows the results of simulation. The results show that even a small force biasing can introduce a relatively large variation in the wear amount. For instance, when the contact forces are biased by 1 to 3 N (corresponding to 4% to 10% of the nominal RMS value of the contact forces) the wear amount increases approximately by 21% to 75% of its nominal value over a time period of 30 years. The analysis of the results also indicate that the trend of variations in the wear is not linearly proportional to the amount of bias. This is due to the fact that the tube wear is a power function of contact forces and also mutually inter-dependent on the wear amount. Since the force biasing employed here is time invariant, it does not submit additional complexity to the wear process trend. In practice, force biasing can occur due to variations in the vibratory excitation forces as a result of power level changes in a steam generator.

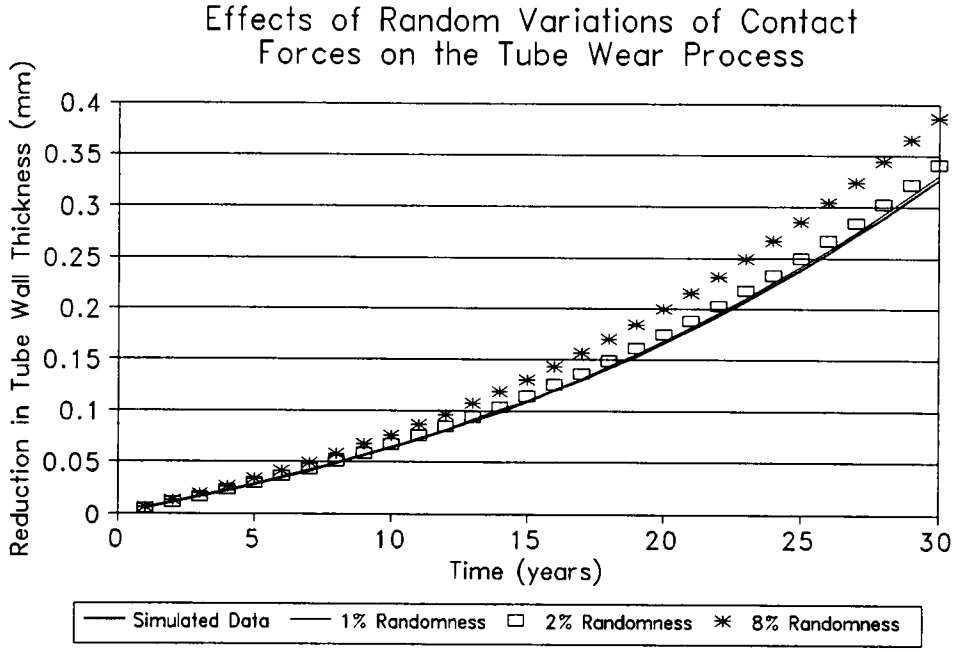


Figure 6.24: Effect of random variations of the contact forces on tube wear.

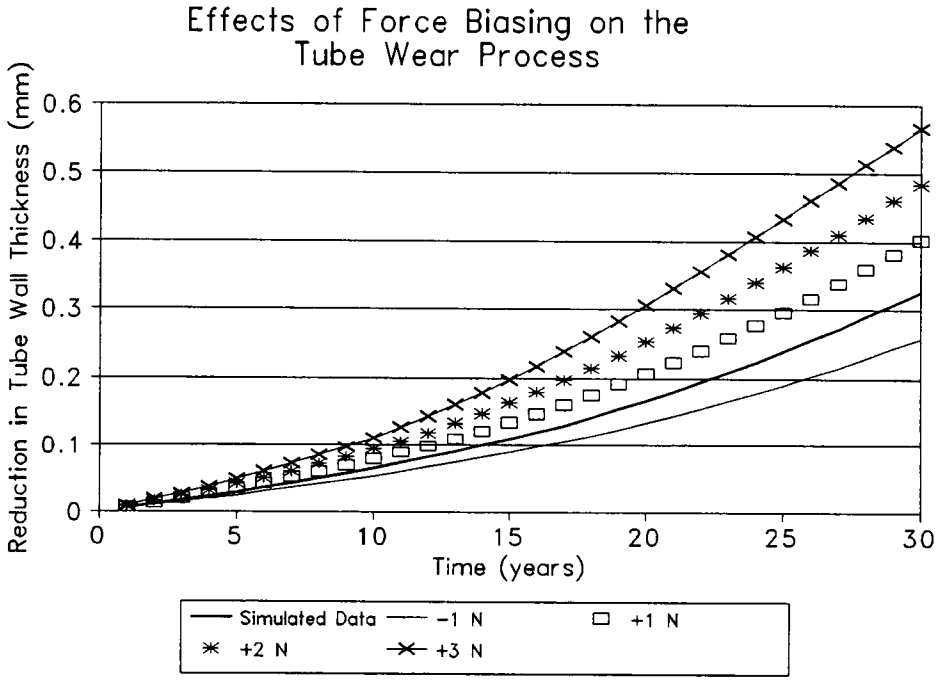


Figure 6.25: Effect of force biasing on tube wear.

6.9 Summary and Suggestions for Implementation

6.9.1 Summary

The life assessment methodology described in Chapter 3 was used to develop a damage process model for the wear mechanism of an OTSG tube. The wear process model was established by combining the models of contact forces, contact duration time, friction coefficient, and shear strength yield point with the tube wear model of Chapter 3. Since the combined model was in a closed form, a computer algorithm was devised to calculate the tube wear amount as a direct function of time over a period of 30 years.

The model was employed to generate various simulated data for the tube wear mechanism by changing the aging parameters in the models of the friction coefficient and the shear strength yield point. The data were used to construct suitable parametric and neural network prediction (NNP) models to forecast the trends of tube wear over time.

Two types of parametric models were used to estimate the trends of tube wear process. They are 1) Power-Law model, and 2) Power-Exponential model. The performance of the models were investigated for both cases of normal and rapid tube wear degradation. The results indicate that the Power-Law model suggested by Ko [15] provides a good prediction only for short-term predictions. The Power-Exponential model, approximated based on the physics of the process, presents a good prediction of the process trends up to the tube wall thickness for both the above cases.

Since real-world data includes some level of measurement noise, the performance

of the models was also examined with the process data containing two, four, and six percent white noise. The results indicate that for a small sample size of data the Power-Law model is less noise-sensitive than the Power-Exponential model.

A dynamic formulation of the historic process data was also incorporated into the above models to improve and enhance their predictions. The inclusion of one-point back in time of the process data [W(t-1)] with the Power-Law model constituted a dynamic model and markedly improved the prediction of the Power-Law model. This shows that the dynamic model is able to capture the dynamic characteristics of the process (which was not explained by the simple model) from the context of the data. This ability was also observed with even a simple second order dynamic model constructed as a linear combination of past data, W(t-1) and W(t-2).

Three types of Neural Network Prediction (NNP) models were constructed according to the guidelines of Chapter 3. They are 3, 5, and 10-point NNP models used for short, intermediate, and long-term prediction, respectively. All the three NNP models were able to estimate the tube wear process trends with a good accuracy within their specified time frame, even for the extrapolated trajectory. Also, their performance did not degrade by the noisy data as much as that of parametric models.

Both parametric and NNP models were used to estimate the residual life of the tube with respect to a maximum allowable wear degradation level. The general procedures for the estimation of residual life for both the parametric and the NNP models were illustrated in Figures 6.16 and 6.17, respectively. It was concluded that if an allowable degradation level is outside the output time-frame of an NNP model, the only definite

result is that the component endures within that time-frame with a certain survival probability as defined in section 6.6. Two examples were also given to demonstrate the estimation of residual life for both parametric and NNP models.

Parametric sensitivity analysis and the simulation of uncertainties were also performed in this chapter. The results of sensitivity analysis showed that the wear rate can change significantly with factors affecting the dynamics of the friction coefficient and the contact forces. The results of simulations of uncertainties indicated that a randomness in the magnitude of contact forces causes negligible variations in the process trends. It was also shown that the presence of a bias in the contact forces can accelerate the degradation process. But it does not introduce additional complexity to the process trend.

6.9.2 Suggestions for Implementation

Based on the investigation of this research study, the following procedure was recommended for the service life prediction of tubes of heat exchangers and steam generators.

1. Identify the main degradation mechanism(s).
2. Develop damage models for such degradation processes.
3. Identify material aging or environmental degradation mechanisms that influence the main degradation mechanism(s).
4. Combine models of steps 2 and 3 to obtain a process model to describe the general trends of the damage mechanism(s) with time. The model may be in a closed form

with respect to time.

5. Construct semi-empirical parametric or computational neural network models based on the physics of the process model and the available field data and information to predict the future trends in the damage mechanism(s).
6. Estimate the service life of tubes by extending the trends of the damage mechanism(s) to an allowable degradation level.

The details of the above procedure are given in Chapter 3.

CHAPTER 7

SUMMARY, CONCLUSIONS AND RECOMMENDATIONS FOR FUTURE RESEARCH

7.1 Summary

A model-based methodology for the life assessment of steam generator tubes subjected to a certain degradation mechanism was developed in this dissertation. The methodology employed the engineering analysis of the degradation process under study to develop a model which characterizes the general physics of the process and identifies its trends during aging, and degradation mechanisms of tubes over time. The degradation model was then used in conjunction with available field data to establish semi-empirical models for forecasting process trends. The projection of the process trends to a pre-defined allowable degradation level was used to estimate the life expectancy of the tubes.

In section 3.2, a procedure was described for developing semi-empirical models using both parametric and non-parametric techniques. The parametric prediction models are derived from the process model in reduced forms and as direct functions of time. The construction methods of these models were guided by the principles of simplicity, physical realism, and applicability to practical problems involved with limited amount of data. An empirical dynamic formulation of the process data was also presented to

improve the prediction of the models. The non-parametric models were established based on artificial neural network methods using a backpropgation training algorithm. They are trained with a wide range of data generated from the process model to recognize the real process trends by an intelligent data mapping and thereby to forecast their future trends within a specified time frame.

As a complex application of trend forecasting, the proposed life assessment approach was used to predict the wear process trends of OTSG tubes at the 15th tube support. At this location the dynamic interaction of tube-to-support, caused by flow-induced tube vibrations, results in the wear of tubes with consequent reduced tube life.

To perform the life assessment analysis for this application, a tube wear model based strictly on mechanical consideration, was developed in Chapter 4 to describe the physics of the tube wear process which takes place during dynamic interaction between a tube and its support.

The model correlates the tube wear rate with the tube-to-support normal contact forces, coefficient of friction and shear stress yield point. The type of model in a qualitative manner agrees with the underlying concept of the wear process described by Archard [70-72], Ko [15,18] and other investigators [5,30]. The definite advantage of this model is that it shows clearly the dependency of the tube wear rate on the coefficient of friction, shear stress yield point of tube materials, and contact parameters. This is important since these factors are subjected to variations because of aging and degradation mechanisms which occur over the life of tubes. The changes in these parameters can result in behavioral changes of the wear process.

The aging models of the coefficient of friction and the shear yield strength points were also identified to satisfy the second step of life assessment methodology. The development of a degradation model so as to describe the changes of the contact parameters (force and duration time) with the tube-to-support clearance required a greater analysis that was carried out in Chapter 5.

To characterize the dynamics of tube-to-support interactions, a one-dimensional finite element vibration model of a multi-span tube was developed in Chapter 5. The model was employed to perform a parametric study to determine the variations of the contact forces and the contact duration time with the clearance at the 15th tube support. The results of the parametric evaluation indicated that the contact forces increased almost linearly with the clearance whereas the contact time reduced exponentially with the clearance.

In Chapter 6, the models of the tube wear parameters were combined with the model of the tube wear degradation mechanism to establish a general model to describe the trends of tube wear process over time. Since the combined model (or process model) was in an implicit form with respect to time, a computer algorithm was devised to perform the simulation of the tube wear process. Several simulations were conducted to understand how the trends of the wear may change over time as a result of aging and degradation mechanisms.

Two types of parametric models were studied in detail. They are 1) Power-Law model (at^b) and 2) Power-Exponential Model [$at^b\exp(ct)$]. The performance of the models were investigated for both normal and rapid cases of the tube wear degradation

with three block sizes of data, each including three, five, and ten data points. The effect of measurement noise on the performance of the models were also examined. To improve the performance of the suggested parametric models, a dynamic formulation of the process data was combined with the models in a time series manner. The performance of a high order nonlinear model was also investigated for the prediction of the wear process.

Three types of Neural Network Prediction (NNP) models were established according to the guidelines of Chapter 6 to forecast the tube wear process trends. They are three, five, and ten-point NNP models corresponding to short term, intermediate, and long term prediction, respectively. Analogous to the parametric models, their performance was investigated for both the normal and the rapid wear degradation processes and for data with noise.

Procedures were devised for the residual life estimation of the tube using both the parametric and the NNP models. Parametric sensitivity analysis and simulation of uncertainties were also carried out to identify parameters and factors that cause the greatest influence on the tube wear process.

7.2 Conclusions

The following conclusions are drawn from the investigations of this research study.

(1) During a normal tube wear process where the only degradation mechanism is the variation of the tube-to-support clearance, the process trends with time appears to be moderately nonlinear. A simple linear model, that often used in practice, can not adequately describe such process trends since it tends to underestimate

the trends.

(2) The degradation of friction coefficient and aging of the tube materials can markedly increase the progress of the wear damage mechanism and thereby reduce the useful life of tubes. They also introduce more complexity and nonlinearity in the wear process trends.

(3) The Power-Law model suggested by Ko [15,16] exhibited a good performance only for short term predictions of both normal and rapid tube wear degradation. For a long term prediction, the model tends to underestimate the process trends. However, a definite advantage of this model over other parametric models is that the estimation of its parameters is slightly affected by noise in the data.

(4) The Power-Exponential model, derived based on a simple approximation of the physics of the tube wear process, provides a satisfactory forecast of the process trend up to the tube wall thickness for both cases of normal and rapid wear degradation. However, a reliable estimation of the model parameters (to diminish the effect of noise) requires a minimum of six to ten data points that somewhat limits its application. This suggests that in practice where the process data are usually contaminated with noise, a simpler model such as at^b should be utilized until sufficient data are gathered.

(5) The results of the dynamic model of at^b reveals that the model can significantly improve the trend predictions of the simple model of at^b. Even when a simple second order linear dynamic model was employed, the model predictions were superior to those of a simple linear model and were analogous to those of the

Power-Exponential model. This implies that such models are able to capture the dynamics of the process from field data.

(6) The high order nonlinear model mathematically produces an excellent prediction of the wear process trends. However, to construct such a model, a large block size of data is needed for the estimation of model parameters. The estimation process also requires a nonlinear regression technique which is tedious to apply in practice.

(7) The performance investigations of the NNP models indicate that they provide excellent predictions of the process trends within their specified time-frame even for the case of the extrapolated trajectory. This is quite evident from the graphical representation of their predictions and small RMS values of the prediction errors as shown in section 6.5. They are also far less noise-sensitive than the parametric models. The satisfactory performance of the NNP models against noisy data should be considered as an important advantage of these models over the classical parametric models.

(8) Generally, a good estimation of the tube residual life requires two key components: (1) a reliable technique for trend forecasting of a given degradation process and (2) an accurate definition of the permissible degradation amount. It was demonstrated that when a value for the allowable tube wear degradation was given, the trending techniques developed in this study were able to estimate the remaining life of the tube with a good accuracy even with a small block size of data (five data points). A limitation of the residual life estimation appears

when the allowable degradation level is situated outside the time frame of an NNP model output. In such situations, the only definite inference that can be made is that the component survives within that time frame with a certain probability, as defined by Equation (6.16). To obtain an indication of the remaining life, as a rule of thumb, a plausible way is to pass a straight line from the last two points of the model predictions and then to make a projection with respect to the given degradation level.

(9) Statistical techniques can be used to establish confidence intervals for the predictions of parametric models though they may not always warrant to cover the true values. For NNP models, however, the construction technique is rather arbitrary. The RMS values of the training errors may be used to establish confidence bounds.

(10) In many practical applications, it is usually desirable to obtain assurances of the functionality and reliability of a component up to a few steps ahead of time or sometimes up to the next component's service inspection time. This is normally the case for nuclear steam generator tubes where the service inspections are performed approximately once a year. In such situations, the NNP models appear to be the best method of choice for the life assessment analysis. This idea is strongly supported by three major reasons that were explored during the course of this study. First, NNP models provide a superior prediction in comparison with that of parametric models when a limited amount of data is available (three to five data points for the case of tube wear). Second, they are

not influenced by noise as much as parametric models. In this dissertation, it was shown that even a correct type of parametric model may produce faulty results if sufficient data are not used for the estimation of model parameters to diminish the impact of noise. Third, as stated in Chapter 3, NNP models can be trained once and used for a class of components subjected to the same degradation process. This is not the case for the parametric models. Thus, the use of NNP models are strongly recommended especially at the beginning of a process where limited field data are usually available.

(11) The life assessment methodology proposed in this dissertation offers the benefits of greater physical insight into a prediction system and of leading to a more reliable forecast with a limited amount of data. It is also general in principle and is expected to be applicable to any degradation mechanism which is simple or as complex as the wear process. A successful application of the methodology was demonstrated for forecasting performance degradation of steam generators.

(12) Finally, it is important to realize that an in-depth life assessment analysis of many mechanical components requires advances in modeling procedures with improved inspection techniques and equipment for data acquisition. This should also be combined with continuing integration of materials, mechanical, and chemical engineering expertise on the subject.

7.3 Recommendations for Future Research

The life assessment methodology developed in this dissertation has been examined only for a single mode of degradation. Thus an obvious extension of the work is to

investigate the effects of multiple degradation modes on the life estimation of a component both methodologically and experimentally. Multiple degradation modes may occur concurrently or sequentially during the life of a component. Notable examples are reactor vessels and steam generator tubes that are subjected to various degradation mechanisms such as nuclear radiation, corrosion, wear, fatigue, and thermal and mechanical stresses. For the case of steam generator tubes, as an example, the combined effects of wear and high cycle fatigue which occur simultaneously can effectively accelerate the mechanical failures of tubes. Thus, a technique is to be developed in order to analyze the combined effects of degradation mechanisms on the service life of tubes. The trends of the combined effects in conjunction with available field data and information should then be used to estimate the useful remaining life of a component. This needs further improvements and developments in the trending techniques that are described in this dissertation for both parametric and NNP models.

Another interesting problem would be to determine how shocks or rapid process transients may reduce the useful life a component. This should be investigated based on the number of occurrences and the duration time of such phenomena. In nuclear steam generators, excessive tube vibration was reported [17] during large power trips in such components. Also, rapid temperature and pressure variations introduced during these events can raise the stress level of tubes, and could eventually lead to their early failures.

REFERENCES

REFERENCES

[1] B. L. Dow, "Steam Generator Progress Report Revision 8," Prepared by Energy Management Services Inc. for EPRI, October 1992.

[2] J. T. Lovett and B. L. Dow, "Steam Generator Performance Degradation" Energy Management Services Inc. EPRI NP-7524, September 1991.

[3] M. J. Pettigrew, H. G. D. Goyder, Z. L. Qiao and F. Axisa, "Damping of Multispan Exchanger Tubes Part 1: In Gases," Symposium on Special Topics of Structural Vibration, ASME Pressure Vessels and Piping Conference, Chicago, July 1986.

[4] M. J. Pettigrew, R. J. Rogers and F. Axisa, "Damping of Multispan Exchanger Tubes Part 2: In Liquids," Symposium on Special Topics of Structural Vibration, ASME Pressure Vessels and Piping Conference, Chicago, July 1986.

[5] M. J. Pettigrew, L. N. Carlucci, C. E. Taylor and N. J. Fisher, "Flow-induced Vibration and Related Technologies in Nuclear Components," Nuclear Engineering and Design Vol. 131, pp 81-100, North-Holland, 1991.

[6] M. J. Pettigrew, C. E. Taylor and B.S. Kim, "Vibration of Tube Bundles in Two-Phase Cross-Flow: Part1--Hydrodynamic Mass and Damping," Journal of Pressure Vessel Technology, Vol. 111, pp 478-487, November 1989.

[7] M. J. Pettigrew, J. H. Tromp, C. E. Taylor and B.S. Kim, "Vibration of Tube Bundles in Two-Phase Cross-Flow: Part2--Fluid-Elastic Instability," Journal of Pressure Vessel Technology, Vol. 111, pp 488-499, November 1989.

[8] C. E. Taylor, I. G. Currie, M. J. Pettigrew and B.S. Kim, "Vibration of Tube Bundles in Two-Phase Cross-Flow: Part3--Turbulence-Induced Excitation, " Journal of Pressure Vessel Technology, Vol. 111, pp 466-477, November 1989.

[9] K. P. Singh and A. I. Soler, "Mechanical Design of Heat Exchangers," Arcturus Publishers, Inc., Cherry Hill, NJ, 1984.

[10] M. K. Au-Yang, "Dynamics of Coupled Fluid-Shells," Trans. of the ASME, Journal of Pressure Vessel Technology, Vol. 108, July 1986.

[11] M. K. Au-Yang, "Turbulent Buffeting of a Multispan Tube Bundle," Trans. of the ASME, Journal of Vibration, Acoustics, Stress, and Reliability in Design,

Vol. 108, April 1986.

[12] M. P. Paidoussis, "A Review of Flow-Induced Vibration in Reactor Components," Nuclear Engineering and Design, Vol. 74, pp. 31-60, 1982, North-Holland Publishing Company.

[13] R. J. Rogers and R. J. Pick, "On the Dynamic Spatial Response of a Heat Exchanger Tube with Intermittent Baffle Contacts," Nuclear Engineering and Design, Vol. 36, pp. 81-90, 1976, North-Holland Publishing Company.

[14] R. J. Rogers and R. J. Pick, "Factors Associated with Support Plate Forces Due to Heat-Exchanger Tube Vibratory Contact," Nuclear Engineering and Design, Vol. 44, pp. 247-253, 1977, North-Holland Publishing Company.

[15] P. L. Ko, "Experimental Studies of Fretting in Steam Generators and Heat Exchangers," Journal of Pressure Vessel Technology, Vol. 101, May 1979.

[16] P. L. Ko and R. J. Rogers, "Analytical and Experimental Studies of Tube/Support Interaction in Multi-Span Heat Exchanger Tubes," Nuclear Engineering and Design, Vol. 65, pp. 399-409, 1981, North-Holland Publishing company.

[17] C. S. Davis, J. M. Thomas, S. W. Winder, and D. E. Allison, "An Engineering and Probablilistic Analysis of Tube Cracking Performance in Once-Through Steam Generators," Volume 1 & 2, EPRI NP_3065, Prepared by Failure Analysis Associates, Palo Alto, California, July 1983.

[18] P. L. Ko and H. Basis, "Correlation of Support Impact Force and Fretting_Wear for a Heat Exchanger Tube," Journal of Pressure Vessel Technology, Vol. 106, pp 69-77, 1984.

[19] K. H. Haslinger and D. A. Steininger, "Steam Generator Tube/Tube Support Plate Interaction Characteristics," Symposium on Flow-Induced Vibrations, ASME Winter Annual Meeting, New Orleans, December, 1984.

[20] R. D. Blevins "A Rational Algorithm for Predicting Vibration Damage to Tube and Shell Heat Exchanger," Symposium on Flow-Induced Vibrations, ASME Winter Annual Meeting, New Orleans, December, 1984.

[21] J. A. Jendrzejczyk, "Dynamic Characteristics of Heat Exchanger Tube Vibrating in a Tube Support Plate Inactive Mode," Journal of Pressure Vessel Technology," Vol. 108, pp 256-266, 1986.

[22] M. Yetisir and D. S. Weaver, "The Dynamics of Heat Exchanger U-Bend Tubes

With Flat Bar Supports," Journal of Pressure Vessel Technology, Vol. 108, pp 406-412, 1986.

[23] R. G. Sauve and W. W. Teper, "Impact Simulation of Process Equipment Tubes and Support Plates--A Numerical Algorithm," Journal of Pressure Vessel Technology, Vol. 109, pp 70-79, February 1987.

[24] N. J. Fisher, M. J. Olesen, R. J. Rogers and P. L. Ko, "Simulation of Tube-to-Support Dynamic Interaction in Heat Exchange Equipment," Journal of Pressure Vessel Technology, Vol. 111, pp 378-384, November 1989.

[25] H. G. D. Goyder and C. E. Teh, "A Study of the Impact Dynamics of Loosely Supported Heat Exchanger Tubes," Journal of Pressure Vessel Technology, Vol. 111, pp 394-401, November 1989.

[26] M. A. Salmon, V. K. Verma and T. G. Youtsos, "Elastic Analysis of Beam-Support Impact," Journal of Pressure Vessel Technology, Vol. 107, pp 64-67, February 1985.

[27] F. Axisa, A. Desseaux, and R. J. Gibert, "Experimental Study of Tube/Support Impact Forces in Multi-Span PWR Steam Generator Tube," ASME Winter Annual Meeting, New Orleans, LA, December 1984.

[28] Y. S. Shin, D. E. Sass and J. A. Jendrzejczyk, "Vibro-Impact Responses of a Tube with Tube-Baffle Interaction," ASME, PVP-20, 1978.

[29] M. J. Pettigrew and C. E. Taylor, "Fluidelastic Instability of Heat Exchanger Tube Bundles: Review and Design Recommendations," Journal of Pressure Vessel Technology, Vol. 113, pp 242-256, May 1991.

[30] N. J. Fisher, J. G. Ing, M. J. Pettigrew and R. J. Rogers, "Tube-to-Support Dynamic Interaction for a Multispan Steam Generator Tube," The American Society of Mechanical Engineers, PVP-Vol. 242, pp 301-316, 1992.

[31] D. J. Gorman, "Exact Analytical Solutions for the Free Vibration of Steam Generator U-Tubes," Trans. of the ASME, Journal of Pressure Vessel Technology, Vol. 110, November 1988.

[32] J. M. Chenoweth, "Fiver- a New Design Concept to Prevent Tube Damage from Flow-Induced Vibration in Shell-and-Tube Heat Exchangers," Symposium on Flow-Induced Vibrations, ASME Winter Annual Meeting, New Orleans, December 1984.

[33] F. Axisa, A. Desseaux and R. J. Gibert, "Experimental Study of Tube/Support

Impact Forces in Multi-span PWR Steam Generator Tubes," Symposium on Flow-Induced Vibrations, ASME Winter Annual Meeting, New Orleans, December 1984.

[34] T. M. Frick, T. E. Sobek and J. R. Reavis, "Overview on the Development and Implementation of Methodologies to Compute Vibration and Wear of Steam Generator Tubes," Symposium on Flow-Induced Vibrations, ASME Winter Annual Meeting, New Orleans, December 1984.

[35] E. R. France and H. J. Connors, "Simulation of flow induced vibration Characteristics of a Steam Generator U-Tube," International Conference on Flow Induced Vibration, Proceedings of the Institution of Mechanical Engineers, Brighton, May 1991.

[36] P. J. Langford and H. J. Connors, "Calculation of Tube/AVB Wear from U-bend Shaker Test Data," International Conference on Flow Induced Vibration, Proceedings of the Institution of Mechanical Engineers, Brighton, May 1991.

[37] H. J. Connors and F. A. Kramer, "U-bend Shaker test Investigation of Tube/AVB Wear Potential," International Conference on Flow Induced Vibration, Proceedings of the Institution of Mechanical Engineers, Brighton, May 1991.

[38] S. S. Chen, "A Review of Dynamic Tube-Support Interaction in Heat Exchanger Tubes," International Conference on Flow Induced Vibration, Proceedings of the Institution of Mechanical Engineers, Brighton, May 1991.

[39] C. E. Teh and H. G. D. Goyder, "Impact Analysis of Loosely Supported Heat Exchanger Tubes," International Conference on Flow Induced Vibration, Proceedings of the Institution of Mechanical Engineers, Brighton, May 1991.

[40] N. J. Fisher, R. J. Rogers, J. G. Ing and M. J. Pettigrew, " Fretting-Wear Damage Prediction in the Inlet Region of Steam Generator," International Conference on Flow Induced Vibration, Proceedings of the Institution of Mechanical Engineers, Brighton, May 1991.

[41] G. Allen, "Flow Induced Vibrations in the Tube Banks of Fossil Fuel Fired Boilers," International Conference on Flow Induced Vibration, Proceedings of the Institution of Mechanical Engineers, Brighton, May 1991.

[42] Steam Generator Reference Book, Electric Power Research Institute, Palo Alto, CA, May 1985.

[43] F. A. Simonen and C. E. Jaske, "A Computational Model for Predicting the Life

of Tubes Used in Petrochemical Heater Service," Journal of Pressure Vessel Technology, Vol. 107, pp 239-246, August 1985.

[44] M. J. Cohn, "Remaining Life of High-Energy Piping Systems Using Equivalent Stress," Journal Pressure Vessel Technology, Vol. 112, pp 260-265, August 1990.

[45] Mitchell/Landgraf, "Advances in Fatigue Lifetime Predictive Techniques," ASTM Publications, STP 1122, Philadelphia, PA, 1992.

[46] Cragnolino and Sridhar, "Application of Accelerated Corrosion Tests to Service Life Prediction of Materials," ASTM Publications, STP 1194, Philadelphia, PA, 1994

[47] I. B. Gertsbakh, "Statistical Reliability Theory," Marcel Dekker Inc., New York, 1989.

[48] D. Kececioglu, "Reliability Engineering Handbook," Prentice Hall, Englewood Cliffs, New Jersey, 1991.

[49] J. Davidson, "The Reliability of Mechanical Systems," Mechanical Engineering Publications, the Institution of Mechanical Engineers, London, 1994

[50] Dominion Engineering, Inc., "Statistical Analysis of Steam Generator Tube Degradation," EPRI NP-7493, Virginia, September 1991.

[51] W. Nelson, "Accelerated Testing, Statistical Models, Test Plans, and data Analyses," John Wiley, New York, 1990.

[52] A. Pankratz, "Forecasting with Dynamic Regression Models," John Wiley & Sons Inc., New York, 1991.

[53] B. R. Upadhyaya, M. Naghedolfeizi and B. Raychaudhuri, "Residual Life Estimation of Plant Components," pp. 22-29, P/PM Technology, June 1994.

[54] M. Naghedolfeizi and B. R. Upadhyaya, "A Methodology for Forecasting Performance Degradation of Steam Generators," Proceedings of the Sixth Predictive Maintenance Conference, Philadelphia, PA, May 16-19, 1994.

[55] P. K. Liaw, A. Saxena and J.S. Perrin, "Life Extension Technology for Steam Pipe Systems-II. Development of Life Prediction Methodology, Engineering Fracture Mechanics, Vol. 45, No. 6, pp 787-798, England, 1993.

[56] P. K. Liaw, A. Saxena and J. Schaefer, "Estimating Remaining Life of Elevated-

Temperature Steam Pipes-Part I. Materials Properties, Engineering Fracture Mechanics, Vol 32, No. 5., pp 675-708, England, 1989.

[57] M. Paz, "Structural Dynamics, Theory and computation," Van Nostrand Reinhold Company, New York, 1985.

[58] N. Kikuchi, "Finite Element Methods in Mechanics," Cambridge University Press, London, 1986.

[59] S. Timoshenko and Goodier, "Theory of Elasticity," McGraw-Hill, New York, 1970.

[60] J. S. Przemieniecki, "Theory of Matrix Structural Analysis," McGraw-Hill Book Company, New York, 1968.

[61] S. S. Rao, "Mechanical Vibrations," Second Edition, Addison-Wesley Publishing Company, New York, 1990.

[62] J. F. Lawless, "Statistical Models and Methods for Lifetime Data," John Wiley & Sons, New York, 1982.

[63] J. A. Collins, "Failure of Materials in Mechanical Design," John Wiley & Sons, New York, 1981.

[64] N. E. Dowling, "Mechanical Behavior of Material," Prentice-Hall Inc., Englewood Cliffs, New Jersey, 1993.

[65] R. W. Hertzberg, "Deformation and Fracture Mechanics of Engineering Materials," John Wiley & Sons, New York, 1983.

[66] E. O. Hall, "Yield Point Phenomena in Metals and Alloys," Macmillan and Co Ltd., London, 1970.

[67] W. J. Shack, "An overview of Environmental Degradation of Materials in Nuclear Power Plant Piping Systems," Proceedings of Third International Symposium on Environmental Degradation of Materials in Nuclear Power System, Traverse City, MI, August 30-September 3, 1987.

[68] G. O. Hayner, et al, "Examination of Tubes Removed from St. Luice Unit 1 and Investigation of Causes of the Corrosion," Proceedings of Third International Symposium on Environmental Degradation of Materials in Nuclear Power System, Traverse City, MI, August 30-September 3, 1987.

[69] M. G. El-Sherbiny and F. B. Salem, "Fretting-Resistant Ion-Plated Coatings,"

Published in Materials Evaluation under Fretting Conditions, ASTM SPT 780, Philadelphia, PA, 1981.

[70] I. V. Kragelsky, M. N. Dobychin, and V. S. Kombalov, "Friction & Wear Calculation Methods," Pergamon Press, Oxford, 1982.

[71] A. D. Sarkar, "Wear of Metals" Pergamon Press, Oxford, 1976.

[72] P. A. Engel, "Impact Wear of Material," Elsevier Scientific Publishing Company, New York, 1976.

[73] Structural Integrity Associates, Inc. "Component Life Estimation: LWR Structural Materials Degradation Mechanisms," EPRI NP-5461, 1987.

[74] Babcock & Wilcox Co., "Steam: Its Generation and Use," New York, 1978.

[75] Combustion Engineering, Inc. "Remaining Life Estimation of Boiler Pressure Parts," EPRI CS-5588, Vol.1-4, 1988.

[76] Steam Generator Eddy Current Data Analysis Performance Demonstration Review Material, Prepared by EPRI NDE Center, June 1993.

[77] W. E. Deeds and C. V. Dodd, "Eddy Current Inspection of Steam Generator Tubing," Electromagnetic Methods of Nondestructive Testing Monograph and Tracts Vol. 3, W. Lord, Ed., Gordon and Breach, New York, 1985.

[78] W. Yan and B. R. Upadhyaya, "Hybrid Digital Signal Processing and Neural Networks for Automated Diagnostics Using Eddy Current Inspection," Proc. ICANN 93, Amsterdam, Sep. 1993.

[79] H. M. Sadek, "Nondestructive Examinations of Heat Exchanger Tubing Ferrous and Non-ferrous Materials," the 1991 International Joint Power Generation Conference, San Diego, CA, October 6-10, 1991.

[80] Y. Liu, B.R. Upadhyaya and M. Naghedolfeizi, "Chemometric Data Analysis Using Artificial Neural Networks," Applied Spectroscopy, Vol. 47, No. 1, 1993.

[81] A. Maren, C. Harston, and R. Pap, "Handbook of Neural Computing Applications," Academic Press, New York, 1990.

[82] P. K. Simpson, "Artificial Neural Systems," Pergammon Press, New York, 1990.

[83] J. Hertz, A. Krogh and R.G. Palmer, "Introduction to the Theory of Neural Computation," Addison-Wesley, Reading, Massachusetts, 1991.

[84] Neural Computing Software system, NeuralWare Inc., Version 4, Pittsburgh, PA, 1991.

[85] C. L. Mantell, "Engineering Material Handbook," McGraw-Hill, New York, 1958.

[86] Statistical Software System (SAS), "System for Regression," Second Edition, SAS Institute Inc., Cary, NC, U.S.A, 1991.

[87] IMSL User's Manual, "FORTRAN Subroutines for Mathematical Applications," Version 2.0, IMSL Inc., U.S.A, 1991.

[88] G. Knudsen, "Coping with Cooling Water Fouling in Tubular Heat Exchangers, American Institute of Chemical Engineering, Symposium Series on Heat Transfer, Philadelphia, 1989.

[89] E. F. C. Somerscales and J. G. Knudsen, "Fouling of Heat Transfer Equipment," McGraw-Hill, New York, 1981.

[90] S. Yokell, " A Working Guide to Shell-and-Tube Heat Exchangers," McGraw-Hill, New York, 1990.

[91] M. Naghedolfeizi and B. R. Upadhyaya, "Dynamic Modeling of a Pressurized Water Reactor Plant for Diagnostics and Control," The University of Tennessee, Report DOE/NE/88ER12824-02, Knoxville, TN, June 1991.

APPENDICES

APPENDIX A

STEAM GENERATOR TUBE FAILURE MODES

This appendix provides a review of steam generator tube wall degradation mechanisms which lead to the failure of tubes. It also presents the industry impact of these failure modes on nuclear power plants in terms of tube plugging and forced power outages. Most of the information presented here is extracted from References [42,76].

A.1 Tube Wall Degradation Mechanisms

As described in Chapter 1, there are seven recognized forms of steam generator tube wall degradation which are divided into two broad categories (1) chemical corrosion and (2) mechanical degradation. The former includes thinning, pitting, primary-water stress corrosion cracking, and intergranular attack/stress corrosion cracking. The mechanical degradation contains wear, fatigue, and impingement damage which are often referred to as erosion-corrosion. The description of these failure modes are given below.

● Thinning

Wall thinning or wastage is defined as the volumetric loss of tube material due to the dissolution of tube material into steam generator coolant. The main reasons leading to the occurrence of this problem are: (1) use of secondary system materials and design

(balance-of- plant) which results in the introduction of corrosion products into the steam generator causing sludge piles, (2) the design of the steam generator which causes these corrosion products settling out in a high-heat flux area where they can not be effectively removed by blowdown flow, and (3) all-solids phosphate secondary-side water chemistry. The occurrence of tube thinning has been confirmed only in recirculating type steam generators. Tube thinning has been observed and detected in 17% of the Westinghouse plants, accounting for 4.5% of the existing plugged tube population. For the Combustion Engineering plants these numbers are 13% and 1.1% respectively.

● **Pitting**

Pitting is a type of corrosion in which degradation is led by local galvanic variations in the tubing. Similar to thinning, pitting ensues by dissolution of surface material but with no preferential grain boundary attack. Pitting appears to be acid attack associated with the introduction of chlorides, sulfur anions, and copper oxides into the steam generator. Unlike thinning, pitting does not tend to grow into a large volume since it is caused by small and localized galvanic differences. The industry impact of pitting has been relatively minor. Only one Combustion Engineering plant and several Westinghouse plant (representing 4.7% of the plant population) have diagnosed with pitting problems.

● **PWSCC**

Primary-water stress-corrosion cracking (PWSCC) is a term used to describe the stress corrosion cracking that typically develops at changes in tube geometry such as roll transition in tube sheet area, dents, and inner row U-bends. This form of tube

degradation has been experienced only in recirculating type steam generators. The affected plant populations by PWSCC for Westinghouse and Combustion Engineering plants are 51.3% and 13.3% respectively. Only one Babcock & Wilcox plant has been diagnosed with PWSCC problem.

● **IGA/SCC**

Intergranular attack/stress corrosion cracking is attributed to the symbiotic action of a sensitive material, aggressive corrosion environment, and stress that occurs on the surface of the tubing. The intergranular attack (IGA) by itself is a term used to characterize a uniform or relatively uniform corrosion attack of grain boundaries over the surface of the tubing. In the formation of IGA, stress is not considered as a strong contributing factor. However stress is believed to be a stronger contributor in a two-dimensional form of intergranular corrosion (often called fingers). The term stress-corrosion cracking (SCC) refers to single or multiple major cracks with minor to moderate amounts of branching. The nature of crack propagation in this phenomenon is predominately intergranular. Depending on the stress state of the material, the type of cracking can be axial, circumferential, or biaxial.

The industry impact of IGA/SCC has been relatively major. It has affected a large percentage of the steam generator population in nuclear power plants. The percentage of the affected plants for Westinghouse, Combustion Engineering, and Babcock & Wilcox plants are 41.2%, 60%, and 50%; respectively. This form of tube degradation has also contributed to a large percentage plugged tubes in existing steam generators.

● **Wear**

Wear is typically regraded as a rubbing mechanical process which causes the removal of material from a surface. In steam generators, the rolling/sliding motions of tubes against their tube supports results in the wear of tubes. The forcing function for the tube wear is the steam generator secondary side fluid flow which induces tube vibrations with subsequent dynamic interaction between the tube and its tube support. The shape of a tube wear scar depends normally on the geometry of tube support and the size of land contact area between tube and tube support. However, visual examination of the pulled-out tubes indicates that the shape of a typical wear scar tends to be somewhat regular resembling a rectangular shape.

Tube wear has affected a large percentage of the operating steam generators in the plants of Westinghouse, Combustion Engineering, and Babcock & Wilcox. The percentage of the affected plant population for Westinghouse is 70.2%, for Babcock & Wilcox is 87.5%, and for Combustion Engineering is 73.3%. It should be noted that tube wear by itself has only caused a small fraction of forced outages in the plants of these vendors.

● **Fatigue**

Tube fatigue develops as a result of alternating stress cycles produced by tube vibration motions. It is often accelerated by chemically aggressive environment or corrosion processes occurring concurrently with the applied stresses (often referred to as corrosion fatigue). The consequence of the tube fatigue is the initiation and/or propagation of cracks on a tube surface which may result in the rupture of the tube.

Tube fatigue has been experienced only in the plants of Westinghouse and Babcock and Wilcox. It has affected 87.5% of the operating once-through steam generator units, but it has only affected 1.8% of the recirculating units.

● Impingement

Tube impingement is defined as a form of erosion (material loss) caused by suspended solids and/or liquid droplets impacting the tube surface. The degree of tube damage can vary depending upon the impinging sizes, velocities, shapes, and hardness of particles. Its occurrence is usually unique to once-through steam generators where flow-induced impingement of tiny particles hit against the tube surface. The source of particles is believed to be debris distributed throughout the steam generator secondary side.

Impingement damage mechanism occurs only in once-through steam generators where it has affected 37.5% of the plant population.

● Denting

Denting is a process where a rapid buildup of corrosion products in the tube-to-support plate annulus squeezes the tube wall and thereby causing dents in the tubes. This process can effectively contribute to the initiation of stress-corrosion-cracking with subsequent tube failure. Thus, the knowledge of its presence is important for the failure analysis of steam generator tubing.

The major factors leading to denting are (1) copper oxide or oxygen introduced to the steam generator, (2) tube support plate hole design in which flow blockage and impurity buildup are likely, and (3) use of tube support material (carbon steel) subject to rapid corrosion.

A.2 Tube Plugging Trend and Forced Power Outages

This section presents a survey of tube plugging trends and forced power outages due to the described tube degradation mechanisms. The tube plugging trends are shown in Figure A.1-A.3 for the steam generators of Babcock & Wilcox, Combustion Engineering, and Westinghouse. Forced power outages due to corrosion and mechanical degradation mechanisms are illustrated in Figure A.4 and A.5, respectively. These figures, indicate that tube fatigue and IGA/SCC have caused the largest percentage of forced power outages.

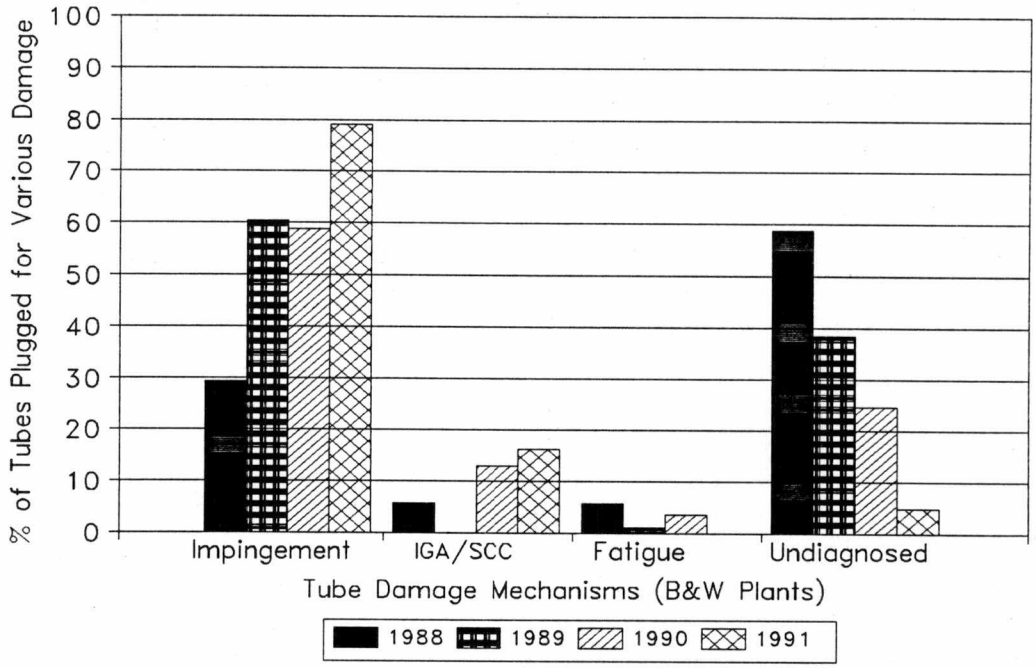


Figure A.1: Tube plugging trends of Babcock & Wilcox steam generators [76].

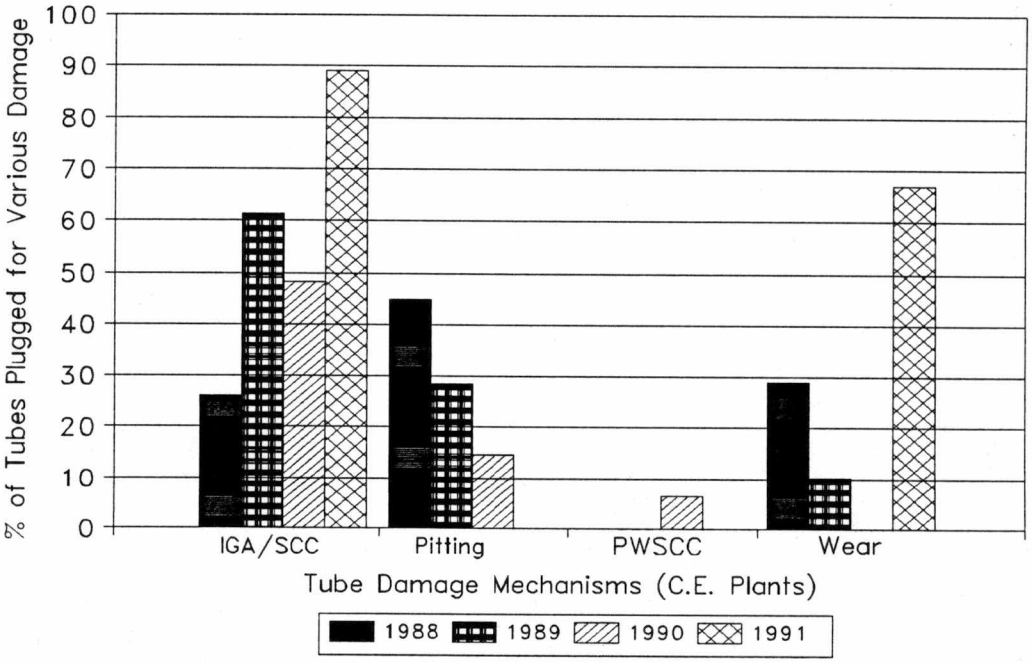


Figure A.2: Tube plugging trends of Combustion Engineering steam generators [76].

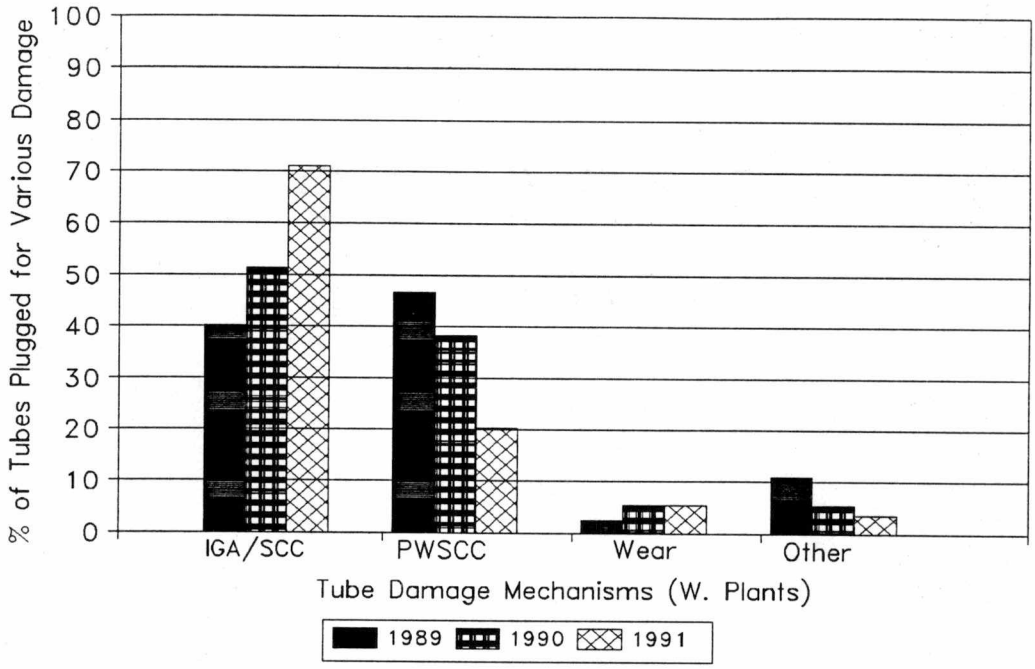


Figure A.3: Tube plugging trends of Westinghouse steam generators [76].

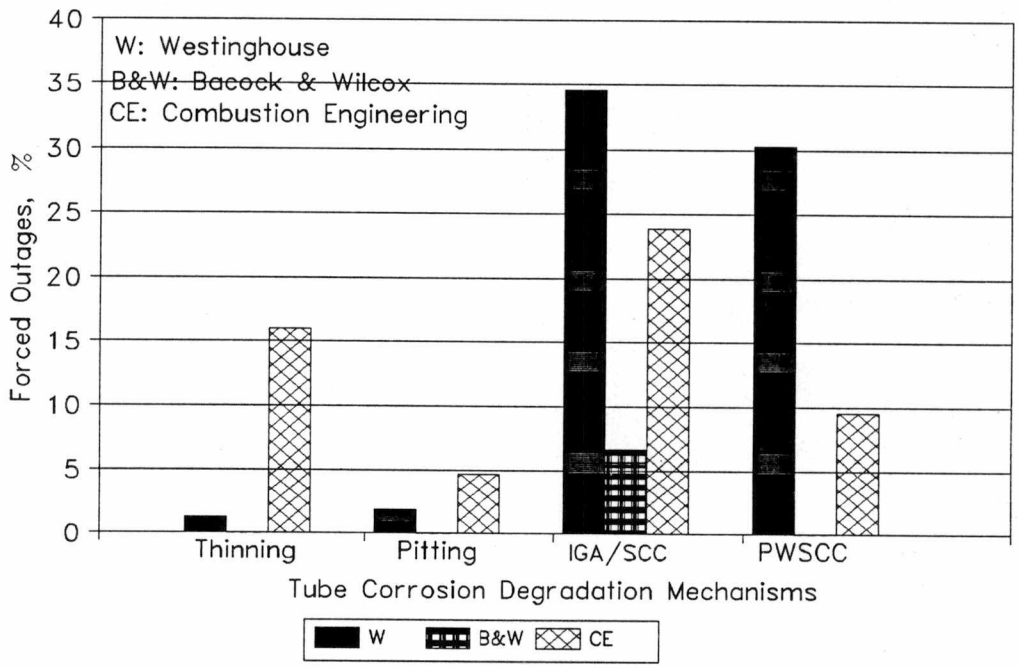


Figure A.4: Percent of forced power outages due to corrosion degradation mechanisms [76].

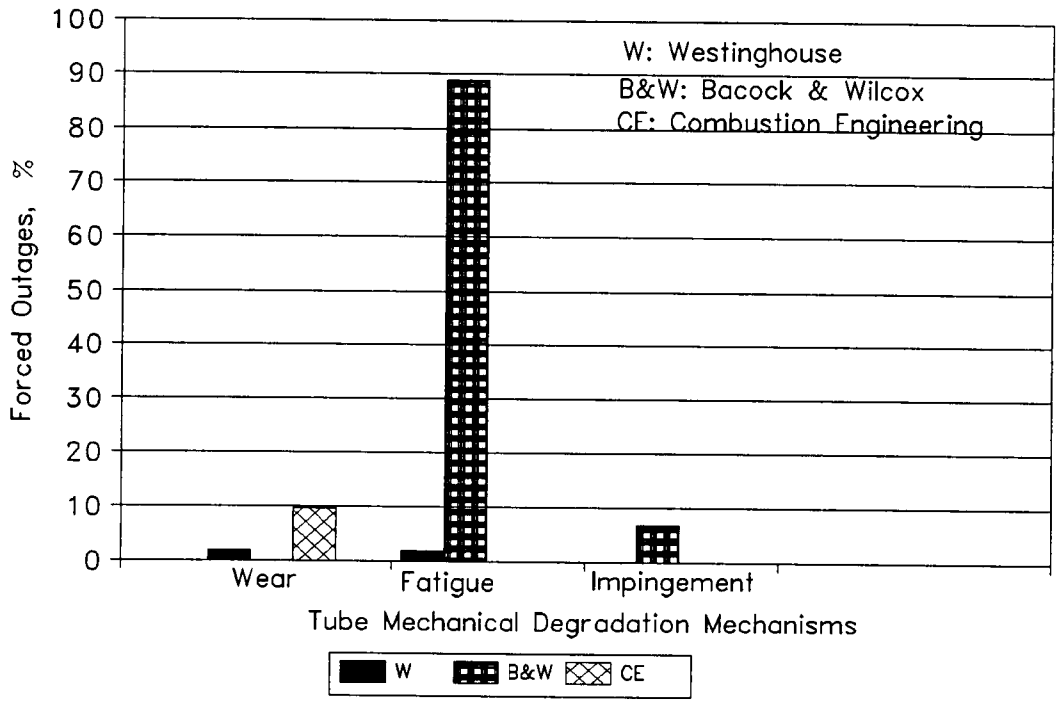


Figure A.5: Percent of forced power outages due to mechanical degradation mechanisms [76].

APPENDIX B

MASS AND STIFFNESS MATRICES

This appendix presents mass and stiffness matrices used in the construction of the one- dimensional finite element vibration model of a multi-span tube (see Chapter 5). The derivation of these matrices are well documented in various text books and literature describing finite element methods and/or vibration analysis [58,60,61].

The mass matrix [m], for a uniform beam element of length l with its two ends (joint) undergoing both translational and rotational displacement is derived as

$$[m] = \frac{\rho A l}{420} \begin{bmatrix} 156 & 22l & 54 & -13l \\ 22l & 4l^2 & 13l & -3l^2 \\ 54 & 13l & 156 & -22l \\ -13l & -3l^2 & -22l & 4l^2 \end{bmatrix}$$

where ρ is the density of the beam and A is the area of cross section. The corresponding stiffness matrix of such a beam is

$$[k] = \frac{EI}{l^3} \begin{bmatrix} 12 & 6l & -12 & 6l \\ 6l & 4l^2 & -6l & 2l^2 \\ -12 & -6l & 12 & -6l \\ 6l & 2l^2 & -6l & 4l^2 \end{bmatrix}$$

where E is Young's modulus and I is the moment inertia of the cross section.

APPENDIX C

LISTING OF COMPUTER PROGRAMS

In this appendix, two computer codes are listed. The first code performs the simulation of tube-to-support dynamic interaction of a multi-span tube using a finite element technique as described in Chapter 5. To execute this program the IMSL software package [87] should be complied with this program. The code is written for workstation or mainframe that supports Vax operating system. It requires minor modifications to run on any personal computer equipped with an IMSL [87] package.

The other program performs the simulation of the tube wear process according to the algorithm described in section 6.3. The program can be run on any personal computer or work station that supports DOS, Unix or Vax operating system.

Computer Program of a Multi-Span Tube Vibration Model

```
************************************************************************
        DEFINITION OF VARIABLES
************************************************************************

c NE        NUMBER OF ELEMENTS
c NE1       NUMBER OF ELEMENTS IN SPAN 1
c NE2       // // // // // // // // 2
c N         NUMBER OF DEGREES OF FREEDOM
c ND        TOTAL NUMBER OF DEGREES OF FREEDOM
c NB        NUMBER OF BAFFLES
c TL        TOTAL LENGTH OF TUBE
c BL        LENGTH OF BAFFLE
c E         YOUNG'S MODULUS
c G         TORSIONAL MODULUS
```

```
c K          STIFFNESS MATRIX
c M          MASS MATRIX
c C          DAMPING MATRIX
c FN         TOTAL NUMBER OF TIME STEPS
c FR         FREQUENCY OF THE FORCES
c CM         COEFFICIENT OF DYNAMIC MASS
c CR         TUBE-TO-SUPPORT CLEARANCE
c FSP        IMPACT FORCES DUE TO SPRING ACTION OF SUPPORTS
c FDA        IMPACT DAMPING FORCES
c LM         SPAN LENGTH
c MMM        OVERALL MASS MATRIX
c KKK        OVERALL STIFFNESS MATRIX
c MOD        MODAL MASS MATRIX
c KMOD       MODAL STIFFNESS MATRIX
c CMOD       MODAL DAMPING MATRIX

*************************************************************************
c                          M A I N   P R O G R A M
*************************************************************************

    PARAMETER (PI = 3.14159,MXPARM=50)
    INTEGER  IDO,ISTEP,OPTION(50),JS
    INTEGER*4 IJ
    REAL*8 M(4,1),MMM(50,1),K(4,4),KKK(50,50),F(4,1),
   &     FFF(50,1), XLE(50),KINV(50,50),V(50),MMOD(50),
   &     KMOD(50),PARAM(MXPARM),F1(50),YPRIME(50),YP1(50),FMOD(50),
   &     T,TOL,Y(50),Y1(50),X(50),FLOAT,W(50),P1(50),
   &     CMOD(50),PART1,MT,MI,MA,MH,LM,KSP,XDOT(50),FSP(50),FDA(50),
   &     FTOTAL(50),FFF1(50,1),SMEAN,SRMS,MEAN,RMS,GA,YY,YY1,G1,G2,
   &     SUM,SUM1,WD,TERM1,DT,DF,F2,T1,T2,ALFAD,ksp1,KSP2
      COMPLEX*16   EVAL(50), EVEC(50,50)
      INTRINSIC FLOAT


    OPEN(60,FILE='SUP1.DAT',STATUS='UNKNOWN')
    OPEN(61,FILE='RUN.DAT',STATUS='OLD')
    OPEN(90,FILE='SUP1.INF',STATUS='UNKNOWN')
    OPEN(100,FILE='FEM.OUT',STATUS='UNKNOWN')
    OPEN(110,FILE='FEM.IN',STATUS='OLD')
    OPEN(30,FILE='FORCE.TYP',STATUS='OLD')
    OPEN(25,FILE='ELMNT.LEG',STATUS='OLD')

    WRITE(6,*)'ENTER  THE FINAL TIME AND THE TIME STEP SIZE'
    READ(61,*)TEND,FN
    WRITE(6,*)'ENTER  THE AMOUNT OF NOISE (PERCENT)'
    read(61,*)G1
    WRITE(6,*)'ENTER  THE NUMBER DATA POINTS TO SKIP'
    READ(61,*)JS
    WRITE(6,*)'ENTER  THE AMOUNT OF EXICITING FORCE'
    READ(61,*)G2
    READ(110,*) NE,NE1,NE2,NE3,NB
```

```
      READ(110,*) TL,BL,DI,DO,PITCH
      READ(110,*) E,G,ROHM
      READ(110,*) ZETA,ZETA1
      READ(110,*)BC1,BC2,BC3,BC4
      READ(110,*)FR
      READ(110,*)CM,CR0,CR1,CR2,CR3,CR4,CR5
      READ(110,*)ALFAD,KSP

       LDA =50
       LDEVEC = 50
     TLE = TL-BL*NB
     AREA  = PI*(DO**2 - DI**2)/4.
     XI    = PI*(DO**4 - DI**4)/64.
     Rp    = 0.85*PITCH
     ETA   = DO/(2*Rp)
     LM    = TLE/(FLOAT(NB)-1.)

      COEF2 = E*XI

*****************************************************************
c             MASS MATRIX OF ONE BEAM ELEMENT
*****************************************************************

     SMT=0.
     SROHO =0.
     SRMEU =0.
     II=1
     L=1
     DO KK1 = 1,NE
     READ(25,*) XLE(KK1),ROHI,ROHO,RMEU
     ROHave = ROHM +(ROHI*(DI**2) + CM*ROHO*(DO**2))/
    &       (DO**2 - DI**2)

     COEF1 = ROHave*AREA/2.
     MA = CM*PI*(DO**2)*XLE(KK1)*ROHO/4.
     MI = PI*(DI**2)*XLE(KK1)*ROHI/4.
     MT = MA+MI+ROHM*AREA*XLE(KK1)
     SMT = SMT+MT
     SROHO = SROHO+ROHO
     SRMEU = SRMEU+RMEU

     M(1,1) = COEF1*XLE(KK1)
     M(2,1) = COEF1*(XLE(KK1)**2)/12.
     M(3,1) = M(1,1)
     M(4,1) = M(2,1)

     CALL MASTERM(II,L,KK1,NE,BC1,BC2,BC3,BC4,M,MMM,NR,NC)
     L=L+2

     END DO
```

```
      MTave  = SMT/TL
      RMEUav = SRMEU/FLOAT(NE)
      ROHOav = SROHO/FLOAT(NE)

**********************************************************************
c              STIFFNESS MATRIX OF ONE BEAM ELEMENT
**********************************************************************

      II=0
      L=1
      ksp1=0.
      ksp2=0.
      DO KK1 =1,NE

      K(1,1) = (COEF2*12./(XLE(KK1)**3))+KSP2
      K(1,2) = COEF2*6./(XLE(KK1)**2)
      K(1,3) = COEF2*(-12.)/(XLE(KK1)**3)
      K(1,4) = COEF2*6./(XLE(KK1)**2)
      K(2,1) = K(1,2)
      K(2,2) = COEF2*4./XLE(KK1)
      K(2,3) = COEF2*(-6.)/(XLE(KK1)**2)
      K(2,4) = COEF2*2./XLE(KK1)
      K(3,1) = K(1,3)
      K(3,2) = K(2,3)
      K(3,3) = (COEF2*12./(XLE(KK1)**3))+ksp1
      K(3,4) = COEF2*(-6.)/(XLE(KK1)**2)
      K(4,1) = K(1,4)
      K(4,2) = K(2,4)
      K(4,3) = K(3,4)
      K(4,4) = COEF2*4./XLE(KK1)

      CALL MASTERM(II,L,KK1,NE,BC1,BC2,BC3,BC4,K,KKK,NR,NC)
      L=L+2
      END DO
      KNC=NC

**********************************************************************
c              FORCE VECTOR OF A DISTRIBUTED LOAD
**********************************************************************

      II=1
      L=1
      DO KK1 = 1,NE
      READ(30,*) P,P1(KK1),OPTION(KK1)
      IF (OPTION(KK1) .EQ. 0) THEN
      F(1,1) = -P*XLE(KK1)/2.
      F(2,1) = -P*(XLE(KK1)**2)/12.
      F(3,1) = -P*XLE(KK1)/2.
      F(4,1) = P*(XLE(KK1)**2)/12.
      END IF
```

```
**********************************************************************
c          FORCE VECTOR OF A CONCENTRATED LOAD
**********************************************************************

      IF (OPTION(KK1) .EQ. 1)THEN
      F(1,1) = 0.
      F(2,1) = 0.
      F(3,1) = -P
      F(4,1) = 0.
      END IF

      CALL MASTERM(II,L,KK1,NE,BC1,BC2,BC3,BC4,F,FFF,NR,NC)
      L=L+2
      END DO

**********************************************************************
c          NORMALIZATION OF THE DISTRIBUTED FORCE
**********************************************************************

      II=1
      L=1
      DO KK1 = 1,NE
      IF (OPTION(KK1) .EQ. 0) THEN
      F(1,1) = -P1(KK1)*XLE(KK1)/2.
      F(2,1) = -P1(KK1)*(XLE(KK1)**2)/12.
      F(3,1) = -P1(KK1)*XLE(KK1)/2.
      F(4,1) = P1(KK1)*(XLE(KK1)**2)/12.
      END IF

**********************************************************************
c          NORMALIZATION OF THE CONCENTERATED FORCE
**********************************************************************
      IF (OPTION(KK1) .EQ. 1)THEN
      F(1,1) = 0.
      F(2,1) = 0.
      F(3,1) = -P1(KK1)
      F(4,1) = 0.
      END IF

      CALL MASTERM(II,L,KK1,NE,BC1,BC2,BC3,BC4,F,FFF1,NR,NC)
      L=L+2
      END DO


**********************************************************************
c        MATRIX INVERSION SUBROUTINE (IMSL SOFTWARE)
**********************************************************************

      CALL DLINRG(NR,KKK,50,KINV,5)

**********************************************************************
```

```
c          CALCULATION OF THE TUBE DEFLECTION
*****************************************************************

      DO I =1,NR
      DO J = 1,KNC
      SUM = SUM + KINV(I,J)*FFF(J,1)
      END DO
      V(I) =SUM
      SUM = 0.
      END DO

*****************************************************************************
c   ECHO-PRINT OF MASS, STIFFNESS, DAMPING, AND FORCE MATRICES
*****************************************************************************

      WRITE(100,*)'M=['
      DO I =1,NR
      WRITE(100,15)MMM(I,1)
      END DO
      WRITE(100,*)'];'

      WRITE(100,*)

       WRITE(100,*)'K=['
       DO I = 1,NR
       WRITE(100,15)(KKK(I,J),J=1,KNC)
       END DO
       WRITE(100,*)'];'

      WRITE(100,*)

      WRITE(100,*)'F=['
      DO I =1,NR
      WRITE(100,15)FFF(I,1)
      END DO
      WRITE(100,*)'];'

*****************************************************************************
c  CALCULATION OF THE DYNAMIC MATRIX FOR EIGENVALUE PROBLEM
*****************************************************************************

      DO I =1,NR
      DO J = 1,KNC
      KINV(I,J)=KINV(I,J)*MMM(J,1)
      END DO
      END DO

*****************************************************************************
c IMSL SUBROUTINE FOR EIGENVALUE AND EIGENVECTOR CALCULATION
*****************************************************************************
```

```
      CALL DEVCRG(NR, KINV, LDA, EVAL, EVEC, LDEVEC)

      DO I =1,NR
      DO J = 1,KNC
      SUM=SUM+(EVEC(J,I)**2)*MMM(J,1)
      END DO
      MMOD(I)=SUM
      SUM=0.
      END DO

      DO I =1,NR
      DO LI = 1,NR
      DO J = 1,KNC
      SUM=SUM+EVEC(J,I)*KKK(J,LI)*EVEC(LI,I)
      END DO
      END DO
      KMOD(I)=SUM
      SUM=0.
      END DO

      DO I =1,NR
      W(I) = (KMOD(I)/MMOD(I))**.5
      END DO

      PART1 = ( PI/SQRT(8.) )*( ROHOav*(DO**2)/MTave )*
     &       ( 2.*SQRT(RMEUav)/DO )*( (1+ETA**3)/((1-ETA**2)**2) )

      DO I =1,NR
       CMOD(I)=2*(ZETA + ZETA1)*W(I)
      END DO

      SUM=0.
      DO I =1,NR
      DO J =1,NR
      SUM = SUM+EVEC(J,I)*FFF(J,1)
      END DO
      FMOD(I)=SUM/MMOD(I)
      SUM=0.
      END DO

**********************************************************************
c     ECHO-PRINT OF NEW STIFFNESS, DAMPING, AND FORCE MATRICES
**********************************************************************

      WRITE(100,*)'M_MODAL=['
      DO I =1,NR
      WRITE(100,15)MMOD(I)
      END DO
      WRITE(100,*)'];'

      WRITE(100,*)
```

```
      WRITE(100,*)'K_MODAL=['
      DO I =1,NR
      WRITE(100,15)KMOD(I)
      END DO
      WRITE(100,*)'];'

      WRITE(100,*)

      WRITE(100,*)'C_MODAL=['
      DO I =1,NR
      WRITE(100,15)CMOD(I)
      END DO
      WRITE(100,*)'];'

      WRITE(100,*)

      WRITE(100,*)'OMEGA=['
      DO I =1,NR
      WRITE(100,15)W(I)
      END DO
      WRITE(100,*)'];'

      WRITE(100,*)
      WRITE(100,*)'FMOD=['
      DO I =1,NR
      WRITE(100,15)FMOD(I)
      END DO
      WRITE(100,*)'];'

      WRITE(100,*)


**********************************************************************
c           DETERMINATION  OF THE TUBE MOTION
**********************************************************************

C           ****OUTER LOOP FOR TIME ITERATION****

      WRITE(60,*)'sup1=['

      SMENA=0.
      SRMS=0.
      KJ=0
      IJ=999999999
      NEQ=NR
      DO ISTEP= 1,TEND

C     ****INNER LOOP #1 FOR FORCE CALCULATION  AT EACH STEP OF TIME****

      T2=FLOAT(ISTEP)*FN
      SUM=0.
```

```
C          **** GENERATING GAUSSIAN WHITE NOISE ****

      Z=ran(IJ)
      ga=sqrt( -2.0*alog(Z) )*cos(6.28318*Z1)
      Z1=Z

      DO I =1,NEQ
      DO J =1,NEQ
      SUM = SUM+EVEC(J,I)*(G2*FFF(J,1)*SIN(2*PI*FR*T2)+
     &      GA*G1*FFF1(J,1)-FTOTAL(J))
      END DO
      FMOD(I)=SUM
      SUM=0.
      END DO

      DO I=1,NEQ

      FSP(I)=0.
      FDA(I)=0.
      FTOTAL(I)=0.
      END DO

C     **TIME INTEGRATION OF THE DIFFERENTIAL EQUATIONS**

      DT = T2-T1

      DO I =1,NEQ

      WD = SQRT( (W(I)**2-(CMOD(I)**2)/4.) )
      F2=FMOD(I)
      DF = F2-F1(I)
      TERM1 = EXP(-DT*CMOD(I)/2.)

      Y(I)=( DF/(KMOD(I)*DT) )*( DT-CMOD(I)/(W(I)**2) +
     & TERM1*( (CMOD(I)/(W(I)**2))*COS(DT*WD)-
     & (4.*WD**2-CMOD(I)**2)*SIN(DT*WD)/(4.*(W(I)**2)*WD)  )) +
     & ( F1(I)/KMOD(I) )*( 1.-TERM1*( COS(WD*DT) +
     & CMOD(I)*SIN(WD*DT)/(2.*WD)  ) ) + TERM1*
     & ( Y1(I)*COS(WD*DT) + (YP1(I)+CMOD(I)*Y1(I)/2.)*SIN(WD*DT)/WD  )


      YPRIME(I)=( DF/(KMOD(I)*DT) )*( 1.- TERM1*( COS(WD*DT)+
     & CMOD(I)*SIN(WD*DT)/(2.*WD)  ) ) + ( F1(I)/KMOD(I) )*
     & TERM1*(W(I)**2)*SIN(WD*DT)/WD  + TERM1*
     & ( YP1(I)*COS(WD*DT)-( CMOD(I)*YP1(I)/(2*WD)+
     &  (W(I)**2)*Y1(I)/WD )*SIN(WD*DT) )

C     ****CALCULATION OF FORCE, NORMALIZED SPEED, AND NORMALIZED****
C                    ** DISPLACEMENT **
```

```
      F1(I) = FMOD(I)
      Y1(I) = Y(I)
      YP1(I) = YPRIME(I)

C                ****END OF INTEGRATION LOOP****
      END DO

      T1 = FLOAT(ISTEP)/FN


      SUM=0.
      DO I =1,NEQ

      DO J=1,NEQ
      SUM=SUM+EVEC(I,J)*Y(J)
      SUM1 =SUM1+EVEC(I,J)*YPRIME(J)
      END DO

      X(I)=SUM
      XDOT(I)=SUM1

C     **** CALCULATION OF TUBE-TO-SUPPORT CONTACT FORCES ****

      If (I .EQ. 2*NE1-1) THEN

      IF (X(2*NE1-1) .GT. CR0) THEN
      KJ=KJ+1
      FSP(2*NE1-1) =KSP*(X(2*NE1-1) - CR0)
      FDA(2*NE1-1) = 1.5*ALFAD*ABS(XDOT(2*NE1-1))*FSP(2*NE1-1)
      FTOTAL(2*NE1-1)=FDA(2*NE1-1)+FSP(2*NE1-1)
      SMEAN = SMEAN+ABS(FTOTAL(2*NE1-1))
      SRMS  = SRMS+(FTOTAL(2*NE1-1))**2
      END IF


      IF (-X(2*NE1-1) .GT. CR1) THEN
      KJ=KJ+1
      FSP(2*NE1-1) =KSP*(X(2*NE1-1) + CR1)
      FDA(2*NE1-1) = 1.5*ALFAD*ABS(XDOT(2*NE1-1))*FSP(2*NE1-1)
      FTOTAL(2*NE1-1)=FDA(2*NE1-1)+FSP(2*NE1-1)
      SMEAN = SMEAN+ABS(FTOTAL(2*NE1-1))
      SRMS  = SRMS+(FTOTAL(2*NE1-1))**2
      END IF

      END IF

      IF (I .EQ. 2*(NE1+NE2)-1) THEN

      IF (X(2*(NE1+NE2)-1) .GT. CR2) THEN
      FSP(2*(NE1+NE2)-1) =KSP*(X(2*(NE1+NE2)-1) - CR2)
      FDA(2*(NE1+NE2)-1) = 1.5*ALFAD*ABS(XDOT(2*(NE1+NE2)-1))*
```

```
     & FSP(2*(NE1+NE2)-1)
       FTOTAL(2*(NE1+NE2)-1)=FDA(2*(NE1+NE2)-1)+FSP(2*(NE1+NE2)-1)
       END IF


       IF (-X(2*(NE1+NE2)-1) .GT. CR3) THEN
       FSP(2*(NE1+NE2)-1) =KSP*(X(2*(NE1+NE2)-1) + CR3)
       FDA(2*(NE1+NE2)-1) = 1.5*ALFAD*ABS(XDOT(2*(NE1+NE2)-1))*
     & FSP(2*(NE1+NE2)-1)
       FTOTAL(2*(NE1+NE2)-1)=FDA(2*(NE1+NE2)-1)+FSP(2*(NE1+NE2)-1)
       END IF

       END IF

       IF (I .EQ. 2*(NE1+NE2+NE3)-1) THEN

       IF (X(2*(NE1+NE2+NE3)-1) .GT. CR4) THEN
       FSP(2*(NE1+NE2+NE3)-1) =KSP*(X(2*(NE1+NE2+NE3)-1) - CR4)
       FDA(2*(NE1+NE2+NE3)-1)=1.5*ALFAD*ABS(XDOT(2*(NE1+NE2+NE3)-1))*
     & FSP(2*(NE1+NE2+NE3)-1)
       FTOTAL(2*(NE1+NE2+NE3)-1)=FDA(2*(NE1+NE2+NE3)-1)+
     & FSP(2*(NE1+NE2+NE3)-1)
       END IF


       IF (-X(2*(NE1+NE2+NE3)-1) .GT. CR5) THEN
       FSP(2*(NE1+NE2+NE3)-1) =KSP*(X(2*(NE1+NE2+NE3)-1) + CR5)
       FDA(2*(NE1+NE2+NE3)-1)=1.5*ALFAD*ABS(XDOT(2*(NE1+NE2+NE3)-1))*
     & FSP(2*(NE1+NE2+NE3)-1)
       FTOTAL(2*(NE1+NE2+NE3)-1)=FDA(2*(NE1+NE2+NE3)-1)+
     & FSP(2*(NE1+NE2+NE3)-1)
       END IF

       END IF



       IF ( ISTEP .EQ. (ISTEP/JS)*JS) THEN

       IF ( I .EQ. 2*NE1-1) WRITE(60,16)T2,X(I),XDOT(I),
     & GA*G1*FFF1(I,1),FTOTAL(I)
       END IF

      SUM1=0.
      SUM=0.

      END DO

C              ****END OF THE OUTER LOOP****
      END DO
```

```
      IF (KJ .EQ. 0) KJ=1
      MEAN = SMEAN/FLOAT(KJ)
      RMS  = SQRT(SRMS/FLOAT(KJ))

       WRITE(60,*)'];'

      WRITE(90,*)' TIME STEP SIZE =',1./FN
      WRITE(90,17)E,CR0,CR1,KSP,FR
      WRITE(90,18)TEND/FN,FLOAT(KJ)/FN
      WRITE(90,19)MEAN,RMS
      WRITE(90,*)'  NUMBER OF CONTACTS= ',KJ

 15    FORMAT(24(1X,E12.4))
 16    FORMAT(5(1X,E14.6))
 17    FORMAT(2X,'MODULUS  OF ELASTICITY=',3X,E14.6  /
     &  2X,'TUBE CLEARANCE AT 15TH SUPPORT (L)=',3X,E14.6/
     &  2X,'TUBE CLEARANCE AT 15TH SUPPORT (R)=',3X,E14.6/
     &  2X,'SPRING COEFFICIENT OF THE SUPPORTS=',3X,E14.6  /
     &  2X,'FREQUENCY  OF EXCITATION  FORCES =',3X,F5.1 /)
 18    FORMAT(2X,'TOTAL  TIME (sec)=',3X,F7.4  /
     &  2X,'TOTAL CONTACT TIME BETWEEN TUBE AND SUPPORT=',3X,E14.6  /)
 19    FORMAT(2X,'MEAN  VALUE OF IMPACT FORCES=',3X,F12.7  /
     &  2X,'RMS VALUE OF IMPACT FORCES=',3X,F12.7)


       END

*************************************************************************
c    SUBROUTINE FOR MAKING A MASTER MATRIX OF THE ENTIRE TUBE
c                       BEAM ELEMENTS
*************************************************************************

      SUBROUTINE MASTERM(II,L,KK1,NE,XBC1,XBC2,XBC3,XBC4,X,XXXX,NR,NC)
      REAl*8 X(4,4),XXX(50,50),XXXX(50,50),XX(50,50)
      INTEGER XSTART, XCOUNT

      IF (KK1 .GT. 1) GOTO 30

      XSTART = 1
      COUNT = (NE-1)*2+4
      XCOUNT = COUNT
      COUNT1 = COUNT



      DO I=1,COUNT
      DO J=1,COUNT1
      XXX(I,J)=0.
      END DO
      END DO
```

```
30    CONTINUE


      DO I=1,COUNT
      DO J=1,COUNT1
      XX(I,J)=0.
      END DO
      END DO


      IF (II .EQ. 1) COUNT1=1

*****************************************************************
c                 END OF INITIALIZATION
*****************************************************************

      LC=3
      LL=L

      IF (II .EQ. 1)THEN
      LL=1
      LC=0
      END IF

      DO I=L,L+3
      DO J=LL,LL+LC
      XX(I,J)=X(I+1-L,J+1-LL)
      END DO
      END DO


      DO I= 1,COUNT
      DO J= 1,COUNT1
      XXX(I,J) =XXX(I,J)+XX(I,J)

      END DO
      END DO

      IF (KK1 .NE. NE) GO TO 20

*****************************************************************
c                 BOUNDARY CONDITIONS
*****************************************************************

      IF (XBC1 .EQ. 0.)  XSTART = 2
      IF(XBC1 .EQ. 0. .AND. XBC2 .EQ. 0) XSTART = 3
      IF (XBC3 .EQ. 0.) XCOUNT = COUNT-1
      IF (XBC3 .EQ. 0. .AND. XBC4 .EQ. 0.) XCOUNT = COUNT-2

      NR = XCOUNT-XSTART+1
```

```
      NC =NR
      XSTART1=XSTART
      IF (II .EQ. 1) THEN
      NC=1
      XSTART1 = 1
      END IF

      DO I = 1,NR
      DO J = 1,NC
      XXXX(I,J) = XXX(I+XSTART-1,J+XSTART1-1)
      END DO
      END DO

 20   CONTINUE
      END
```

Computer Program for the Simulation of Tube Wear Mechanism

```
************************************************************************
        DEFINITION OF VARIABLES
************************************************************************

c
c W             = Wear amount
c a1-6          = Coefficients of Equations
c Cr            = Tube-to-Support Clearance
c Cr0           = Initial Tube-to-Support Clearance
c MU            = Coefficient of Friction between Tube and its Support
c MU0           = Initial Coefficient of Friction between Tube and Support
c Tc            = Overall Contact Time between Tube and Support
c TAU           = Yield Shear Stress Point of Tube
c TAU0          = Initial Yield Shear Stress Point of Tube
c Fn            = Normal Force between Tube and Support
c nd            = Number of data points
c T_range       = The time that the coefficient of friction Includes higher
c                 order terms (nonlinear terms).
c P             = Time interval for printing data points
c Alpha1-3      = Parameters of the coefficient of friction polynomial
c Mcr           = Reduction of tube wall thickness due to wear
c

************************************************************************
c                          MAIN PROGRAM
************************************************************************

      Character*150 Answer,Answer1,Answer2,String
      Parameter (PI = 3.14159)
      Integer*4 i,ii,k,choice4,nd
      Real*8 MU,MU0,N,a(10),a0(10),Cr,Cr0,Tc,TAU,TAU0,Fn,coeff1,
     &       coeff2,coeff3,time,p,alpha1,alpha2,alpha3,alph,alpha1_0,
     &       alpha2_0,o,T_range,percent,mcr,Cr_0,Cr_1,Cr_2
```

```
Open(100, File='Wear.inf',Status='old')
Open(110, File='wear.dat',Status='Unknown')
Open(95,  File='wearno.ise',status='Unknown')
Do I =1,6
Read(100,*) a(i)
a0(i)=a(i)
End do

Read (100, '(a)' )String
Read (100,*)Bl,Do,Cr0
Read (100,'(a)' ) String
Read (100,*)MU0,Roh,TAU0
Read (100, '(a)') String
Read (100,*)N,Time,Cycle
Read (100, '(a)') String
Read (100,*)Coeff1,p,T_range
Read (100, '(a)')String
Read (100,*)alpha1,alpha2,o
Read (100,'(a)')String
Read (100,*)percent

Alpha1_0 = alpha1
Alpha2_0 = alpha2
ii       = 999999999

Area   = Bl*PI*Do/3.
Coeff2 = (Roh*Area*1000000.)
Coeff3 = 3600.*6.8*10e-15*cycle/mu0
nd     = int(Time/p)

Write (6,*) 'Enter The Choice of Fuction for the
& Coefficient Of Friction'
Write (6,*)
Write (6,*) '1. Power '
Write (6,*) '2. Linear'
Write (6,*) '3. Piece-wise Polynomial <Default>'
Read (5,*)Choice1

Write (6,*) 'Enter The Choice of Fuction for the
& Contact Forces'
Write (6,*)
Write (6,*) '1. Linear <Default>'
Write (6,*) '2. Exponential'
Read (5,*)Choice2

Write (6,*) 'Enter The Choice of Fuction for the
& the Contact Time'
Write (6,*)
Write (6,*) '1. Linear <Default>'
Write (6,*) '2. Exponential'
```

```
      Read (5,*)Choice3
      Cr = Cr0

      Write(6,*) ' Do you want to perform a parametric study? (Y/N)'
      Read (5,'(a)')Answer
      Write(6,*) ' Do you want to add WHITE NOISE to the wear results?'
      Read (5,'(a)')Answer2

      If ((Answer .eq. 'Y') .OR. (Answer .eq. 'y')) then
      Go to 200
      else
      go to 210
      end if

200   Write(6,*) ' Your Choices are:'
      Write(6,*)
      Write(6,*) ' Code              Choice'
      Write(6,*)
      Write(6,*) ' 1    Rate Coefficient of Contact Forces'
      Write(6,*) ' 3    Rate Coefficient of Contact Time'
      Write(6,*) ' 5    Rate Coefficient of Coefficient of Friction'
      Write(6,*) ' 6    Rate Coefficient of Shear Yield Point'
      Write(6,*) ' 0    QUIT'
      Write(6,*)
      Write(6,*) ' Enter one of the above Codes (Integer Only)'
      Read (5,*) Choice4

      If (Choice4 .eq. 0) GO to 240

      K = Choice4
      a5 = a0(5)
      a6 = a0(6)
      alpha1_00 = alpha1_0
      alpha2_00 = alpha2_0

      I = -1
230   I = I +1

      If ( I .eq. 0) then

      a0(5)=0.
      a0(6)=0.
      alpha1_0 = 0.
      alpha2_0 = 0.

      Else

      a0(5)=a5
      a0(6)=a6
      alpha1_0 = alpha1_00
      alpha2_0 = alpha2_00
```

```
      End if

      a(K) = a0(K)*(1. + float(I)/10.)
      alpha1 = alpha1_0*(1. + float(I)/10.)
      alpha2 = alpha2_0*(1. + float(I)/10.)
      If ( (Choice1 .NE. 1.) .and. (Choice1 .NE. 2.) ) alpha1=alpha1_0

210   Continue

      Cr_0 = Cr0
      Cr = Cr0
      alph = 0.

      Do T= 1,time

      If ( (T/coeff1) .Gt. T_range) alph=alpha2

      If ( (Choice1 .NE. 1.) .and. (Choice1 .NE. 2.) ) then
      MU = Mu0+alpha1*(T/coeff1)+alph*(abs(T/coeff1-T_range)**o)
      end if

      If (Choice1 .Eq. 1.) MU  = MU0+0.002*((T/coeff1)**a(5)  )
      If (Choice1 .Eq. 2.) MU  = MU0+alpha1*(T/coeff1)
      If (t .le. coeff1 ) Mu=mu0+0.002
      If (Mu .GE. 0.75) Mu = 0.75

      TAU = TAU0*(  Exp( a(6)* T/coeff1 )  )

      If ( Choice2 .NE. 2. )  Fn  = a(1)*(Cr/Cr0) + a(2)
      If ( Choice2 .Eq. 2. )  Fn  = a(2)*Exp( (Cr/Cr0)*a(1) )

      If ( Choice3 .Ne. 2. ) Tc  = 900*( a(3)*(Cr/Cr0) + a(4) )
      If ( Choice3 .Eq. 2.)  Tc  = 900*( a(4)*Exp( (Cr/Cr0)*a(3) ) )

      Y    = ran(ii)
      Ga   = sqrt( -2.0 * alog(Y) )*cos(6.28318*y1)
      Y1   = Y
      Cr   = Cr + Coeff3*(MU*(Fn**N)*Tc)/(Coeff2*TAU)
      If ( (answer2 .Ne. 'Y') .and. (Answer2 .Ne. 'y') ) Ga = 0.
      Mcr  = (Cr-Cr0)*(1.0 + Percent*abs(Ga)/100.)

      If ( Int(t/p)*p .eq. T) then

      Write(110,10) T/8760.,Mcr*1000.,Fn,Tau,Mu
      Write(95,11) T/8760.,Mcr*1000.,Cr,ga
      End if

      End Do


      If (( Answer .eq. 'Y') .OR. (Answer .eq. 'y')) then
```

```
      Go to 250
      Else
      Go to 240
      End if

250   Continue
      If ( I .eq. 18) Go to 220
      Go to 230

 10   Format(1X,F6.2,3x,f12.9,3x,F7.3,3x,E15.8,3x,F12.2,3x,F6.5)
 11   format(1x,f4.1,2x,5(e12.6,1x))

220   Continue
      close(110)

      Call Data(k,nd)

      Write(6,*) ' Do You Want to Continue the Parametric Study?'
      Read (5,'(a)') Answer1

      If ((Answer1 .eq. 'Y') .or. (Answer1 .eq. 'y'))then
      cr=cr0
      Go to 200
      Else
      Go to 240
      End if

240   Continue
      End

*************************************************************************
C              DATA PREPARATION FOR PLOTTING
*************************************************************************

      Subroutine DATA (k,nd)

      Character*200,  filename(7),filenam1(7)
      Integer i,k,nd,jd
      real T1(400),D(400),Force(400),TCO(400),TAU1(400),MU(400)
      open(110,file='wear.dat',status='old')
      open(24,file='filename.inf',status='old')
      Rewind(24)

      Do i =1,6
      read(24,7)filename(i),filenam1(i)
      end do

      J=0
      rewind (110)
      Do while (.true.)
```

```
      j=j+1
      read(110,*,end=11)t1(j),d(j),force(j),tco(j),Tau1(j),mu(j)

      end do

11    close(110)

      Open (25,file = filename(k),status='unknown')

      Do I=1,nd
      write(25,20)t1(i),(d(i+jd),jd=0,4*nd,nd)
      end do
      write(25,20)

      Do I=1,nd
      write(25,20)t1(i),(d(i+jd),jd=5*nd,9*nd,nd)
      end do
      write(25,*)'                    Force'

      Do I=1,nd
      write(25,20)t1(i),(force(i+jd),jd=0,4*nd,nd)
      end do
      write(25,*)

      Do I=1,nd
      write(25,20)t1(i),(force(i+jd),jd=5*nd,9*nd,nd)
      end do
      write(25,*)'                    Contact Time'

      Do I=1,nd
      write(25,20)t1(i),(tco(i+jd),jd=0,4*nd,nd)
      end do
      write(25,*)

      Do I=1,nd
      write(25,20)t1(i),(tco(i+jd),jd=5*nd,9*nd,nd)
      end do
      write(25,*)'                Coefficient of Friction'

      Do I=1,nd
      write(25,20)t1(i),(mu(i+jd),jd=0,4*nd,nd)
      end do
      write(25,*)

      Do I=1,nd
      write(25,20)t1(i),(mu(i+jd),jd=5*nd,9*nd,nd)
      end do
      write(25,*)'                Shear Yield Strength Point'

      Do I=1,nd
      write(25,20)t1(i),(tau1(i+jd),jd=0,4*nd,nd)
```

```
      end do
      write(25,*)

      Do I=1,nd
      write(25,20)t1(i),(tau1(i+jd),jd=5*nd,9*nd,nd)
      end do
      write(25,*)

      close(25)

      Open (26,file = filenam1(k),status='unknown')

      Write(26,*) '                          Time 5 Year'
      Do I = 5,9*nd,30
      write(26,20)t1(i),d(i),force(i),Tco(i),tau1(i),mu(i)
      end do

      Write(26,*) '                          Time 10 Year'
      Do I = 10,9*nd,30
      write(26,20)t1(i),d(i),force(i),Tco(i),tau1(i),mu(i)
      end do

      Write(26,*) '                          Time 15 Year'
      Do I = 15,9*nd,30
      write(26,20)t1(i),d(i),force(i),Tco(i),tau1(i),mu(i)
      end do

      Write(26,*) '                          Time 20 Year'
      Do I = 20,9*nd,30
      write(26,20)t1(i),d(i),force(i),Tco(i),tau1(i),mu(i)
      end do

      Write(26,*) '                          Time 25 Year'
      Do I = 25,9*nd,30
      write(26,20)t1(i),d(i),force(i),Tco(i),tau1(i),mu(i)
      end do

20    format(1x,f4.1,2x,5(e12.6,1x))
 7    format(a11,1x,a12)
      return
      end
```

VITA

Masoud Naghedolfeizi was born in Tehran, Iran on May 4, 1961. He received his Bachelor of Science degree in Mechanical Engineering from Tehran Science and Technology University in February 1986. In August 1988, he entered The University of Tennessee to purse his graduate studies in the field of nuclear engineering. He obtained his M.S. degree in Nuclear Engineering in December 1990. From August 1988 to May 1989, he was a graduate teaching assistant for computer programming courses at the College of Engineering of The University of Tennessee. He was a graduate research assistant at the Nuclear Engineering Department from May 1989 to December 1994. He received the Doctor of Philosophy degree in Nuclear Engineering in December 1994. His research interests are life assessment analysis of plant components, thermal-hydraulics, nuclear shielding, and signal processing.